ISSN 1949-8462 (online)

World Journal of *Cardiology*

World J Cardiol 2013 December 26; 5(12): 442-494

Baishideng Publishing Group
www.wjgnet.com

World Journal of Cardiology

A peer-reviewed, online, open-access journal of Cardiology

Editorial Board

2009-2013

The *World Journal of Cardiology* Editorial Board consists of 362 members, representing a team of worldwide experts in cardiology. They are from 43 countries, including Argentina (4), Australia (9), Belgium (2), Brazil (5), Canada (24), Chile (1), China (18), Colombia (1), Czech (1), Denmark (4), France (3), Germany (32), Greece (14), Hungary (2), India (8), Iran (2), Ireland (1), Israel (2), Italy (44), Japan (24), Kosovo (1), Lebanon(1), Malaysia (1), Mexico (1), Morocco (1), Netherlands (9), Nigeria (1), Oman (1), Pakistan (1), Poland (3), Portugal (1), Russia (1), Singapore (1), Slovenia (2), South Africa (2), South Korea (6), Spain (10), Switzerland (1), Thailand (1), Turkey (8), United Kingdom (14), United States (93), and Uruguay (1).

Denmark

Morten Grunnet, *Ballerup*
Won Yong Kim, *Aarhus*
Ole Dyg Pedersen, *Copenhagen*
Jacob Tfelt-Hansen, *Copenhagen*

France

Philippe Commeau, *Ollioules*
Yves D Durandy, *Massy*
Thierry Lefèvre, *Massy*

Germany

Ferruh Artunc, *Tübingen*
Muhammet A Aydin, *Hamburg*
Alexander Bauer, *Heidelberg*
Peter Bernhardt, *Ulm*
Torsten Bossert, *Jena*
Marcus Dörr, *Greifswald*
Holger Eggebrecht, *Essen*
Tommaso Gori, *Mainz*
Dariusch Haghi, *Mannheim*
Stefan E Hardt, *Heidelberg*
Klaus Hertting, *Hamburg*
Thomas Jax, *Neuss*
Thorsten Kälsch, *Mannheim*
Klaus Kettering, *Frankfurt*
Grigorios Korosoglou, *Heidelberg*
Horst J Kuhn, *Planegg*
Lorenz H Lehmann, *Heidelberg*
Huige Li, *Mainz*
Veselin Mitrovic, *Bad Nauheim*
Ulrich Nellessen, *Stendal*
Guenter Pilz, *Hausham*
Peter W Radke, *Lübeck*
Obaida Rana, *Aachen*
Tienush Rassaf, *Düsseldorf*
Oliver Ritter, *Wuerzburg*
Erol Saygili, *Aachen*
Dirk Skowasch, *Bonn*
Tim Süselbeck, *Mannheim*
Dirk Taubert, *Cologne*
Theodor Tirilomis, *Goettingen*
Stephen Wildhirt, *Ulm*
Thomas Zeller, *Bad Krozingen*

Greece

Yiannis S Chatzizisis, *Thessaloniki*
Moses S Elisaf, *Ioannina*
Gerasimos Filippatos, *Athens*
Panagiotis Korantzopoulos, *Ioannina*
Nicholas G Kounis, *Patras*
Antigone Lazou, *Thessaloniki*
Konstantinos P Letsas, *Athens*
Athanassios N Manginas, *Athens*
Lampros Michalis, *Ioannian*
Serafim Nanas, *Athens*
Loukianos S Rallidis, *Athens*
Georgios I Tagarakis, *Thessaloniki*
Dimitrios Tziakas, *Alexandroupolis*
Theodoros Xanthos, *Athens*

Hungary

Gergely Feher, *Pecs*
Albert Varga, *Szeged*

India

MPS Chawla, *Roorkee*
S Dwivedi, *Delhi*
Rajeev Gupta, *Jaipur*
Deepak Kaul, *Chandigarh*
Prabhakaran Prabhakaran, *New Delhi*
KV Pugalendi, *Tamilnadu*
Rajesh Vijayvergiya, *Chandigarh*

Iran

VR Dabbagh Kakhki, *Mashhad*
Roya Kelishadi, *Isfahan*

Ireland

Jonathan D Dodd, *Dublin*

Israel

Jacob George, *Tel Aviv*
E Goldhammer, *Haifa*

Italy

Maria Grazia Andreassi, *Massa*
Giuseppe Barbaro, *Rome*
Riccardo Bigi, *Milan*
Tonino Bombardini, *Pisa*
Filippo Cademartiri, *Parma*
Alessandro Capucci, *Piacenza*
Sergio Coccheri, *Bologna*
Antonio Colombo, *Milan*
Alberto Cuocolo, *Napoli*
Roberto De Ponti, *Varese*
Gianluca Di Bella, *Messina*
Giovanni Fazio, *Palermo*
Vittorio Fineschi, *Foggia*
Antonio F Folino, *Padova*
Gabriele Fragasso, *Milano*
Carmine Gazzaruso, *Vigevano*
Massimo Imazio, *Torino*
Federico Lombardi, *Milan*
Roberto Marchioli, *Santa Maria Imbaro*
Giovan Giuseppe Mattera, *Pomezia*
Germano Melissano, *Milano*
Pietro A Modesti, *Florence*
Eraldo Occhetta, *Novara*
Pasquale Pagliaro, *Orbassano*
Emilio Maria G Pasanisi, *Pisa*
Vincenzo Pasceri, *Rome*
Salvatore Patanè, *Messina*
Nunzia Rosa Petix, *Florence*
Eugenio Picano, *Pisa*
Rita Rezzani, *Brescia*
Manfredi Rizzo, *Palermo*
Gian Paolo Rossi, *Padua*
Speranza Rubattu, *Rome*
Andrea Rubboli, *Bologna*
Rosa Sicari, *Pisa*
Giuseppe Tarantini, *Padua*
Luigi Tavazzi, *Cotignola*
Luca Testa, *Milan*
Maurizio Turiel, *Milan*
Cristina Vassalle, *Pisa*
Massimo Volpe, *Rome*

Japan

Yoshifusa Aizawa, *Niigata*
Junichiro Hashimoto, *Sendai*
Hajime Kataoka, *Oita*
Akinori Kimura, *Tokyo*
Sei Komatsu, *Amagasaki*
Ikuo Fukuda, *Hirosaki*
Satoshi Kurisu, *Hiroshima*
Yoshihiro Matsumoto, *Shizuoka*
Tetsuo Minamino, *Osaka*
Yoko Miyasaka, *Osaka*
Kenichi Nakajima, *Kanazawa*
Mashio Nakamura, *Tsu*
Kazuaki Nishio, *Tokyo*
Koichi Sakabe, *Kagawa*
Masataka Sata, *Tokushima*
Shinji Satoh, *Fukuoka*
Yoshihide Takahashi, *Kanagawa*
Masamichi Takano, *Chiba*
Kengo Tanabe, *Tokyo*
Hiroki Teragawa, *Hiroshima*
Hiroyasu Ueda, *Osaka*
Takanori Yasu, *Okinawa*
Hiroshi Yoshida, *Chiba*

Kosovo

Gani Bajraktari, *Prishtina*

Lebanon

Habib A Dakik, *Beirut*

Malaysia

Eric Tien Siang Lim, *Johor*

Mexico

Enrique Vallejo, *Mexico*

Morocco

Abdenasser Drighil, *Casablanca*

Netherlands

Folkert Wouter Asselbergs, *Groningen*
Jeroen J Bax, *Leiden*
JJ Brugts, *Rotterdam*
Peter W de Leeuw, *AZ Maastricht*
Corstiaan A Den Uil, *Rotterdam*
PA Doevendans, *Utrecht*
D Poldermans, *Rotterdam*
PW Serruys, *Rotterdam*

Nigeria

OS Ogah, *Ibadan*

Pakistan

Fahim H Jafary, *Karachi*

Poland

Pawel Buszman, *Katowice*
Maciej Kurpisz, *Poznan*
Sebastian Szmit, *Warsaw*

Russia

Nadezda Bylova, *Moscow*

Singapore

Jinsong Bian, *Singapore*

Slovenia

Mitja Lainscak, *Golnik*
Matej Podbregar, *Ljublajna*

South Africa

Benjamin Longo-Mbenza, *Pretoria*
JP Smedema, *Capetown*

South Korea

Jang-Ho Bae, *Daejeon*
Young-Guk Ko, *Seoul*
Sang-Hak Lee, *Seoul*
Pil-Ki Min, *Seoul*
Seung-Jung Park, *Seoul*

Spain

Miguel A Arias, *Toledo*
Antoni Bayés-Genís, *Barcelona*
Alberto Dominguez-Rodriguez, *Tenerife*
Lorenzo Facila, *Castellon*
José Luis Pérez-Castrillon, *Valladolid*
Jesus Peteiro, *Coruña*
Pedro L Sánchez, *Madrid*
José L Zamorano, *Madrid*

Switzerland

Paul Erne, *Luzern*

Thailand

Nipon Chattipakorn, *Chiang Mai*

Turkey

Turgay Çelik, *Etlik-Ankara*
Yengi U Celikyurt, *Kocaeli*
Hamza Duygu, *Yesilyurt*
Cemil Gürgün, *İzmir*
T Fikret Ilgenli, *Kocaeli*
Ergün Barış Kaya, *Ankara*
Mehmet Ozaydin, *Isparta*
Mustafa Yildiz, *Istanbul*

United Kingdom

AD Blann, *Birmingham*
Geoffrey Burnstock, *London*
John GF Cleland, *Kingston upon Hull*
Armen Yuri Gasparyan, *Dudley*
Derek J Hausenloy, *London*
Farhad Kamali, *Newcastle upon Tyne*
Juan Carlos Kaski, *London*
Rajesh G Katare, *Bristol*
Sohail Q Khan, *Manchester*
Khalid Rahman, *Liverpool*
Alexander M Seifalian, *London*
Mark Slevin, *Manchester*
Anastasis Stephanou, *London*

United States

Kamran Akram, *Omaha*
Arshad Ali, *Ashland*
Mouaz Al-Mallah, *Detroit*
Naser M Ammash, *Rochester*
Vignendra Ariyarajah, *Philadelphia*
Wilbert S Aronow, *Valhalla*
S Serge Barold, *Tampa*
Gregory W Barsness, *Rochester*
Daniel S Berman, *Los Angeles*
John F Beshai, *Chicago*
William E Boden, *Buffalo*
Somjot S Brar, *Los Angeles*
David W Brown, *Decatur*
Lu Cai, *Louisville*
Christopher Paul Cannon, *Boston*
Ricardo Castillo, *Brooklyn*
Jun R Chiong, *Loma Linda*
Steven G Chrysant, *Oklahoma*
Timm Dickfeld, *Baltimore*
Dayue Darrel Duan, *Reno*
Rosemary B Duda, *Boston*
Michael E Farkouh, *New York*
Arthur Michael Feldman, *Philadelphia*
Ronald Freudenberger, *Allentown*
Jalal K Ghali, *Detroit*
Lev G Goldfarb, *Bethesda*
Samuel Z Goldhaber, *Boston*
Hitinder S Gurm, *Ann Arbor*
Julia H Indik, *Tucson*
Antony Leslie Innasimuthu, *Pittsburgh*
Ami E Iskandrian, *Birmingham*
Rovshan M Ismailov, *Pittsburgh*
Diwakar Jain, *Philadelphia*
Shahrokh Javaheri, *Mason*
Jacob Joseph, *West Roxbury*
Bobby V Khan, *Atlanta*
Christopher M Kramer, *Charlottesville*
Rakesh C Kukreja, *Richmond*
Roberto M Lang, *Chicago*
Marzia Leacche, *Nashville*
Jingping Lin, *Bethesda*
Yi-Hwa Liu, *New Haven*
Angel López-Candales, *Pittsburgh*
Frank Marcus, *Tucson*
Malek G Massad, *Chicago*
Jawahar L Mehta, *Little Rock*
Robert M Mentzer Jr, *Detroit*
J Gary Meszaros, *Rootstown*
Michael Miller, *Baltimore*
Emile R Mohler III, *Philadelphia*
Patrick M Moriarty, *Kansas City*
Jeffrey W Moses, *New York*
Mohammad-Reza Movahed, *Tucson*
Gerald V Naccarelli, *Hershey*
Andrea Natale, *Austin*
Tien MH Ng, *Los Angeles*
Steven Nissen, *Cleveland*
Gian M Novaro, *Weston*
Brian Olshansky, *Iowa*
Robert Lee Page II, *Aurora*
Weihong Pan, *Baton Rouge*
Linda Pauliks, *Hershey*
Philip Jack Podrid, *Boston*
Vikas K Rathi, *Midlothian*
Jun Ren, *Laramie*
Harmony R Reynolds, *New York*
Clive Rosendorff, *Bronx*
Samir Saba, *Pittsburgh*
Rajesh Sachdeva, *Little Rock*
Sandeep A Saha, *Spokane*
Tiziano M Scarabelli, *Detroit*
Robert H Schneider, *Maharishi Vedic*
Frank W Sellke, *Providence*
Samin K Sharma, *New York*
Jamshid Shirani, *Danville*
Boris Z Simkhovich, *Los Angeles*
Krishna Singh, *Johnson City*
Laurence S Sperling, *Atlanta*
Jonathan S Steinberg, *New York*
Ernst R von Schwarz, *Los Angeles*
Richard Gary Trohman, *Chicago*
Tong Tang, *San Diego*
Qing Kenneth Wang, *Cleveland*
Yi Wang, *Wilmington*
Adam Whaley-Connell, *Columbia*
Bruce L Wilkoff, *Cleveland*
Qinglin Yang, *Birmingham*
Xing Sheng Yang, *Atlanta*
Yucheng Yao, *Los Angeles*
Midori A Yenari, *San Francisco*
Cuihua Zhang, *Columbia*

Uruguay

Juan C Grignola, *Montevideo*

WJC

World Journal of Cardiology

Contents

Monthly Volume 5 Number 12 December 26, 2013

World Journal of Cardiology
Volume 5 Number 12 December 26, 2013

Contents

NAME OF JOURNAL
World Journal of Cardiology

ISSN
ISSN 1949-8462 (online)

LAUNCH DATE
December 31, 2009

FREQUENCY
Monthly

EDITORIAL OFFICE
Jin-Lei Wang, Director
Xiu-Xia Song, Vice Director
World Journal of Cardiology
Room 903, Building D, Ocean International Center,
No. 62 Dongsihuan Zhonglu, Chaoyang District,
Beijing 100025, China
Telephone: +86-10-85381891
Fax: +86-10-85381893
E-mail: bpgoffice@wjgnet.com
http://www.wjgnet.com

PUBLISHER
Baishideng Publishing Group Co., Limited
Flat C, 23/F., Lucky Plaza, 315-321 Lockhart Road,
Wan Chai, Hong Kong, China
Fax: +852-65557188
Telephone: +852-31779906
E-mail: bpgoffice@wjgnet.com
http://www.wjgnet.com

PUBLICATION DATE
December 26, 2013

INSTRUCTIONS TO AUTHORS
Full instructions are available online at http://www.wjgnet.com/1949-8462/g_info_20100316161927.htm.

ONLINE SUBMISSION
http://www.wjgnet.com/esps/

World Journal of Cardiology

Online Submissions: http://www.wjgnet.com/esps/
bpgoffice@wjgnet.com
doi:10.4330/wjc.v5.i12.442

World J Cardiol 2013 December 26; 5(12): 442-443
ISSN 1949-8462 (online)

TOPIC HIGHLIGHT

Zhonghua Sun, PhD, Associate Professor, *Series Editor*

Coronary CT angiography: State of the art

Zhonghua Sun, Akmal Sabarudin

Zhonghua Sun, Discipline of Medical Imaging, Department of Imaging and Applied Physics, Curtin University, Perth 6845, Western Australia, Australia
Akmal Sabarudin, Diagnostic Imaging and Radiotherapy Program, School of Diagnostic and Applied Health Sciences, Faculty of Health Sciences, University Kebangsaan Malaysia, Kuala Lumpur 50300, Malaysia
Author contributions: Both authors wrote the paper.
Correspondence to: Zhonghua Sun, PhD, Associate Professor, Discipline of Medical Imaging, Department of Imaging and Applied Physics, Curtin University, GPO Box U1987, Perth 6845, Western Australia, Australia. z.sun@curtin.edu.au
Telephone: +61-8-9266 7509 Fax: +61-8-9266 2377
Received: July 3, 2013 Revised: July 24, 2013
Accepted: August 28, 2013
Published online: December 26, 2013

Core tip: This article provides an overview of a series of articles that focus on individual topic highlight related to coronary computed tomography (CT) angiography. In particular, use of beta-blocker protocol, radiation dose measurements, dose-reduction strategies, diagnostic and prognostic value of coronary CT angiography will be described in detail in each series. Furthermore, potential applications of coronary CT angiography beyond luminal visualization and future directions will also be discussed.

Sun Z, Sabarudin A. Coronary CT angiography: State of the art. *World J Cardiol* 2013; 5(12): 442-443 Available from: URL: http://www.wjgnet.com/1949-8462/full/v5/i12/442.htm DOI: http://dx.doi.org/10.4330/wjc.v5.i12.442

Abstract

Coronary computed tomography (CT) angiography has been recognized as the most rapidly developed imaging technique in the diagnosis of coronary artery disease due to the emergence and technological advances in multislice CT scanners. Coronary CT angiography has been confirmed to demonstrate high diagnostic and predictive value in coronary artery disease when compared to invasive coronary angiography. However, it suffers from high radiation dose which raises concerns in the medical field. Various dose-reduction strategies have been proposed with effective outcomes having been achieved to reduce radiation exposure to patients. This article provides an introduction and overview of the series of articles that will focus on each particular topic related to coronary CT angiography.

Key words: Coronary artery disease; Coronary computed tomography angiography; Radiation dose; Diagnostic value; Predictive value

CORONARY CT ANGIOGRAPHY

Over the last decade a great deal of interest has been focused on imaging and diagnosis of coronary artery disease (CAD) using coronary computed tomography (CT) angiography due to its less invasive nature and improved spatial and temporal resolution. With latest multislice CT scanners (64- and post-64 slice CT), coronary CT angiography has been reported to have high diagnostic value, and it can be used as a reliable alternative to invasive coronary angiography in selected patients[1-7]. In addition to the diagnostic value, coronary CT angiography has demonstrated the ability to assess coronary plaques in terms of morphology and plaque characterization, thus providing prognostic information for prediction of major adverse cardiac events[8-11].

Despite these promising reports and increasing studies available in the literature, coronary CT angiography suffers from a major limitation, which is high radiation dose. This has raised serious concerns in the medical field, as radiation-induced cancer is not negligible. Awareness of this issue plays an important role in ensuring that use of

coronary CT angiography is medically justified, and dose-reduction strategies are implemented whenever possible, while diagnostic image quality is still acceptable[12].

This series consists of 5 articles on the clinical applications of coronary CT angiography in CAD. Part I deals with beta-blocker administration protocol as beta-blocker is the most commonly used drug to achieve heart rate control during coronary CT angiography. It has become a routine protocol to use beta-blocker to slow down heart rate in patients with heart rate more than 70 beats/min prior to coronary CT angiography, thus, understanding the preparations and patient care is important for clinicians (in particular for those who are inexperienced in performing the coronary CT angiography) to effectively utilize this imaging technique.

Part II focuses on radiation dose measurements in coronary CT angiography. As mentioned above, coronary CT angiography is associated with high radiation dose, therefore, awareness of the basic dosimeters for dose measurement will help clinicians to understand the radiation risks. Part III is about dose-reduction strategies in coronary CT angiography. This part contributes to an overview of different dose-saving methods that are currently recommended in the clinical practice.

Part IV focuses on the diagnostic and prognostic value of coronary CT angiography in CAD. A systematic review of the literature on these two aspects will provide readers with updated information with regard to the current status of coronary CT angiography in terms of diagnostic accuracy and prediction of disease outcomes.

Part V is the last article of this series presenting information on the emerging diagnostic value of coronary CT angiography in CAD, which is entitled coronary CT angiography: beyond luminal visualization. In addition to the evaluation of coronary wall morphology and plaque assessment, coronary CT angiography is able to provide functional information such as assessment of myocardial ischemia which is available with dual-energy CT; hemodynamic analysis of coronary stenosis and plaque, as well as determination of patient-specific lesions (CT-derived fractional flow reserve) with use of computational fluid dynamics. This research area represents some novel applications of coronary CT angiography, although its applications are still at infancy.

In summary, this series provides a comprehensive coverage of different topics related to the coronary CT angiography in CAD, ranging from the patient preparation of heart rate control to dose measurements, dose reduction to the diagnostic and prognostic value. Finally, future research directions of coronary CT angiography are discussed and highlighted in the last part. We believe these articles contribute to improving our knowledge and understanding on coronary CT angiography and its corresponding clinical value.

REFERENCES

1 **Sun Z**, Lin C, Davidson R, Dong C, Liao Y. Diagnostic value of 64-slice CT angiography in coronary artery disease: a systematic review. *Eur J Radiol* 2008; **67**: 78-84 [PMID: 17766073 DOI: 10.1016/j.ejrad.2007.07.014]

2 **Mowatt G**, Cook JA, Hillis GS, Walker S, Fraser C, Jia X, Waugh N. 64-Slice computed tomography angiography in the diagnosis and assessment of coronary artery disease: systematic review and meta-analysis. *Heart* 2008; **94**: 1386-1393 [PMID: 18669550 DOI: 10.1136/hrt.2008.145292]

3 **Stein PD**, Yaekoub AY, Matta F, Sostman HD. 64-slice CT for diagnosis of coronary artery disease: a systematic review. *Am J Med* 2008; **121**: 715-725 [PMID: 18691486 DOI: 10.1016/j.amjmed.2008.02.039]

4 **Otero HJ**, Steigner ML, Rybicki FJ. The "post-64" era of coronary CT angiography: understanding new technology from physical principles. *Radiol Clin North Am* 2009; **47**: 79-90 [PMID: 19195535 DOI: 10.1016/j.rcl.2008.11.001]

5 **Hurlock GS**, Higashino H, Mochizuki T. History of cardiac computed tomography: single to 320-detector row multislice computed tomography. *Int J Cardiovasc Imaging* 2009; **25** Suppl 1: 31-42 [PMID: 19145476 DOI: 10.1007/s10554-008-9408-z]

6 **Abdulla J**, Asferg C, Kofoed KF. Prognostic value of absence or presence of coronary artery disease determined by 64-slice computed tomography coronary angiography a systematic review and meta-analysis. *Int J Cardiovasc Imaging* 2011; **27**: 413-420 [PMID: 20549366 DOI: 10.1007/s10554-010-9652-x]

7 **Sun Z**, Choo GH, Ng KH. Coronary CT angiography: current status and continuing challenges. *Br J Radiol* 2012; **85**: 495-510 [PMID: 22253353 DOI: 10.1259/bjr/15296170]

8 **Rana JS**, Gransar H, Wong ND, Shaw L, Pencina M, Nasir K, Rozanski A, Hayes SW, Thomson LE, Friedman JD, Min JK, Berman DS. Comparative value of coronary artery calcium and multiple blood biomarkers for prognostication of cardiovascular events. *Am J Cardiol* 2012; **109**: 1449-1453 [PMID: 22425333 DOI: 10.1016/j.amjcard.2012.01.358]

9 **Gottlieb I**, Miller JM, Arbab-Zadeh A, Dewey M, Clouse ME, Sara L, Niinuma H, Bush DE, Paul N, Vavere AL, Texter J, Brinker J, Lima JA, Rochitte CE. The absence of coronary calcification does not exclude obstructive coronary artery disease or the need for revascularization in patients referred for conventional coronary angiography. *J Am Coll Cardiol* 2010; **55**: 627-634 [PMID: 20170786 DOI: 10.1016/j.jacc.2009.07.072]

10 **Carrigan TP**, Nair D, Schoenhagen P, Curtin RJ, Popovic ZB, Halliburton S, Kuzmiak S, White RD, Flamm SD, Desai MY. Prognostic utility of 64-slice computed tomography in patients with suspected but no documented coronary artery disease. *Eur Heart J* 2009; **30**: 362-371 [PMID: 19153177 DOI: 10.1093/eurheartj/ehn605]

11 **Budoff MJ**, Nasir K, McClelland RL, Detrano R, Wong N, Blumenthal RS, Kondos G, Kronmal RA. Coronary calcium predicts events better with absolute calcium scores than age-sex-race/ethnicity percentiles: MESA (Multi-Ethnic Study of Atherosclerosis). *J Am Coll Cardiol* 2009; **53**: 345-352 [PMID: 19161884 DOI: 10.1016/j.jacc.2008.07.072]

12 **Sun Z**, Ng KH. Coronary computed tomography angiography in coronary artery disease. *World J Cardiol* 2011; **3**: 303-310 [PMID: 21949572 DOI: 10.4330/wjc.v3.i9.303]

P- Reviewers: Firstenberg MS, Kasai T
S- Editor: Zhai HH **L- Editor**: A **E- Editor**: Liu XM

World Journal of Cardiology

Online Submissions: http://www.wjgnet.com/esps/
bpgoffice@wjgnet.com
doi:10.4330/wjc.v5.i12.444

World J Cardiol 2013 December 26; 5(12): 444-452
ISSN 1949-8462 (online)

TOPIC HIGHLIGHT

Zhonghua Sun, PhD, Associate Professor, *Series Editor*

Coronary CT angiography: Beyond morphological stenosis analysis

Zhonghua Sun

Zhonghua Sun, Discipline of Medical Imaging, Department of Imaging and Applied Physics, Curtin University, Perth, Western Australia 6845, Australia
Author contributions: Sun Z solely contributed to this paper.
Correspondence to: Zhonghua Sun, Associate Professor, Discipline of Medical Imaging, Department of Imaging and Applied Physics, Curtin University, GPO Box, U1987, Perth, Western Australia 6845, Australia. z.sun@curtin.edu.au
Telephone: +61-8-92667509 Fax: +61-8-92662377
Received: September 16, 2013 Revised: October 24, 2013
Accepted: November 18, 2013
Published online: December 26, 2013

Abstract

Rapid technological developments in computed tomography (CT) imaging technique have made coronary CT angiography an attractive imaging tool in the detection of coronary artery disease. Despite visualization of excellent anatomical details of the coronary lumen changes, coronary CT angiography does not provide hemodynamic changes caused by presence of plaques. Computational fluid dynamics (CFD) is a widely used method in the mechanical engineering field to solve complex problems through analysing fluid flow, heat transfer and associated phenomena by using computer simulations. In recent years, CFD is increasingly used in biomedical research due to high performance hardware and software. CFD techniques have been used to study cardiovascular hemodynamics through simulation tools to assist in predicting the behaviour of circulatory blood flow inside the human body. Blood flow plays a key role in the localization and progression of coronary artery disease. CFD simulation based on 3D luminal reconstructions can be used to analyse the local flow fields and flow profiling due to changes of vascular geometry, thus, identifying risk factors for development of coronary artery disease. The purpose of this article is to provide an overview of the coronary CT-derived CFD applications in coronary artery disease.

Key words: Computational fluid dynamics; Coronary artery disease; Hemodynamics; Modelling

Core tip: Coronary computed tomography (CT) angiography is limited to the visualization of anatomical details of coronary artery tree, while computational fluid dynamics (CFD) overcomes this limitation by providing hemodynamic changes to the coronary artery due to presence of plaques. CFD has been increasingly used in the investigation of cardiovascular disease due to its ability of providing flow changes and variations. This article provides an overview of the clinical applications of coronary CT-derived CFD in coronary artery disease.

Sun Z. Coronary CT angiography: Beyond morphological stenosis analysis. *World J Cardiol* 2013; 5(12): 444-452 Available from: URL: http://www.wjgnet.com/1949-8462/full/v5/i12/444.htm
DOI: http://dx.doi.org/10.4330/wjc.v5.i12.444

INTRODUCTION

Coronary artery disease (CAD) is the leading cause of death in advanced countries and its prevalence is increasing among developing countries[1]. Traditionally, diagnosis of CAD is performed by invasive coronary angiography which is considered the gold standard technique, since it has superior spatial and temporal resolution leading to excellent diagnostic accuracy. However, it is an invasive and expensive procedure associated with a small but distinct procedure-related morbidity (1.5%) and mortality (0.2%)[2]. Furthermore, invasive coronary angiography usually requires patients to stay for a short period in the hospital after the examination and this causes discomfort for the patients. Thus, a non-invasive technique for imaging and

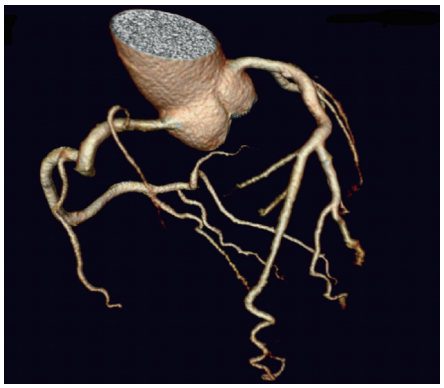

Figure 1 3D volume rendering shows normal right and left coronary arteries with excellent demonstration of main and side branches.

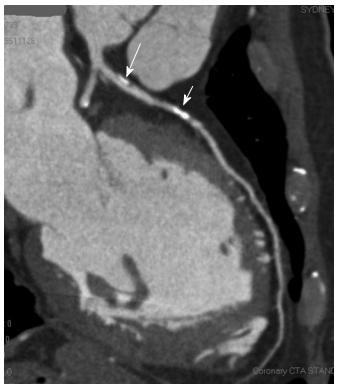

Figure 2 Curved planar reformation image shows significant stenosis of the left anterior descending coronary artery due to presence of plaques. The long arrow refers to the mixed plaque at the proximal segment of left left anterior descending (LAD), while the short arrow points to the calcified plaque at the proximal segment of LAD.

diagnosis of CAD is highly desirable.

Cardiac imaging has experienced rapid growth in recent years. Several techniques have been investigated for diagnosis and prognosis of patients with proven or suspected CAD. Although currently there is no less-invasive imaging modality that can replace invasive coronary angiography, the development of computed tomography (CT), magnetic resonance imaging (MRI), single photon emission computed tomography and positron emission tomography contribute to the detection and diagnosis of CAD less invasively when compared to the invasive coronary angiography[3-11].

Despite promising results achieved with these less-invasive modalities, the application is still limited to the visualization of anatomical details such as stenosis or occlusion, while the hemodynamic interference due to the presence of coronary plaques and subsequent flow changes cannot be assessed by traditional imaging techniques. Thus, identification of plaques that may cause cardiac events is of paramount importance for reducing the mortality and improving healthcare in patients suspected of CAD.

Computational fluid dynamics (CFD) enables analysis of hemodynamic changes of the blood vessel, even before the atherosclerotic plaques are actually formed in the artery wall. Therefore, to some extent, CFD allows for an early detection of atherosclerotic disease and improves understanding of the progression of plaques[12-14]. The purpose of this article is to provide an overview of the applications of CFD in the diagnosis of coronary artery disease based on coronary CT angiography examination.

CORONARY CT ANGIOGRAPHY VISUALIZATION OF CAD

Over the last decade a great deal of interest has been focused on imaging and diagnosis of CAD using coronary CT angiography due to its less invasive nature and improved spatial and temporal resolution (Figure 1). Moderate to high diagnostic accuracy was achieved with 64- or post-64 slice CT, owing to further technical improvements[15-19]. These studies have indicated that coronary CT angiography has high accuracy for the diagnosis of CAD and could be used as an effective alternative to invasive coronary angiography in selected patients (Figure 2).

In addition to the diagnostic value, coronary CT angiography demonstrates the potential to visualize coronary artery wall morphology, characterize atherosclerotic plaques and identify non-stenotic plaques that may be undetected by invasive coronary angiography (Figure 3). Studies have shown that coronary CT angiography demonstrates high prognostic value in CAD, as it is able to differentiate low-risk from high-risk patients, with very low rate of adverse cardiac events occurring in patients with normal coronary CT angiography, and significantly high rate of these events in patients with obstructive CAD[20-22].

According to the guidelines of the European Society of Cardiology, and the American College of Cardiology/American Heart Association, the decision to perform interventional procedures such as coronary angioplasty or bypass surgery should integrate anatomical information with a test that provides objective proof of ischemia[23,24]. Echocardiography is a multimodality imaging technique which allows accurate assessment of myocardial structure, function and perfusion. Stress echocardiography has become widely used for evaluation of patients with suspected or known CAD, and it has been reported to be a cost-effective and feasible modality in the diagnosis of CAD[25,26]. Although coronary CT angiography has been reported to provide potentially important additional information on myocardial perfusion and chronic myocardial infarction, a limited correlation between stenotic coronary disease and single photon emission computed tomography (SPECT) findings was noticed[27]. However, with the emergence of dual-energy CT (DECT), which offers fascinating new applications such as the mapping of the iodine distribution, acquisition of both anatomic and functional information is possible[28,29]. Early studies have reported that DECT had more than 90% diagnostic accuracy for detecting myocardial perfusion defect compared to myocardial perfusion SPECT imaging[29,30], although large patient cohorts are needed to confirm the potential application of DECT

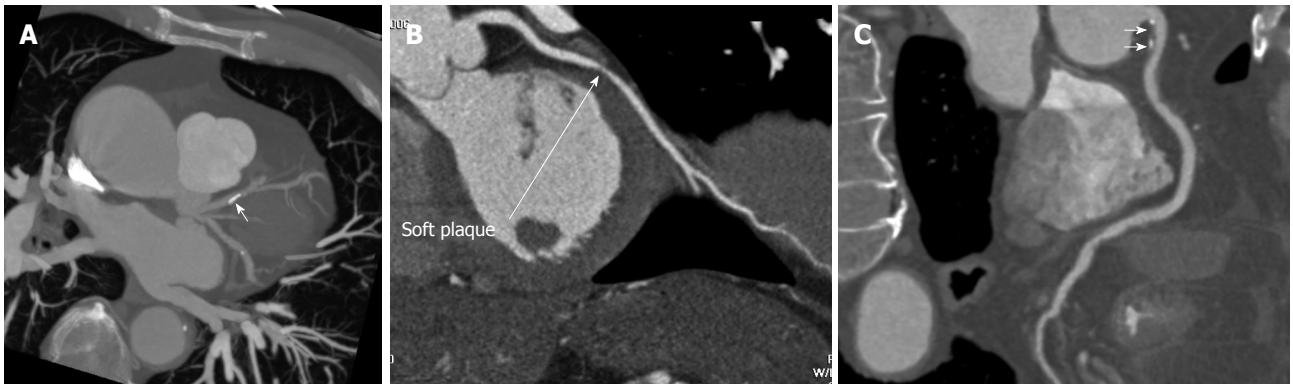

Figure 3 Characterization of coronary plaques on coronary computed tomography angiography. Coronal maximum intensity projection shows a calcified plaque (A, arrow) at the proximal segment of left coronary artery. A non-calcified plaque is present at the mid-segment of right coronary artery (B, arrow) on a curved planar reformation image. A mixed plaque is present at the proximal segment of right coronary artery (C, arrows) on a curved planar reformation image.

for both anatomic and myocardial perfusion assessment of CAD.

Coronary CT angiography provides excellent views of anatomical changes of the artery wall due to presence of plaques, thus enabling assessment of the degree of coronary stenosis. Coronary CT angiography claims to not only identify flow-limiting coronary stenosis, but also detect calcified and non-calcified plaques, measure atherosclerotic plaque burden and its response to treatment, and differentiate stable plaques from those that tend to rupture[31,32]. However, these expectations have not yet been met. In contrast, CFD enables analysis of hemodynamic changes of the blood vessel, thus improving our understanding of the progression of plaques formation and development of atherosclerosis.

COMPUTATIONAL FLUID DYNAMICS

CFD is a general term of all numerical techniques that are used to describe and analyse the flow of fluid elements at each location in certain geometry. The basic principle in CFD is that a complex geometry is separated into a large number of small finite elements. Those elements create a grid on which the equations describing the flow are analysed. The merit of CFD is developing new and improved devices and system designs, and optimization is conducted on existing equipment through computational simulations resulting in enhanced efficiency and lower operating costs[33]. However, CFD is still emerging in the biomedical field due to complexity of human anatomy and human body fluid behaviour. With high performance hardware and software easily available due to advances in computer science, biomedical research with CFD has become more accessible in recent years[34].

APPLICATIONS OF CFD IN CAD

Recently, CFD techniques have been increasingly used to study cardiovascular hemodynamics through simulation tools to assist in predicting the behaviour of circulatory blood flow inside the human body. Mechanical forces and intravascular hemodynamics can chronically affect and regulate blood vessels structure which induces a chronic inflammatory response in the arterial walls resulting in atherosclerosis[35,36]. Early CFD-based hemodynamic studies were conducted to represent *in vitro* conditions within restrictive assumptions[37-40]. Later reports demonstrated that CFD methods have the potential to enhance the data obtained from *in vivo* methods (CT or MRI) by providing a complete characterization of hemodynamic conditions (blood velocity and pressure as a function of space and time) under precisely controlled conditions (Figure 4)[41-44].

Knight *et al*[41] performed an analysis of the hemodynamic parameters including average wall-shear stress gradient, wall shear stress and oscillatory shear index obtained through a CFD study on the right coronary arteries of 30 patients. These parameters were correlated to each patient's specific plaque profile with aim of predicting the particular plaque location. Their results showed a statistically significant difference between average wall shear stress and oscillatory shear index in sensitivity and positive predictive value for the identification of atherosclerotic plaque sites in the right coronary artery. These findings further strengthen the theory that low shear stress is a contributor to the initiation of atherosclerosis.

In addition to the CFD analysis of main coronary arteries, impact of side branches on local wall shear stress should not be neglected. Wellnhofer *et al*[42] studied the impact of side branches on wall shear stress calculation in 17 patients and they concluded that side branches showed significant impact on coronary flow and wall shear stress profile in the right coronary artery. In contrast, Chaichana *et al*[43] investigated the influence of realistic coronary plaques on coronary side branches, based on a sample patient with coronary artery stenosis at the left coronary bifurcation. A direct correlation was found between coronary plaques and subsequent wall shear stress and wall pressure stress gradient changes in the coronary side branches (Figure 5). These research findings improve the understanding of the development of

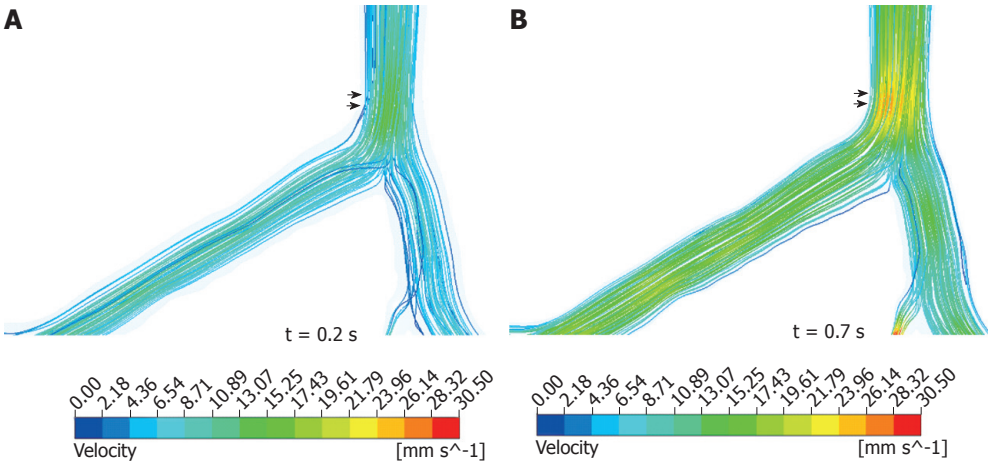

Figure 4 Local impact of flow velocity observed in a normal coronary model during systolic phase of 0.2 s (A) and diastolic phase of 0.7 s (B). Double arrows reveal high flow velocity locations at bifurcation in the left coronary artery model.

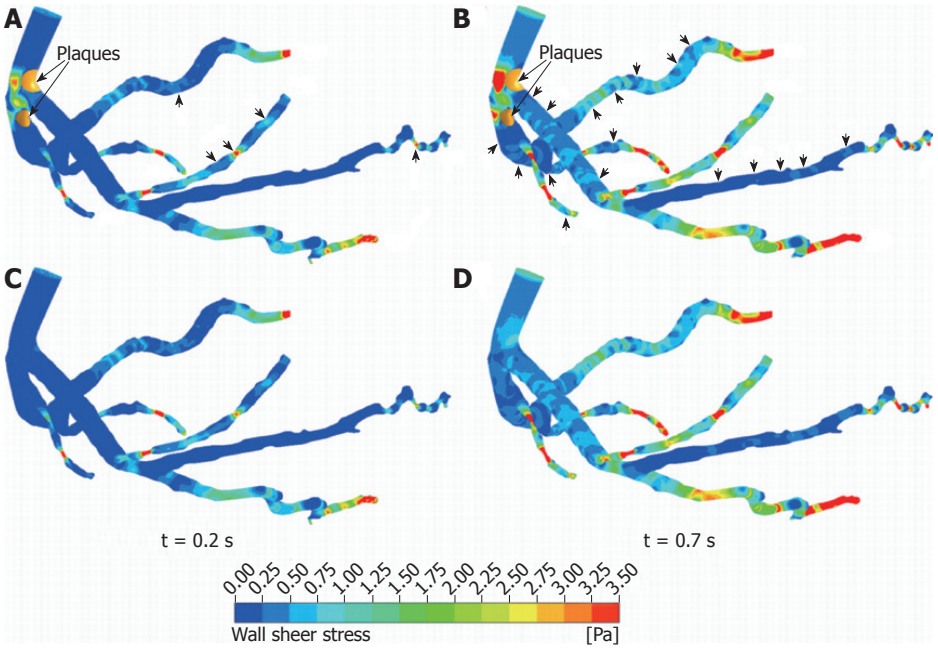

Figure 5 Computational fluid dynamics analysis of wall shear stress in 3D realistic models generated from coronary computed tomography angiography during systolic phase of 0.2 s and diastolic phase of 0.7 s. A, B: Coronary models with presence of plaques in the left anterior descending; C, D: Computational fluid dynamics analysis simulation in coronary models without presence of plaques. Arrows indicate the effect of plaques locations on wall shear stress changes in coronary side branches in the post-plaques-conditions.

atherosclerosis by exploring the hemodynamic effect of coronary plaques using CFD technique, although further studies based on a large cohort are required to verify these results.

Hemodynamic effect of left coronary angulation

The natural history of coronary plaque is dependent not only on the formation and progression of atherosclerosis, but also on the vascular remodelling response. If the local wall shear stress is low, a proliferative plaque will form. Local inflammatory response will stimulate the formation of so-called "vulnerable plaque" which is prone to rupture with superimposed thrombus formation. The vast majority of these inflamed high-risk vulnerable plaques cannot be detected by anatomic imaging and myocardial perfusion imaging. Since the progression and development of vulnerable plaque is associated with low wall shear stress and the presence of expansive remodelling, measurement of these characteristics *in vivo* will enable risk stratification for the entire coronary circulation[12,13,44]. Wong *et al*[45] simulated plaque locations in different angles involving ten patterns of plaques formation in the coronary artery wall, and they studied the effects of blood flow resistance through diseased coronary artery. Their proposed formation of the wall geometry has potential applications in the provision of reduction of flow estimates in angiography equipment and in situations where practical experimental measurement of the

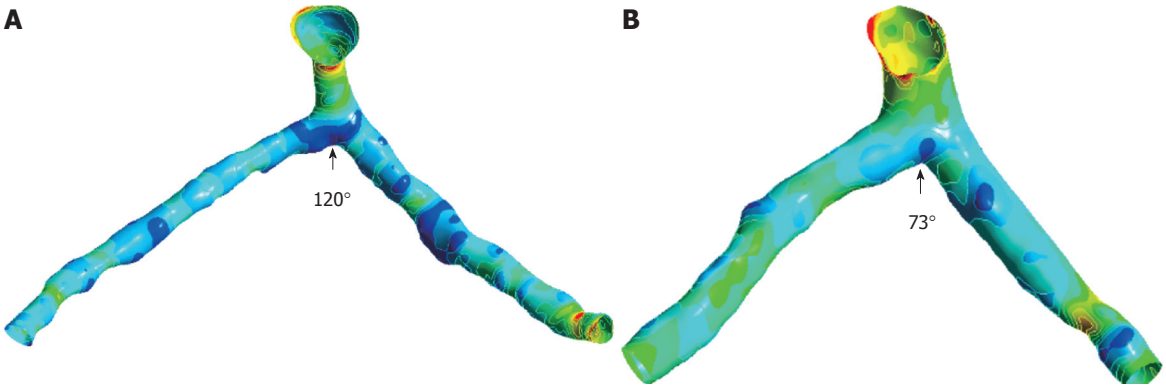

Figure 6 Wall shear stress gradient observed with different angles of the realistic left coronary artery models generated from coronary computed tomography angiography at peak systolic phase of 0.4 s. The arrows display the wall shear stress gradient distributions, with a large region of the low magnitude present at present at a 120° model (A) and a small region at a 73° model (B).

flow is unavailable.

The strong correlation between averaged low wall shear stress and the localization of atherosclerotic lesions in arterial bifurcations has been well established[12,46,47]. Rodriguez-Granillo *et al*[47] in their prospective study reported that atherosclerotic plaques located in the ostial left anterior descending coronary artery demonstrated larger plaque burden, maximal plaque thickness and low shear stress than those located in the distal left main coronary artery. Chaichana *et al*[48] in their recent study based on simulated and realistic coronary models showed a direct relationship between angulations of the left coronary artery and corresponding hemodynamic changes. Low wall shear stress and wall shear stress gradient was observed in the wide-angled models ranging from 75° to 120° when compared to the narrow-angled models ranging from 15° to 60°. Similarly, the magnitude of wall shear stress was significantly lower in the wide angulation models (120° and 110°) than that observed in the narrow angulation models (58°) which were generated based on patient's coronary CT images (Figure 6). This emphasises the potential risk of developing atherosclerosis at the left coronary bifurcation, although further studies are needed to validate these results in more realistic patient' data.

Hemodynamic effect of plaque location at the left coronary artery

Coronary plaque generally originates in the bifurcation region due to the angulations. The angulations cause a region of low wall shear stress, as confirmed by previous reports[48-53]. Medical imaging modalities such as intravascular ultrasound and coronary CT angiography have been commonly used to detect plaque locations in the left main coronary artery[54,55]. These imaging techniques provide valuable diagnostic information, such as assessment of plaque components and corresponding coronary lumen changes, however, they offer no tangible insight into the resultant hemodynamics. CFD provides an opportunity to predict the hemodynamic behaviour. Thus, the characterization of hemodynamic variations due to the various types of bifurcation plaque in the configurations can be further explored with flow visualizations; this exceeds the traditional anatomical analysis of coronary stenosis or occlusion.

According to a recent study by Chaichana *et al*[56], various types of plaques were simulated in different positions of the left coronary artery to reflect the realistic distribution of coronary plaques, as shown in Figure 7A. The wall shear stress, velocity and pressure gradient were computed and compared using CFD method. Figure 7B shows hemodynamic effects corresponding to different types of plaque in the left coronary artery, with significant difference among these plaques, while Figure 7C demonstrates the pressure gradient variations in relation to the plaque locations. These findings indicate that extra plaque located in the left coronary artery may increase the risk of plaque rupture, although further studies are needed to analyse the realistic plaque at the coronary artery based on different configurations (concentric *vs* eccentric plaques) and compositions (calcified *vs* non-calcified plaques).

Coronary CT angiography-derived fractional flow reserve

A technique to reveal the culprit CAD during invasive coronary angiography is the fractional flow reserve (FFR) measurement using a pressure-sensing guiding wire. FFR is the gold standard assessment of the hemodynamic significance of coronary stenoses as it is a measurement of the functional severity of a stenosis based on the pressure changes over a lesion during maximal coronary hyperemia. FFR is defined as maximal blood flow in a stenotic artery as a ratio to normal maximal flow[57]. FFR is measured at the time of invasive coronary angiography. An FFR of 0.80 is used as a cut off value to determine coronary stenoses responsible for ischemia with an accuracy of more than 90%[58,59]. FFR has been shown to improve detection of lesions that cause ischemia when compared with coronary CT angiography stenosis, thus, reducing the rates of false positive lesions incorrectly classified by stenosis alone[60].

Computation of FFR_{CT} is performed by computational fluid dynamics modelling after segmentation of coronary arteries and left ventricular myocardium. 3D

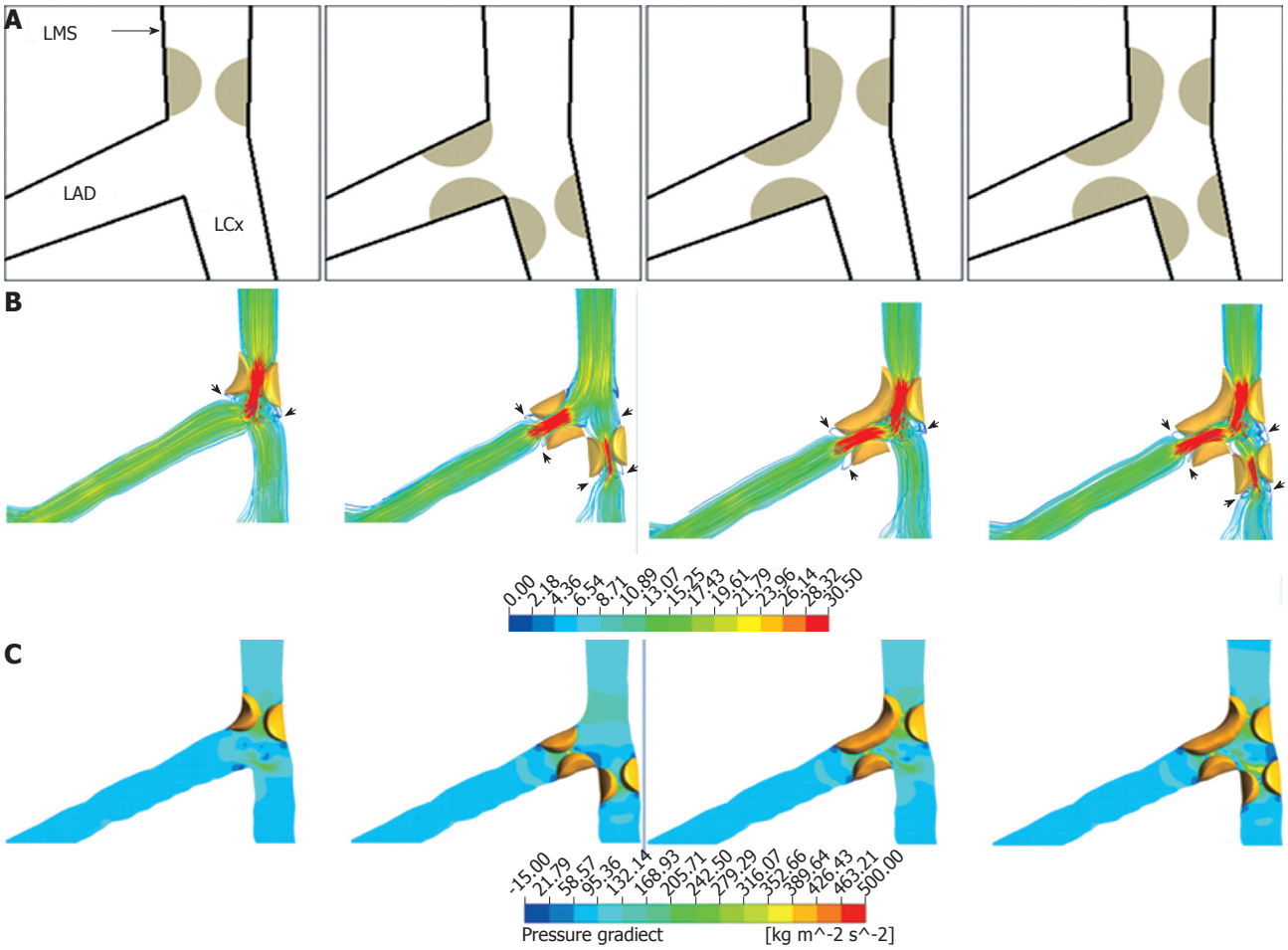

Figure 7 Computational fluid dynamics simulation of left coronary models with measurement of flow velocity and pressure gradient. A: Diagram shows characterization of the four different types of bifurcation plaques in the left coronary artery; B: The velocity patterns inside left bifurcation at effective plaque locations with these types of bifurcation plaques during the diastolic phase (0.7 s); C: The pressure gradient patterns inside left bifurcation at plaque locations with different types of bifurcation plaques during the systolic phase (0.2 s) (C). Arrows refer to the flow changes in the location of plaques. It is noticed that high velocity and high pressure gradient are present in the models with more plaques formed in the left coronary artery branches. LMS: Left main stem; LAD: Left anterior descending; LCx: Left circumflex.

blood flow simulations of the coronary arteries are performed with blood modelled as a Newtonian fluid using incompressible Navier-Stokes equations, with implementation of appropriate initial and boundary conditions to the models using a finite element method on a supercomputer. In order to ensure that the analysis reflects the realistic simulation *in vivo* conditions, realistic physiological boundary conditions are applied for 3D numerical analysis. The transient simulation is performed using accurate hemodynamic rheological and material properties, as described in previous studies[43,48]. Coronary blood flow is simulated under conditions modelling adenosine-mediated coronary hyperemia. The FFR$_{CT}$ ratio is obtained by dividing the mean pressure distal to the coronary stenosis by the mean aortic pressure, which can be measured during CFD simulations.

The FFR measurement was tested with coronary CT angiography and CFD technique and results are promising[61-63]. Min *et al*[61] in their multicenter study involving 252 stable patients with suspected or known CAD compared CT-derived FFR (FFR$_{CT}$) with coronary CT angiography and invasive coronary angiography for the diagnosis of hemodynamically significant coronary stenosis. Their results showed that FFR$_{CT}$ is considered a potentially promising non-invasive method for identification of individuals with ischemia. FFR$_{CT}$ plus CT improved diagnostic performance in terms of sensitivity and specificity when compared to CT alone. Similarly, Koo *et al*[62] in their DISCOVER-FLOW multicenter study further confirmed the usefulness of FFR derived from coronary CT angiography in the identification of ischemic coronary stenosis. On a per-vessel analysis (FFR$_{CT}$ was performed on 159 vessels in 103 patients), the diagnostic accuracy, sensitivity, specificity, positive predictive value and negative predictive value were 84.3%, 87.9%, 82.2%, 73.9%, 92.2%, respectively, for FFR$_{CT}$, and were 58.5%, 91.4%, 39.6%, 46.5%, 88.9%, respectively, for coronary CT angiography. These findings together with others indicate that FFR computed from coronary CT angiography provides better diagnostic performance for the diagnosis of lesion-specific ischemia and offers incremental value for the depiction of the culprit lesion in CAD compared to

coronary CT angiography[62-65]. In addition to the assessment of coronary stenosis, FFR_{CT} could be further applied to evaluate the in-stent restenosis or for coronary artery bypass grafts, although reports are limited in these areas.

Despite the promising results of FFR_{CT} in the detection of flow-limiting coronary stenosis, this technique suffers from some limitations. In order to confirm the diagnostic accuracy of FFR_{CT}, it needs to be compared with the gold standard, FFR which is measured by invasive coronary angiography. Furthermore, coronary CT angiography is associated with high radiation dose, although dose-reduction strategies have been recommended to reduce radiation exposure to patients[15]. Currently, myocardial perfusion SPECT imaging remains a widely accepted technique for functional assessment of coronary artery disease[27].

SUMMARY AND CONCLUSION

Although many risk factors predispose development of atherosclerosis, it tends to develop at locations where disturbed flow patterns occur, suggesting that lesion-prone areas may be due to biomechanically related factors. Furthermore, regional hemodynamics such as flow velocity, wall shear stress and wall pressure have been regarded as other risk factors for developing coronary artery disease[66-69].

CFD has been increasingly used to analyse coronary artery hemodynamics and implicate atherosclerosis progression. CFD method applied to coronary CT angiography has enabled non-invasive assessment of lesion-specific ischemia by FFR_{CT}. Furthermore, these methods also assist prediction of changes in coronary flow and pressure from therapeutic procedures (*e.g.*, percutaneous coronary intervention, coronary artery bypass graft)[70]. More research is being conducted on realistic *in vivo* coronary geometry models, and it is expected that research findings will provide potential valuable information for improving our understanding of the biomechanical pathophysiology of atherosclerosis and its complications.

REFERENCES

1 **American Heart Association**, American Stroke Association. 2002 Heart disease and stroke statistical update. Dallas, Texas: The American Heart Association, 2002

2 **Noto TJ**, Johnson LW, Krone R, Weaver WF, Clark DA, Kramer JR, Vetrovec GW. Cardiac catheterization 1990: a report of the Registry of the Society for Cardiac Angiography and Interventions (SCA& amp; I). *Cathet Cardiovasc Diagn* 1991; **24**: 75-83 [PMID: 1742788]

3 **Hingorani A**, Ascher E, Marks N. Preprocedural imaging: new options to reduce need for contrast angiography. *Semin Vasc Surg* 2007; **20**: 15-28 [PMID: 17386360 DOI: 10.1053/j.semvascsurg.2007.02.005]

4 **Sun Z**, Jiang W. Diagnostic value of multislice computed tomography angiography in coronary artery disease: a meta-analysis. *Eur J Radiol* 2006; **60**: 279-286 [PMID: 16887313 DOI: 10.1016/j.ejrad.2006.06.009]

5 **Sun Z**, Lin C, Davidson R, Dong C, Liao Y. Diagnostic value of 64-slice CT angiography in coronary artery disease: a systematic review. *Eur J Radiol* 2008; **67**: 78-84 [PMID: 17766073 DOI: 10.1016/j.ejrad.2007.07.014]

6 **Sommer T**, Hackenbroch M, Hofer U, Schmiedel A, Willinek WA, Flacke S, Gieseke J, Träber F, Fimmers R, Litt H, Schild H. Coronary MR angiography at 3.0 T versus that at 1.5 T: initial results in patients suspected of having coronary artery disease. *Radiology* 2005; **234**: 718-725 [PMID: 15665221 DOI: 10.1148/radiol.2343031784]

7 **Stuber M**, Botnar RM, Fischer SE, Lamerichs R, Smink J, Harvey P, Manning WJ. Preliminary report on in vivo coronary MRA at 3 Tesla in humans. *Magn Reson Med* 2002; **48**: 425-429 [PMID: 12210906 DOI: 10.1002/mrm.10240]

8 **Hachamovitch R**, Berman DS, Shaw LJ, Kiat H, Cohen I, Cabico JA, Friedman J, Diamond GA. Incremental prognostic value of myocardial perfusion single photon emission computed tomography for the prediction of cardiac death: differential stratification for risk of cardiac death and myocardial infarction. *Circulation* 1998; **97**: 535-543 [PMID: 9494023]

9 **van der Vaart MG**, Meerwaldt R, Slart RH, van Dam GM, Tio RA, Zeebregts CJ. Application of PET/SPECT imaging in vascular disease. *Eur J Vasc Endovasc Surg* 2008; **35**: 507-513 [PMID: 18180182 DOI: 10.1016/j.ejvs.2007.11.016]

10 **Husmann L**, Wiegand M, Valenta I, Gaemperli O, Schepis T, Siegrist PT, Namdar M, Wyss CA, Alkadhi H, Kaufmann PA. Diagnostic accuracy of myocardial perfusion imaging with single photon emission computed tomography and positron emission tomography: a comparison with coronary angiography. *Int J Cardiovasc Imaging* 2008; **24**: 511-518 [PMID: 18158612 DOI: 10.1007/s10554-007-9288-7]

11 **Bateman TM**, Heller GV, McGhie AI, Friedman JD, Case JA, Bryngelson JR, Hertenstein GK, Moutray KL, Reid K, Cullom SJ. Diagnostic accuracy of rest/stress ECG-gated Rb-82 myocardial perfusion PET: comparison with ECG-gated Tc-99m sestamibi SPECT. *J Nucl Cardiol* 2006; **13**: 24-33 [PMID: 16464714]

12 **Soulis JV**, Farmakis TM, Giannoglou GD, Louridas GE. Wall shear stress in normal left coronary artery tree. *J Biomech* 2006; **39**: 742-749 [PMID: 16439244 DOI: 10.1016/j.jbiomech.2004.12.026]

13 **Shanmugavelayudam SK**, Rubenstein DA, Yin W. Effect of geometrical assumptions on numerical modeling of coronary blood flow under normal and disease conditions. *J Biomech Eng* 2010; **132**: 061004 [PMID: 20887029 DOI: 10.1115/1.4001033]

14 **Katritsis DG**, Theodorakakos A, Pantos I, Andriotis A, Efstathopoulos EP, Siontis G, Karcanias N, Redwood S, Gavaises M. Vortex formation and recirculation zones in left anterior descending artery stenoses: computational fluid dynamics analysis. *Phys Med Biol* 2010; **55**: 1395-1411 [PMID: 20150685 DOI: 10.1088/0031-9155/55/5/009]

15 **Sun Z**, Choo GH, Ng KH. Coronary CT angiography: current status and continuing challenges. *Br J Radiol* 2012; **85**: 495-510 [PMID: 22253353 DOI: 10.1259/bjr/15296170]

16 **Mowatt G**, Cook JA, Hillis GS, Walker S, Fraser C, Jia X, Waugh N. 64-Slice computed tomography angiography in the diagnosis and assessment of coronary artery disease: systematic review and meta-analysis. *Heart* 2008; **94**: 1386-1393 [PMID: 18669550 DOI: 10.1136/hrt.2008.145292]

17 **Stein PD**, Yaekoub AY, Matta F, Sostman HD. 64-slice CT for diagnosis of coronary artery disease: a systematic review. *Am J Med* 2008; **121**: 715-725 [PMID: 18691486 DOI: 10.1016/j.amjmed.2008.02.039]

18 **Otero HJ**, Steigner ML, Rybicki FJ. The "post-64" era of coronary CT angiography: understanding new technology from physical principles. *Radiol Clin North Am* 2009; **47**: 79-90 [PMID: 19195535 DOI: 10.1016/j.rcl.2008.11.001]

19 **Hurlock GS**, Higashino H, Mochizuki T. History of cardiac computed tomography: single to 320-detector row multislice computed tomography. *Int J Cardiovasc Imaging* 2009; **25** Suppl 1: 31-42 [PMID: 19145476 DOI: 10.1007/s10554-008-9408-z]

20 **Abdulla J**, Asferg C, Kofoed KF. Prognostic value of absence or presence of coronary artery disease determined by 64-slice computed tomography coronary angiography a systematic review and meta-analysis. *Int J Cardiovasc Imaging* 2011; **27**: 413-420 [PMID: 20549366 DOI: 10.1007/s10554-010-9652-x]

21 **van Werkhoven JM**, Gaemperli O, Schuijf JD, Jukema JW, Kroft LJ, Leschka S, Alkadhi H, Valenta I, Pundziute G, de Roos A, van der Wall EE, Kaufmann PA, Bax JJ. Multislice computed tomography coronary angiography for risk stratification in patients with an intermediate pretest likelihood. *Heart* 2009; **95**: 1607-1611 [PMID: 19581272 DOI: 10.1136/hrt.2009.167353]

22 **Liu YC**, Sun Z, Tsay PK, Chan T, Hsieh IC, Chen CC, Wen MS, Wan YL. Significance of coronary calcification for prediction of coronary artery disease and cardiac events based on 64-slice coronary computed tomography angiography. *Biomed Res Int* 2013; **2013**: 472347 [PMID: 23586041 DOI: 10.1155/2013/472347]

23 **Silber S**, Albertsson P, Avilés FF, Camici PG, Colombo A, Hamm C, Jørgensen E, Marco J, Nordrehaug JE, Ruzyllo W, Urban P, Stone GW, Wijns W. Guidelines for percutaneous coronary interventions. The Task Force for Percutaneous Coronary Interventions of the European Society of Cardiology. *Eur Heart J* 2005; **26**: 804-847 [PMID: 15769784 DOI: 10.1093/eurheartj/ehi138]

24 **Smith SC**, Feldman TE, Hirshfeld JW, Jacobs AK, Kern MJ, King SB, Morrison DA, O'Neil WW, Schaff HV, Whitlow PL, Williams DO, Antman EM, Adams CD, Anderson JL, Faxon DP, Fuster V, Halperin JL, Hiratzka LF, Hunt SA, Nishimura R, Ornato JP, Page RL, Riegel B. ACC/AHA/SCAI 2005 guideline update for percutaneous coronary intervention: a report of the American College of Cardiology/American Heart Association Task Force on Practice Guidelines (ACC/AHA/SCAI Writing Committee to Update 2001 Guidelines for Percutaneous Coronary Intervention). *Circulation* 2006; **113**: e166-e286 [PMID: 16490830 DOI: 10.1161/CIRCULATIONAHA.106.173220]

25 **Jeetley P**, Burden L, Stoykova B, Senior R. Clinical and economic impact of stress echocardiography compared with exercise electrocardiography in patients with suspected acute coronary syndrome but negative troponin: a prospective randomized controlled study. *Eur Heart J* 2007; **28**: 204-211 [PMID: 17227784 DOI: 10.1093/eurheartj/ehl444]

26 **Shah BN**, Balaji G, Alhajiri A, Ramzy IS, Ahmadvazir S, Senior R. Incremental diagnostic and prognostic value of contemporary stress echocardiography in a chest pain unit: mortality and morbidity outcomes from a real-world setting. *Circ Cardiovasc Imaging* 2013; **6**: 202-209 [PMID: 23258477 DOI: 10.1161/CIRCIMAGING.112.980797]

27 **Cheng W**, Zeng M, Arellano C, Mafori W, Goldin J, Krishnam M, Ruehm SG. Detection of myocardial perfusion abnormalities: standard dual-source coronary computed tomography angiography versus rest/stress technetium-99m single-photo emission CT. *Br J Radiol* 2010; **83**: 652-660 [PMID: 20413446 DOI: 10.1259/bjr/82257160]

28 **Schwarz F**, Ruzsics B, Schoepf UJ, Bastarrika G, Chiaramida SA, Abro JA, Brothers RL, Vogt S, Schmidt B, Costello P, Zwerner PL. Dual-energy CT of the heart--principles and protocols. *Eur J Radiol* 2008; **68**: 423-433 [PMID: 19008064 DOI: 10.1016/j.ejrad.2008.09.010]

29 **Ruzsics B**, Schwarz F, Schoepf UJ, Lee YS, Bastarrika G, Chiaramida SA, Costello P, Zwerner PL. Comparison of dual-energy computed tomography of the heart with single photon emission computed tomography for assessment of coronary artery stenosis and of the myocardial blood supply. *Am J Cardiol* 2009; **104**: 318-326 [PMID: 19616661 DOI: 10.1016/j.amjcard.2009.03.051]

30 **Nagao M**, Kido T, Watanabe K, Saeki H, Okayama H, Kurata A, Hosokawa K, Higashino H, Mochizuki T. Functional assessment of coronary artery flow using adenosine stress dual-energy CT: a preliminary study. *Int J Cardiovasc Imaging* 2011; **27**: 471-481 [PMID: 20686853 DOI: 10.1007/s10554-010-9676-2]

31 **Kitagawa T**, Yamamoto H, Horiguchi J, Ohhashi N, Tadehara F, Shokawa T, Dohi Y, Kunita E, Utsunomiya H, Kohno N, Kihara Y. Characterization of noncalcified coronary plaques and identification of culprit lesions in patients with acute coronary syndrome by 64-slice computed tomography. *JACC Cardiovasc Imaging* 2009; **2**: 153-160 [PMID: 19356549 DOI: 10.1016/j.jcmg.2008.09.015]

32 **Takumi T**, Lee S, Hamasaki S, Toyonaga K, Kanda D, Kusumoto K, Toda H, Takenaka T, Miyata M, Anan R, Otsuji Y, Tei C. Limitation of angiography to identify the culprit plaque in acute myocardial infarction with coronary total occlusion utility of coronary plaque temperature measurement to identify the culprit plaque. *J Am Coll Cardiol* 2007; **50**: 2197-2203 [PMID: 18061065]

33 **Lee BK**. Computational fluid dynamics in cardiovascular disease. *Korean Circ J* 2011; **41**: 423-430 [PMID: 21949524 DOI: 10.4070/kcj.2011.41.8.423]

34 **Tu J**, Yeoh GH, Liu C. Computational Fluid dynamics. A Practical Approach. 1st ed. Oxford: Elesevier, 2008: 1-27

35 **Caro CG**, Fitz-Gerald JM, Schroter RC. **Arterial wall shear** and distribution of early atheroma in man. *Nature* 1969; **223**: 1159-1160 [PMID: 5810692]

36 **Malek AM**, Alper SL, Izumo S. Hemodynamic shear stress and its role in atherosclerosis. *JAMA* 1999; **282**: 2035-2042 [PMID: 10591386 DOI: 10.1001/jama.282.21.2035]

37 **Perktold K**, Resch M, Peter RO. **Three-dimensional numerical** analysis of pulsatile flow and wall shear stress in the carotid artery bifurcation. *J Biomech* 1991; **24**: 409-420 [PMID: 1856241]

38 **Lei M**, Archie JP, Kleinstreuer C. Computational design of a bypass graft that minimizes wall shear stress gradients in the region of the distal anastomosis. *J Vasc Surg* 1997; **25**: 637-646 [PMID: 9129618]

39 **Perktold K**, Rappitsch G. Computer simulation of local blood flow and vessel mechanics in a compliant carotid artery bifurcation model. *J Biomech* 1995; **28**: 845-856 [PMID: 7657682]

40 **Steinman DA**, Ethier CR. The effect of wall distensibility on flow in a two-dimensional end-to-side anastomosis. *J Biomech Eng* 1994; **116**: 294-301 [PMID: 7799630]

41 **Knight J**, Olgac U, Saur SC, Poulikakos D, Marshall W, Cattin PC, Alkadhi H, Kurtcuoglu V. Choosing the optimal wall shear parameter for the prediction of plaque location-A patient-specific computational study in human right coronary arteries. *Atherosclerosis* 2010; **211**: 445-450 [PMID: 20466375 DOI: 10.1016/j.atherosclerosis.2010.03.001]

42 **Wellnhofer E**, Osman J, Kertzscher U, Affeld K, Fleck E, Goubergrits L. Flow simulation studies in coronary arteries--impact of side-branches. *Atherosclerosis* 2010; **213**: 475-481 [PMID: 20934704 DOI: 10.1016/j.atherosclerosis.2010.09.007]

43 **Chaichana T**, Sun Z, Jewkes J. Impact of plaques in the left coronary artery on wall shear stress and pressure gradient in coronary side branches. *Comput Methods Biomech Biomed Engin* 2014; **17**: 108-118 [PMID: 22443493 DOI: 10.1080/10255842.2012.671308]

44 **Rikhtegar F**, Knight JA, Olgac U, Saur SC, Poulikakos D, Marshall W, Cattin PC, Alkadhi H, Kurtcuoglu V. Choosing the optimal wall shear parameter for the prediction of plaque location-A patient-specific computational study in human left coronary arteries. *Atherosclerosis* 2012; **221**: 432-437 [PMID: 22317967 DOI: 10.1016/j.atherosclerosis.2012.01.018]

45 **Wong K**, Mazumdar J, Pincombe B, Worthley SG, Sanders P, Abbott D. Theoretical modeling of micro-scale biological phenomena in human coronary arteries. *Med Biol Eng Comput* 2006; **44**: 971-982 [PMID: 17048027 DOI: 10.1007/s11517-006-0113-6]

46 **Katritsis D**, Kaiktsis L, Chaniotis A, Pantos J, Efstathopoulos EP, Marmarelis V. Wall shear stress: theoretical considerations and methods of measurement. *Prog Cardiovasc Dis* 2007; **49**: 307-329 [PMID: 17329179 DOI: 10.1016/j.pcad.2006.11.001]

47 **Rodriguez-Granillo GA**, García-García HM, Wentzel J, Valgimigli M, Tsuchida K, van der Giessen W, de Jaegere P, Regar E, de Feyter PJ, Serruys PW. Plaque composition and its relationship with acknowledged shear stress patterns in coronary arteries. *J Am Coll Cardiol* 2006; **47**: 884-885 [PMID: 16487861 DOI: 10.1016/j.jacc.2005.11.027]

48 **Chaichana T**, Sun Z, Jewkes J. Computation of hemodynamics in the left coronary artery with variable angulations. *J Biomech* 2011; **44**: 1869-1878 [PMID: 21550611 DOI: 10.1016/j.jbiomech.2011.04.033]

49 **Sun Z**, Cao Y. Multislice CT angiography assessment of left coronary artery: correlation between bifurcation angle and dimensions and development of coronary artery disease. *Eur J Radiol* 2011; **79**: e90-e95 [PMID: 21543178 DOI: 10.1016/j.ejrad.2011.04.015]

50 **Fuster V**. Lewis A. Conner Memorial Lecture. Mechanisms leading to myocardial infarction: insights from studies of vascular biology. *Circulation* 1994; **90**: 2126-2146 [PMID: 7718033]

51 **Gziut AI**. [Comparative analysis of atherosclerotic plaque distribution in the left main coronary artery and proximal segments of left anterior descending and left circumflex arteries in patients qualified for percutaneous coronary angioplasty]. *Ann Acad Med Stetin* 2006; **52**: 51-62; discussion 62-63 [PMID: 17633397]

52 **Han SH**, Puma J, García-García HM, Nasu K, Margolis P, Leon MB, Lerman A. Tissue characterisation of atherosclerotic plaque in coronary artery bifurcations: an intravascular ultrasound radiofrequency data analysis in humans. *EuroIntervention* 2010; **6**: 313-320 [PMID: 20884408 DOI: 10.4244/EIJV6I3A53]

53 **Gijsen FJ**, Wentzel JJ, Thury A, Lamers B, Schuurbiers JC, Serruys PW, van der Steen AF. A new imaging technique to study 3-D plaque and shear stress distribution in human coronary artery bifurcations in vivo. *J Biomech* 2007; **40**: 2349-2357 [PMID: 17335832 DOI: 10.1016/j.jbiomech.2006.12.007]

54 **Grayburn PA**, Willard JE, Haagen DR, Brickner ME, Alvarez LG, Eichhorn EJ. Measurement of coronary flow using high-frequency intravascular ultrasound imaging and pulsed Doppler velocimetry: in vitro feasibility studies. *J Am Soc Echocardiogr* 1992; **5**: 5-12 [PMID: 1531416]

55 **Rodriguez-Granillo GA**, Rosales MA, Degrossi E, Durbano I, Rodriguez AE. Multislice CT coronary angiography for the detection of burden, morphology and distribution of atherosclerotic plaques in the left main bifurcation. *Int J Cardiovasc Imaging* 2007; **23**: 389-392 [PMID: 17028928 DOI: 10.1007/s10554-006-9144-1]

56 **Chaichana T**, Sun Z, Jewkes J. Hemodynamic impacts of various types of stenosis in the left coronary artery bifurcation: a patient-specific analysis. *Phys Med* 2013; **29**: 447-452 [PMID: 23453845 DOI: 10.1016/j.ejmp.2013.02.001]

57 **Pijls NH**, De Bruyne B, Peels K, Van Der Voort PH, Bonnier HJ, Bartunek J Koolen JJ, Koolen JJ. Measurement of fractional flow reserve to assess the functional severity of coronary-artery stenoses. *N Engl J Med* 1996; **334**: 1703-1708 [PMID: 8637515]

58 **Watkins S**, McGeoch R, Lyne J, Steedman T, Good R, McLaughlin MJ, Cunningham T, Bezlyak V, Ford I, Dargie HJ, Oldroyd KG. Validation of magnetic resonance myocardial perfusion imaging with fractional flow reserve for the detection of significant coronary heart disease. *Circulation* 2009; **120**: 2207-2213 [PMID: 19917885 DOI: 10.1161/CIRCULATIONAHA.109.872358]

59 **Berger A**, Botman KJ, MacCarthy PA, Wijns W, Bartunek J, Heyndrickx GR, Pijls NH, De Bruyne B. Long-term clinical outcome after fractional flow reserve-guided percutaneous coronary intervention in patients with multivessel disease. *J Am Coll Cardiol* 2005; **46**: 438-442 [PMID: 16053955 DOI: 10.1016/j.jacc.2005.04.041]

60 **Kristensen TS**, Engstrøm T, Kelbæk H, von der Recke P, Nielsen MB, Kofoed KF. Correlation between coronary computed tomographic angiography and fractional flow reserve. *Int J Cardiol* 2010; **144**: 200-205 [PMID: 19427706 DOI: 10.1016/j.ijcard.2009.04.024]

61 **Min JK**, Leipsic J, Pencina MJ, Berman DS, Koo BK, van Mieghem C, Erglis A, Lin FY, Dunning AM, Apruzzese P, Budoff MJ, Cole JH, Jaffer FA, Leon MB, Malpeso J, Mancini GB, Park SJ, Schwartz RS, Shaw LJ, Mauri L. Diagnostic accuracy of fractional flow reserve from anatomic CT angiography. *JAMA* 2012; **308**: 1237-1245 [PMID: 22922562 DOI: 10.1001/2012.jama.11274]

62 **Koo BK**, Erglis A, Doh JH, Daniels DV, Jegere S, Kim HS, Dunning A, DeFrance T, Lansky A, Leipsic J, Min JK. Diagnosis of ischemia-causing coronary stenoses by noninvasive fractional flow reserve computed from coronary computed tomographic angiograms. Results from the prospective multicenter DISCOVER-FLOW (Diagnosis of Ischemia-Causing Stenoses Obtained Via Noninvasive Fractional Flow Reserve) study. *J Am Coll Cardiol* 2011; **58**: 1989-1997 [PMID: 22032711 DOI: 10.1016/j.jacc.2011.06.066]

63 **Yoon YE**, Choi JH, Kim JH, Park KW, Doh JH, Kim YJ, Koo BK, Min JK, Erglis A, Gwon HC, Choe YH, Choi DJ, Kim HS, Oh BH, Park YB. Noninvasive diagnosis of ischemia-causing coronary stenosis using CT angiography: diagnostic value of transluminal attenuation gradient and fractional flow reserve computed from coronary CT angiography compared to invasively measured fractional flow reserve. *JACC Cardiovasc Imaging* 2012; **5**: 1088-1096 [PMID: 23153908 DOI: 10.1016/j.jcmg.2012.09.002]

64 **Grunau GL**, Min JK, Leipsic J. Modeling of fractional flow reserve based on coronary CT angiography. *Curr Cardiol Rep* 2013; **15**: 336 [PMID: 23264169 DOI: 10.1007/s11886-012-0336-0]

65 **Min JK**, Berman DS, Budoff MJ, Jaffer FA, Leipsic J, Leon MB, Mancini GB, Mauri L, Schwartz RS, Shaw LJ. Rationale and design of the DeFACTO (Determination of Fractional Flow Reserve by Anatomic Computed Tomographic AngiOgraphy) study. *J Cardiovasc Comput Tomogr* 2011; **5**: 301-309 [PMID: 21930103 DOI: 10.1016/j.jcct.2011.08.003]

66 **Lee BK**, Kwon HM, Hong BK, Park BE, Suh SH, Cho MT, Lee CS, Kim MC, Kim CJ, Yoo SS, Kim HS. Hemodynamic effects on atherosclerosis-prone coronary artery: wall shear stress/rate distribution and impedance phase angle in coronary and aortic circulation. *Yonsei Med J* 2001; **42**: 375-383 [PMID: 11519078]

67 **Friedman MH**, Deters OJ, Mark FF, Bargeron CB, Hutchins GM. Arterial geometry affects hemodynamics. A potential risk factor for athersoclerosis. *Atherosclerosis* 1983; **46**: 225-231 [PMID: 6838702]

68 **Felsenthal G**, Butler DH, Shear MS. Across-tarsal-tunnel motor-nerve conduction technique. *Arch Phys Med Rehabil* 1992; **73**: 64-69 [PMID: 1729977]

69 **Lee BK**, Kwon HM, Kim D, Yoon YW, Seo JK, Kim IJ, Roh HW, Suh SH, Yoo SS, Kim HS. Computed numerical analysis of the biomechanical effects on coronary atherogenesis using human hemodynamic and dimensional variables. *Yonsei Med J* 1998; **39**: 166-174 [PMID: 9587258]

70 **Pijls NH**, van Schaardenburgh P, Manoharan G, Boersma E, Bech JW, van't Veer M, Bär F, Hoorntje J, Koolen J, Wijns W, de Bruyne B. Percutaneous coronary intervention of functionally nonsignificant stenosis: 5-year follow-up of the DEFER Study. *J Am Coll Cardiol* 2007; **49**: 2105-2111 [PMID: 17531660 DOI: 10.1016/j.jacc.2007.01.087]

P- Reviewers: Peteiro J, Rodriguez-Granillo GA, Ueda H
S- Editor: Zhai HH **L- Editor**: A **E- Editor**: Liu XM

World Journal of Cardiology

Online Submissions: http://www.wjgnet.com/esps/
bpgoffice@wjgnet.com
doi:10.4330/wjc.v5.i12.453

World J Cardiol 2013 December 26; 5(12): 453-458
ISSN 1949-8462 (online)

TOPIC HIGHLIGHT

Zhonghua Sun, Associate Professor, *Series Editor*

Beta-blocker administration protocol for prospectively ECG-triggered coronary CT angiography

Akmal Sabarudin, Zhonghua Sun

Akmal Sabarudin, Diagnostic Imaging and Radiotherapy Program, School of Diagnostic and Applied Health Sciences, Faculty of Health Sciences, University Kebangsaan Malaysia, Kuala Lumpur 50300, Malaysia
Zhonghua Sun, Discipline of Medical Imaging, Department of Imaging and Applied Physics, Curtin University, Perth 6845, Western Australia, Australia
Author contributions: Sabarudin A prepared and reconstructed the manuscript; Sun Z editted the manuscript.
Correspondence to: Zhonghua Sun, Associate Professor, Discipline of Medical Imaging, Department of Imaging and Applied Physics, Curtin University, GPO Box, U1987, Perth 6845, Western Australia, Australia. z.sun@curtin.edu.au
Telephone: +61-8-92667509 Fax: +61-8-92662377
Received: July 3, 2013 Revised: September 13, 2013
Accepted: October 16, 2013
Published online: December 26, 2013

Core tip: This article provides the protocol of beta-blocker as guidance for prospective ECG-triggered coronary computed tomography angiography (CCTA). With the use of beta-blocker, patients' heart rate can be regulated and controlled to suit the protocol of prospective ECG-triggering CCTA. We believe that this article can give an insight on the management of beta-blocker administration in the coronary computed tomography protocol.

Sabarudin A, Sun Z. Beta-blocker administration protocol for prospectively ECG-triggered coronary CT angiography. *World J Cardiol* 2013; 5(12): 453-458 Available from: URL: http://www.wjgnet.com/1949-8462/full/v5/i12/453.htm DOI: http://dx.doi.org/10.4330/wjc.v5.i12.453

Abstract

The aim of this article is to discuss the protocol of beta-blockers that is commonly used for prospectively ECG-triggered coronary computed tomography angiography (CCTA). It is essential to ensure a low and regular heart rate in patients undergoing prospectively ECG-triggered CCTA for optimal visualization of coronary arteries. Although early generations of computed tomography-scanners are not applicable to be tailored according to patients' heart rate, a low and regular heart rate is possible to be achieved by the administration of medications according to the beta-blocker protocol. Beta-blocker can be safely administered to reduce patients' heart rate for CCTA examination if patients are screened for certain contraindications.

Key words: Beta-blockers; Coronary computed tomography angiography; Heart rate; Prospective ECG-triggering

INTRODUCTION

Prospectively ECG-triggered coronary computed tomography angiography (CCTA) is increasingly used in the diagnosis of coronary artery disease (CAD) due to its very low radiation dose with acceptable image quality[1-3]. This technique not only provides comparable diagnostic accuracy to that of conventional approach, retrospectively ECG-gated CCTA, but also shows superior advantage in reducing radiation dose (up to 83%), which is significantly lower than that from retrospectively ECG-gated protocol[1-4]. However, in order to ensure that image quality is acceptable for clinical diagnosis, prospectively ECG-triggered CCTA is restricted to patients with low (heart rates less than 65 bpm) and regular (HR variability < ± 5 bpm) during the scan[1,2,5].

With the advancements of computed tomography (CT) technology, the latest generation of multislice CT scanners enables customization of the scanning protocol to tailor individual patient's condition such as using multiple heartbeat scanning modes or application of additional padding windows[5,6]. Thus, the prospectively ECG-triggered CCTA

Table 1 Beta-blocking agents

B-blockers	Selectivity	Partial agonist activity	Lipid solubility	Onset		Hemodynamic effect		Plasma half-life	Elimination's route
Generic name				Oral	Ⅳ	Oral	Ⅳ		
Acebutolol hydrochloride	β_1	Yes	Low	1-2 h	No	> 24 h	No	3-4 h	Hepatic, renal
Atenolol	β_1	No	Low	1 h	1-2 min	24 h	12 h	6-9 h	Renal
Betaxolol hydrochloride	β_1	No	Low	24 h	No	> 24 h	No	12-22 h	Hepatic, renal
Bisoprolol	β_1	No	Low	1-4 h	No	24 h	No	7-15 h	Hepatic, renal
Esmolol	β_1	No	Low	No	1-4 min	No	5-10 min	4-9 min	Erythrocyte, renal
Metoprolol tartrate	β_1	No	Moderate	1 h	5-10 min	5-8 h		3-7 h	Hepatic
Metoprolol succinate	β_1	No	Moderate	2-3 h	No	24 h	No	3-7 h	Hepatic
Nadolol	None	No	Low	1-2 h	No	24 h	No	20-24 h	Renal
Pindolol	None	Yes	Moderate	1-2 h	No	24 h	No	3-4 h	Hepatic, renal
Propranolol hydrochloride	None	No	High	30 min	< 1 min	6-12 h	4-6 h	3.5-6 h	Hepatic

could be extended to more patients with variable heart rates. However, these protocols suffer from radiation dose which limits the widespread use of the prospectively ECG-triggering technique in cardiac imaging. Therefore, the use of beta-blockers is an option which is widely used in CCTA studies to reduce the heart rate to less than 65-70 bpm and to make the cardiac rhythm more regular[7].

All of the beta-blockers used in clinical practice are competitive pharmacologic antagonists. Drugs in beta-blocker group can be classified into subgroups on the basis of β1 selectivity, partial agonist activity, local anesthetic action and lipid solubility (Table 1)[7,8]. Most of the organ-level effects of beta-blockers are predictable blockade of the beta-receptor-mediated effects of sympathetic discharge. The clinical applications of beta-blockade are broad ranging from treating glaucoma to cardiovascular disease[8].

The applications of beta-blockers in cardiovascular disease treatment are of paramount importance, especially in the situations such as hypertension, angina and arrhythmias[8]. However, adverse cardiovascular effects such as bradycardia, atrioventricular blockade and heart failure may occur due to beta-blockade toxicity. Patient with airway disease may suffer severe asthma attacks. In addition, adverse effects of central nervous system include sedation, fatigue and sleep alterations might only occur with use of lipid soluble beta-blockers. Sexual dysfunction has been reported in some patients using the beta blockers[8,9].

It has been shown in clinical studies that Beta-blocking agents have a preferential effect on β_1 adrenoreceptors, mainly located in the cardiac muscle[8,10,11]. Beta-blockers lessen cardiac contractility and heart rates by blocking myocardial beta-receptors, and therefore prevent exercise-induced increase in oxygen demands by the heart[9]. Clinical pharmacology studies have confirmed that beta-blocking activity had enormous effect on the reduction in heart rate and cardiac output at rest and upon exercise, reduction of systolic blood pressure upon exercise, reduction of reflex orthostatic tachycardia and inhibition of isoproterenol-induced tachycardia[8,10,11]. Therefore, beta-blockers are recommended to be administered prior to CCTA scanning. The purpose of this article is to provide an overview of the use of beta-blockers administration protocol for prospectively ECG-triggered CCTA.

PATIENT PREPARATION

There are several common indications for prospectively ECG-triggered CCTA inclusive of the CAD indications and non-CAD indications. CAD indications are inclusive of evaluation of coronary arteries in patients with new-onset heart failure to assess etiology, symptomatic patients at intermediate preset probability of CAD, patients with a chest pain syndrome regardless of acute or chronic with interpretable stress test. In certain circumstances, CCTA is required although non-CAD detection indications are presented such as suspected pulmonary embolism or aortic dissection or aneurysm, assessment of complex congenital heart disease, suspected coronary anomalies in symptomatic patients, evaluation of pulmonary vein anatomy prior to atrial fibrillation radiofrequency ablation, evaluation of cardiac venous anatomy prior to biventricular pacing and evaluation of cardiac mass or pericardial condition when non-radiation imaging modalities are limited[12,13].

However, there are some contraindications to CCTA procedure which include pregnancy, severe anaphylactic contrast reaction, unable to comply with the scanning instructions such as fail to hold long breath-hold, renal insufficiency and clinically unstable patients[12,13]. In addition, identification to contraindicated drug must be clarified before undergoing CCTA procedure inclusive of the pre-scan nitroglycerine such as severe aortic stenosis, hypertrophic cardiomyopathy and phosphodiesterase-5 (PDE-5) inhibitor and beta-blockers[8,12]. For patients who are considered to undergo beta-blocker protocol, some guidelines have been suggested to avoid complications including screening contraindications to beta-blockers[7]. The contraindications include sinus bradycardia, which is defined as a heart rate of < 60 bpm with systolic pressure of less than 100 mmHg; allergic to beta-adrenergic antagonists or its constituents; decompensated cardiac failure; asthma on beta-agonist inhalers; active bronchospasm; second or third-degree of atrioventricular (AV) block[14-16]. Patients who are likely to have second- or third-degree AV block can be evaluated by generating a single-lead ECG strip[7].

Patient's vital signs and pulse are also monitored and documented upon arrival. In patients with a sinus rhythm with heart rate < 65 bpm, no beta-blockers are required and therefore, the patient can be prepared for CCTA ex-

amination. In patients with irregular rhythm or/and higher heart rate (> 65 bpm), the beta-blockers are given according to the protocol setting (Figure 1).

In addition, patients are required to follow all standard instructions for contrast-enhanced studies including fasting for at least 4 h prior to the scan, maintaining oral hydration with clear fluid up to 1 h before scan and need to hold metformin for a minimum of 48 h following the scan. Patients with non-severe anaphylactic contrast reaction in the past should receive pre-medication treatment to avoid the risk of current contrast reaction. A pre-medication protocol suggested as 50 mg of prednisone is administered orally 13, 7 and 1 h prior to scan with additional of 50 mg oral diphenhydramine (*Benadryl*) is taken 1 h prior to scan[12,17].

With regards to optimal heart rate control, caffeine product is not permitted within 12 h of CCTA. Moreover, severe hypotension can occur if PDE-5 inhibitors interact with nitrates. Therefore, patients are refrained from undertaking PDE-5 inhibitor drugs such as sildenafil (*Viagra*), vardenafil (*Levitra*) and tadalafil (*Cialis*) for at least 48 h before CCTA[12,18,19]. However, usual cardiovascular medications are advisable to be taken continuously.

ADMINISTRATION OF BETA-BLOCKERS AND OTHER ALTERNATIVE DRUG IN HEART RATE-LOWERING THERAPY

Several cardio selective beta-blockers are available with distinct pharmacokinetic profiles such as acebutolol hydrochloride, atenolol, betaxolol hydrochloride, bisoprolol, esmolol, metoprolol succinate and metoprolol tartrate. However, metoprolol tartrate (*Lopressor*) was selected due to its convenient method of administration, dosage form availability and cardioselectivity[7]. Unlike oral metoprolol tartrate, intravenous metoprolol dosage form is recommended due to its fast onset reaction (between 5 and 10 min) after administration. On the other hand, metoprolol tablets (oral) effect can only be seen within 1 hour after administration and the peak plasma concentrations are seen at 90 min. Although the onset reaction in both oral and IV routes differ significantly, the plasma half-life for metoprolol tartrate is similar in both oral and IV which ranges from 3 to 4 h in a healthy adult[7,15,16].

Oral pre-medication in heart rate-lowering therapy is another alternative to achieve lower heart rate prior to the CT scanning. Pre-medicating the patient with tablet metoprolol gives an advantage which may reduce the risk of being injected with IV of metoprolol. However, without proper scanning arrangement, the effect of the oral metoprolol might not be effective and other factors such as anxiety and nervousness may also increase the patients' heart rate on the day of the examination. Thus, administration of metoprolol intravenously is most commonly performed prior to the CT scanning due to its fast onset and clinically feasibility.

Most previous practices injected their first bolus of metoprolol once the patient is lying down supine on the CT examination table. Our practice suggests that first bolus administration of metoprolol (2.5 mg) is given before the patient is brought on the CT examination table; right after the IV line is set (pre-procedure). Then, the patient's heart rate is monitored at the designated area under supervision of medically authorized personnel. This aims to avoid interruption of the procedure workflow and the delay time for beta-blockers to respond.

Although beta-blockers helped in lowering the heart rate, they also have negative inotropic effect and could decrease left ventricular contractility which may affect the assessment of ventricular function[7]. However, ventricular function is only being evaluated by echocardiography or nuclear medicine studies and CCTA study is mainly performed for assessment of coronary arteries and degree of stenosis. Initially, two 2.5 mg doses of metoprolol are given with 5 min interval. Then two doses of 5 mg each are given 5 min apart with a total maximum dose of no more than 15 mg. Blood pressure and HR are monitored before each of the IV dose as stated in Figure 1. The beta-blockers' administration is conducted under the supervision of the radiologists or cardiologists. Blood pressure and continuous ECG monitoring should always be used when giving IV metoprolol.

Ivabradine is another attractive option to reduce patient heart rate for CCTA procedure[20]. Unlike metoprolol, ivabradine selectively inhibits if current in sinoatrial node cells that controls the spontaneous diastolic depolarization, resulting in the reduction of diastolic depolarization rate and heart rate[21,22]. Therefore, it is useful in patients in sinus rhythm, but not in other rhythms such as atrial fibrillation. Ivabradine lowers heart rate at concentrations that do not affect other cardiac ionic currents. Therefore, ivabradine has no other direct cardiovascular effect[20]. Therefore, the main pharmacodynamics of ivabradine in humans is a specific dose-dependent reduction in heart rate. Heart rate reduction is achieved approximately 10 beats/min (bpm) at rest and during exercise at the recommended dosage (no more than 10 mg/d) which leads to a reduction in cardiac workload and myocardial oxygen consumption[21]. Ivabradine has a relatively short half-life of around 2 h and is currently only available as an oral preparation.

HEART RATE CONTROL-LESS COMMONLY APPLIED IN 64- AND POST-64 CT

Heart rate control with use of medications is necessary in 4- and 16-slice CT, but less common in 64- and post-64 slice coronary CT angiography due to improvement in temporal resolution. Pache *et al*[23] in their early study showed that 64-slice CT has high diagnostic accuracy in the assessment of coronary artery bypass grafts, despite the presence of irregular or high heart rates. Recent tech-

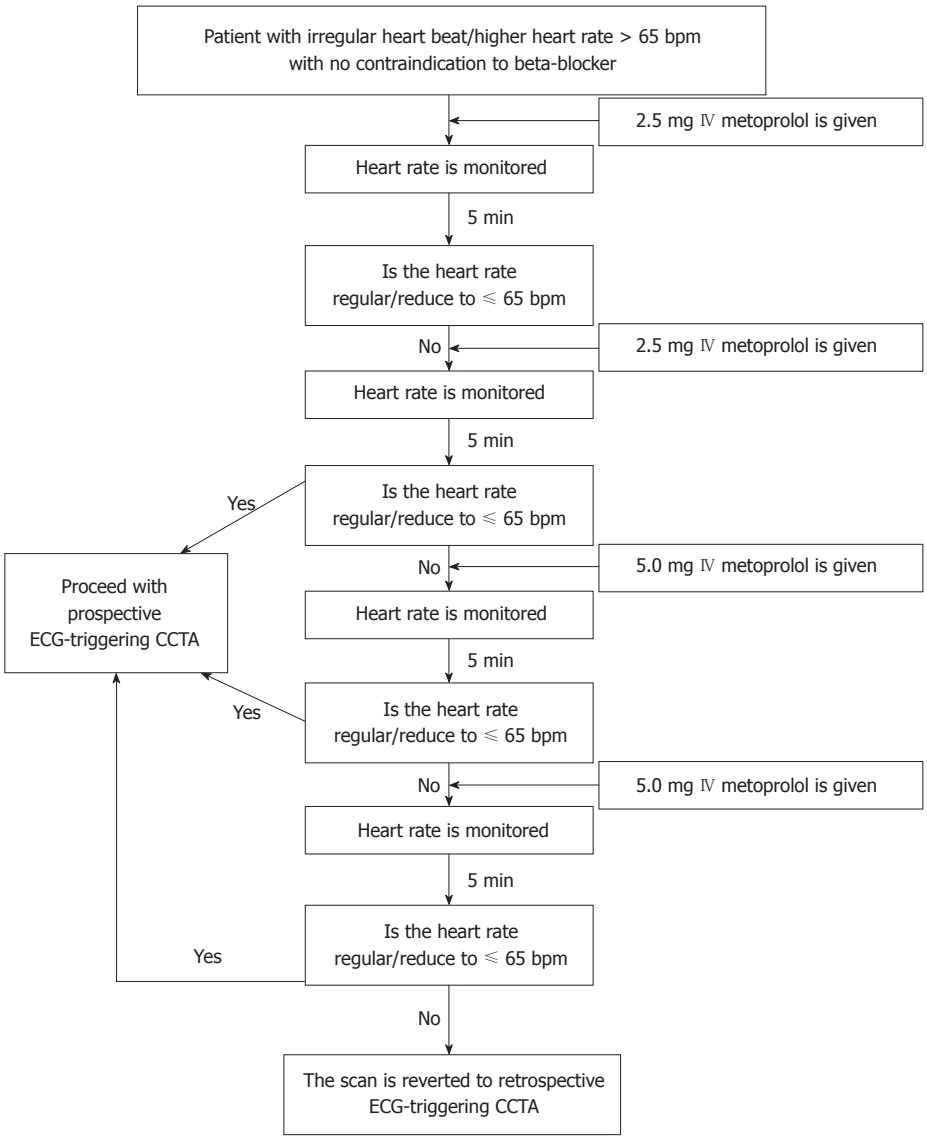

Figure 1 Flow chart showing the intravenous administration of metoprolol protocol in heart rate-lowering therapy. CCTA: Coronary computed tomography angiography.

nological developments with the introduction of dual-source CT and 320-slice CT have overcome the limitation of early generation of multislice CT as the temporal resolution was significantly increased, thus image quality and diagnostic value of coronary CT angiography was less dependent on heart rates[24,25]. It has been reported that dual-source coronary CT angiography shows improved diagnostic performance in patients with a wide range of different heart rates being included[26,27]. Expansion of multislice CT systems from a prototype 256-slice to a 320-slice system has allowed for acquisition of whole heart coverage in one gantry rotation. Studies have shown that 320-slice coronary CT angiography demonstrated high sensitivity and specificity at per-patient, per-vessel and per-segment analysis in patients with atrial fibrillation[28-30]. These results indicate that 320-slice CT has the potential to broaden the use of coronary CT angiography to more patients with high or irregular heart rates or those without responding well to the heart rate control.

POST-PROCEDURE CARE

All patients who are given Ⅳ metoprolol are observed for about 30 min once the scan is completed. If the patient presents with bronchospasm, an albuterol inhaler is given accordingly[7,31]. If the patient's heart rate drops to less than 45 bpm, administration of atropine is considered. However, if the patient is resistant to the atropine while the heart rate drops continuously, resuscitative measures and Ⅳ administration of beta-agonists need to be administered such as dopamine or epinephrine[7].

In general, beta-blockers are helpful in patients with irregular heart rate, either with premature atrial or ventricular contractions, supraventricular tachycardia and arrhythmias such as arterial fibrillation. With atrial fibrillation, the negative chronotropic and dromotropic effects of the beta-blockers lengthen the diastolic portion of the

cardiac cycle[7,8]. In prospectively ECG-triggered CCTA, X-ray exposure occurs during a small portion of the cardiac cycle typically centered at mid-diastole at 75% of R-R interval[1,6]. Therefore, increasing diastole by beta-blockers would improve CCTA image quality. Previous studies showed that the vessel visibility was achieved with the single-segment reconstruction in patients with low heart rates (< 65 bpm) and with multisegment reconstructions in patients with high heart rates (> 65 bpm)[32,33]. Moreover, the visibility of right coronary artery also has been shown to improve significantly with the administration of beta-blockers. The proportion of the cardiac cycle spent in diastole increases as the heart rate decreases. Therefore, use of beta-blockers is suggested to increase the diastolic phase in the cardiac cycle[34].

In conclusion, beta-blockers administration protocol has been discussed in this article with regard to is usefulness in preparing patient's heart rate for prospectively ECG-triggered CCTA. Since use of medication is essential to ensure that coronary CT angiography will provide excellent diagnostic images with few artifacts, understanding the mechanism of beta-blockers in cardiac imaging will contribute to the efficient use of coronary CT angiography technique in clinical diagnosis.

REFERENCES

1 **Earls JP**. How to use a prospective gated technique for cardiac CT. *J Cardiovasc Comput Tomogr* 2009; **3**: 45-51 [PMID: 19201376 DOI: 10.1016/j.jcct.2008.10.013]

2 **Sabarudin A**, Sun Z, Yusof AK. **Coronary CT angiography** with single-source and dual-source CT: comparison of image quality and radiation dose between prospective ECG-triggered and retrospective ECG-gated protocols. *Int J Cardiol* 2013; **168**: 746-753 [PMID: 23098849 DOI: 10.1016/j.ijcard.2012.09.217]

3 **Sun Z**, Lin C, Davidson R, Dong C, Liao Y. Diagnostic value of 64-slice CT angiography in coronary artery disease: a systematic review. *Eur J Radiol* 2008; **67**: 78-84 [PMID: 17766073 DOI: 10.1016/j.ejrad.2007.07.014]

4 **Budoff MJ**, Achenbach S, Blumenthal RS, Carr JJ, Goldin JG, Greenland P, Guerci AD, Lima JA, Rader DJ, Rubin GD, Shaw LJ, Wiegers SE. Assessment of coronary artery disease by cardiac computed tomography: a scientific statement from the American Heart Association Committee on Cardiovascular Imaging and Intervention, Council on Cardiovascular Radiology and Intervention, and Committee on Cardiac Imaging, Council on Clinical Cardiology. *Circulation* 2006; **114**: 1761-1791 [PMID: 17015792 DOI: 10.1161/CIRCULATIONAHA.106.178458]

5 **Hoe J**, Toh KH. First experience with 320-row multidetector CT coronary angiography scanning with prospective electrocardiogram gating to reduce radiation dose. *J Cardiovasc Comput Tomogr* 2009; **3**: 257-261 [PMID: 19577215 DOI: 10.1016/j.jcct.2009.05.013]

6 **Efstathopoulos EP**, Kelekis NL, Pantos I, Brountzos E, Argentos S, Grebác J, Ziaka D, Katritsis DG, Seimenis I. Reduction of the estimated radiation dose and associated patient risk with prospective ECG-gated 256-slice CT coronary angiography. *Phys Med Biol* 2009; **54**: 5209-5222 [PMID: 19671974 DOI: 10.1088/0031-9155/54/17/009]

7 **Pannu HK**, Alvarez W, Fishman EK. Beta-blockers for cardiac CT: a primer for the radiologist. *AJR Am J Roentgenol* 2006; **186**: S341-S345 [PMID: 16714607 DOI: 10.2214/AJR.04.1944]

8 **Trevor AJ**, Katzung BG, Masters SB. **Katzung & Trevor's pharmacology**: examination & board review. 10th ed. New York: McGraw-Hill, 2005: 244-251

9 **Choe JY**. Drug actions and interactions. New York: McGraw-Hill Medical, 2011

10 **Pérez-Schindler J**, Philp A, Baar K, Hernández-Cascales J. Regulation of contractility and metabolic signaling by the β2-adrenergic receptor in rat ventricular muscle. *Life Sci* 2011; **88**: 892-897 [PMID: 21466811 DOI: 10.1016/j.lfs.2011.03.020]

11 **Wachter SB**, Gilbert EM. Beta-adrenergic receptors, from their discovery and characterization through their manipulation to beneficial clinical application. *Cardiology* 2012; **122**: 104-112 [PMID: 22759389 DOI: 10.1159/000339271]

12 **Taylor CM**, Blum A, Abbara S. Patient preparation and scanning techniques. *Radiol Clin North Am* 2010; **48**: 675-686 [PMID: 20705165 DOI: 10.1016/j.rcl.2010.04.011]

13 **Hoffmann U**, Ferencik M, Cury RC, Pena AJ. Coronary CT angiography. *J Nucl Med* 2006; **47**: 797-806 [PMID: 16644750]

14 **Boxtel CJ**, Santoso B, Edwards LR. Drug benefits and risks international textbook of clinical pharmacology. Chichester: John Wiley & Sons, 2001

15 **Hitner H**, Nagle BT. Opioid (narcotic) analgesics, Pharmacology: an introduction. 5th ed. New York: McGraw-Hill, 2005

16 **Burnham WM**. Antiseizure drugs (anticonvulsants). In: **Kalant H**, Roschlau WHE, editors. Principles of Medical Pharmacology. 5th ed. Philadelphia: B.C. Decker, 1989: 203-213

17 **Marshall GD**, Lieberman PL. Comparison of three pretreatment protocols to prevent anaphylactoid reactions to radiocontrast media. *Ann Allergy* 1991; **67**: 70-74 [PMID: 1859044]

18 **Cheitlin MD**, Hutter AM, Brindis RG, Ganz P, Kaul S, Russell RO, Zusman RM. **ACC/AHA expert consensus document**. Use of sildenafil (Viagra) in patients with cardiovascular disease. American College of Cardiology/American Heart Association. *J Am Coll Cardiol* 1999; **33**: 273-282 [PMID: 9935041 DOI: 10.1161/01.CIR.99.1.168]

19 **Kloner RA**, Hutter AM, Emmick JT, Mitchell MI, Denne J, Jackson G. Time course of the interaction between tadalafil and nitrates. *J Am Coll Cardiol* 2003; **42**: 1855-1860 [PMID: 14642699 DOI: 10.1016/j.jacc.2003.09.023]

20 **Guaricci AI**, Schuijf JD, Cademartiri F, Brunetti ND, Montrone D, Maffei E, Tedeschi C, Ieva R, Di Biase L, Midiri M, Macarini L, Di Biase M. Incremental value and safety of oral ivabradine for heart rate reduction in computed tomography coronary angiography. *Int J Cardiol* 2012; **156**: 28-33 [PMID: 21095627 DOI: 10.1016/j.ijcard.2010.10.035]

21 **Murat SN**, Orcan S, Akdemir R, Dogan M, Kara E, Balci M. Arrhythmic effects of ivabradine in patients with coronary artery disease. *Clin Invest Med* 2009; **32**: E322-E326 [PMID: 19796572]

22 **Pichler P**, Pichler-Cetin E, Vertesich M, Mendel H, Sochor H, Dock W, Syeda B. Ivabradine versus metoprolol for heart rate reduction before coronary computed tomography angiography. *Am J Cardiol* 2012; **109**: 169-173 [PMID: 22011557 DOI: 10.1016/j.amjcard.2011.08.025]

23 **Pache G**, Saueressig U, Frydrychowicz A, Foell D, Ghanem N, Kotter E, Geibel-Zehender A, Bode C, Langer M, Bley T. Initial experience with 64-slice cardiac CT: non-invasive visualization of coronary artery bypass grafts. *Eur Heart J* 2006; **27**: 976-980 [PMID: 16527826 DOI: 10.1093/eurheartj/ehi824]

24 **Sun Z**, Choo GH, Ng KH. Coronary CT angiography: current status and continuing challenges. *Br J Radiol* 2012; **85**: 495-510 [PMID: 22253353 DOI: 10.1259/bjr/15296170]

25 **Sun Z**. Multislice CT angiography in coronary artery disease: Technical developments, radiation dose and diagnostic value. *World J Cardiol* 2010; **2**: 333-343 [PMID: 21160611 DOI: 10.4330/wjc.v2.i10.333]

26 **Brodoefel H**, Burgstahler C, Tsiflikas I, Reimann A, Schroeder S, Claussen CD, Heuschmid M, Kopp AF. **Dual-source CT: effect** of heart rate, heart rate variability, and calcification on image quality and diagnostic accuracy. *Radiology* 2008; **247**: 346-355 [PMID: 18372455 DOI: 10.1148/radiol.2472070906]

27 **Xu L**, Yang L, Zhang Z, Li Y, Fan Z, Ma X, Lv B, Yu W. Low-dose adaptive sequential scan for dual-source CT coronary angiography in patients with high heart rate: comparison with

retrospective ECG gating. *Eur J Radiol* 2010; **76**: 183-187 [PMID: 19595528 DOI: 10.1016/j.ejrad.2009.06.003]

28 **Pelliccia F**, Pasceri V, Evangelista A, Pergolini A, Barillà F, Viceconte N, Tanzilli G, Schiariti M, Greco C, Gaudio C. Diagnostic accuracy of 320-row computed tomography as compared with invasive coronary angiography in unselected, consecutive patients with suspected coronary artery disease. *Int J Cardiovasc Imaging* 2013; **29**: 443-452 [PMID: 22806317 DOI: 10.1007/s10554-012-0095-4]

29 **Pasricha SS**, Nandurkar D, Seneviratne SK, Cameron JD, Crossett M, Schneider-Kolsky ME, Troupis JM. Image quality of coronary 320-MDCT in patients with atrial fibrillation: initial experience. *AJR Am J Roentgenol* 2009; **193**: 1514-1521 [PMID: 19933642 DOI: 10.2214/AJR.09.2319]

30 **Uehara M**, Takaoka H, Kobayashi Y, Funabashi N. Diagnostic accuracy of 320-slice computed-tomography for detection of significant coronary artery stenosis in patients with various heart rates and heart rhythms compared with conventional coronary-angiography. *Int J Cardiol* 2013; **167**: 809-815 [PMID: 22429616 DOI: 10.1016/j.ijcard.2012.02.017]

31 **Salpeter SR**, Ormiston TM, Salpeter EE. Cardioselective beta-blockers in patients with reactive airway disease: a meta-analysis. *Ann Intern Med* 2002; **137**: 715-725 [PMID: 12416945 DOI: 10.7326/0003-4819-137-9-200211050-00035]

32 **Giesler T**, Baum U, Ropers D, Ulzheimer S, Wenkel E, Mennicke M, Bautz W, Kalender WA, Daniel WG, Achenbach S. Noninvasive visualization of coronary arteries using contrast-enhanced multidetector CT: influence of heart rate on image quality and stenosis detection. *AJR Am J Roentgenol* 2002; **179**: 911-916 [PMID: 12239036 DOI: 10.2214/ajr.179.4.1790911]

33 **Schroeder S**, Kopp AF, Kuettner A, Burgstahler C, Herdeg C, Heuschmid M, Baumbach A, Claussen CD, Karsch KR, Seipel L. Influence of heart rate on vessel visibility in noninvasive coronary angiography using new multislice computed tomography: experience in 94 patients. *Clin Imaging* 2002; **26**: 106-111 [PMID: 11852217 DOI: 10.1016/S0899-7071(01)00371-0]

34 **Boudoulas H**, Rittgers SE, Lewis RP, Leier CV, Weissler AM. Changes in diastolic time with various pharmacologic agents: implication for myocardial perfusion. *Circulation* 1979; **60**: 164-169 [PMID: 376175 DOI: 10.1161/01.CIR.60.1.164]

P- Reviewers: Di Bella G, Lin SL, Teragawa H
S- Editor: Zhai HH **L- Editor**: A **E- Editor**: Liu XM

World Journal of Cardiology

Online Submissions: http://www.wjgnet.com/esps/
bpgoffice@wjgnet.com
doi:10.4330/wjc.v5.i12.459

World J Cardiol 2013 December 26; 5(12): 459-464
ISSN 1949-8462 (online)

TOPIC HIGHLIGHT

Zhonghua Sun, PhD, Associate Professor, *Series Editor*

Radiation dose measurements in coronary CT angiography

Akmal Sabarudin, Zhonghua Sun

Akmal Sabarudin, Diagnostic Imaging and Radiotherapy Program, School of Diagnostic and Applied Health Sciences, Faculty of Health Sciences, University Kebangsaan Malaysia, Kuala Lumpur 50300, Malaysia
Zhonghua Sun, Discipline of Medical Imaging, Department of Imaging and Applied Physics, Curtin University, Perth 6845, Western Australia, Australia
Author contributions: Both authors wrote the paper.
Correspondence to: Zhonghua Sun, PhD, Associate Professor, Discipline of Medical Imaging, Department of Imaging and Applied Physics, Curtin University, GPO Box U1987, Perth 6845, Western Australia, Australia. z.sun@curtin.edu.au
Telephone: +61-8-9266 7509 Fax: +61-8-9266 2377
Received: July 3, 2013 Revised: July 24, 2013
Accepted: August 28, 2013
Published online: December 26, 2013

Abstract

Coronary computed tomography (CT) angiography is associated with high radiation dose and this has raised serious concerns in the literature. Awareness of various parameters for dose estimates and measurements of coronary CT angiography plays an important role in increasing our understanding of the radiation exposure to patients, thus, contributing to the implementation of dose-saving strategies. This article provides an overview of the radiation dose quantity and its measurement during coronary CT angiography procedures.

Key words: Coronary computed tomography angiography; Dose measurement; Dose quantity; Multislice computed tomography; Radiation dose

Core tip: Various dose parameters are used for measurement of radiation dose associated with coronary computed tomography (CT) angiography. It is important to be aware of the dose quantity and measurement in order to achieve the low-dose coronary CT angiography protocol. This article provides an in-depth review of the dose quantity and dose measurement parameters that are commonly used in coronary CT angiography.

Sabarudin A, Sun Z. Radiation dose measurements in coronary CT angiography. *World J Cardiol* 2013; 5(12): 459-464 Available from: URL: http://www.wjgnet.com/1949-8462/full/v5/i12/459.htm DOI: http://dx.doi.org/10.4330/wjc.v5.i12.459

INTRODUCTION

The introduction of latest multi-slice computed tomography (MSCT) technology has emerged as a useful diagnostic imaging modality for the noninvasive assessment of coronary artery disease. The recent advances in the spatial and temporal resolution with thinner detector widths and the low helical pitch values being required for data acquisition in cardiac computed tomography (CT), mainly in retrospective ECG-gating coronary CT angiography (CCTA) mode, however, resulted in increased radiation dose. Compared with plain film radiography, CT examination produces significant higher radiation dose, resulting in a marked increase in radiation exposure to patients. However, the main concern of exposure to ionizing radiation is the potential risk of radiation-induced cancer, and this has raised serious concerns in the literature[1].

Risks associated with radiation exposure are manifested as either deterministic or stochastic effects. Deterministic effects occur when the radiation dose reaches a threshold dose level. The threshold level in deterministic effects varies in different subjects and the damages are significantly related to the amount of dose received. Skin injury, hair loss and cataract are the examples of deterministic effects associated with radiation dose. For example, skin injuries range from skin erythema, moist desquamation, epilation, laceration to necrosis if the skin is exposed to radiation dose beyond the threshold level of 2 Gy[2]. On the other hand, stochastic

effects can be defined as an effect that occurs without any dose threshold. It happens at all time and the damages are not depending on the amount of dose received. Ionizing radiation-induced cancer and genetic changes belong to the stochastic effects. However, previous studies have reported that the increment of radiation dose could increase the chance of developing cancer[3].

Radiation dose estimates for cardiac CT examinations are best expressed as the CT volume dose index ($CTDI_{vol}$), dose-length product (DLP) and effective dose (E). These parameters are precisely defined to allow comparisons of the radiation doses among different CT imaging protocols. The dose received by a patient from a given CT examination is commonly estimated using $CTDI_{vol}$ or DLP value available on the scanner console[4]. Other than $CTDI_{vol}$, DLP and E, there were several radiation dose parameters widely used in CT study in order to measure or quantify the radiation dose of CT scanning procedure. Therefore, the purpose of this article is to provide an overview of the radiation dose quantity and its measurement during CCTA procedures.

RADIATION DOSE QUANTITY AND MEASUREMENTS

CT dose index

The fundamental radiation dose parameter in CT is the computed tomography dose index (CTDI). $CTDI_{100}$ is a measured parameter of radiation exposure which is more convenient than the CTDI and it is regarded as the measurement of choice performed by medical physicists in the clinical setting. Initially, $CTDI_{100}$ is measured by a 100-mm long pencil-shaped ionization chamber in two different cylindrical acrylic phantoms (16 and 32-cm diameter) which was placed at the iso-center of the CT scanner. Most manufacturers use a 16 cm phantom for head and 32 cm phantom for body examinations during CTDI calculation[5]. The $CTDI_w$ is the weighted average of the $CTDI_{100}$ measurements at the center and the peripheral locations of the phantom. This parameter reflects the average absorbed dose over the two-dimensions (x and y dimensions) of the average radiation dose to a cross-section of a patient's body.

The $CTDI_{vol}$ is different from $CTDI_w$ where $CTDI_{vol}$ represents the average radiation dose over the volume scan (x, y, and z directions) while $CTDI_w$ represents the average exposure in the x-y plane only. $CTDI_{vol}$ is the weighted CTDI divided by the pitch, or $CTDI_{vol} = CTDI_w$/pitch and it is measured in mGy. The $CTDI_{vol}$ is now the preferred radiation dose parameter in CT dosimetry. $CTDI_{vol}$ is commonly used in clinical practice due to its accessibility to the radiologists and CT operators as it specifies the radiation intensity used to perform a specific CT examination and not to quantify how much radiation that each patient receives from the CT examination[6]. Rather than the dose to a specific patient, $CTDI_{vol}$ is a standardized index of the average dose delivered from the scanning series. $CTDI_{vol}$ is available to be displayed on the control console. This allows the clinicians or operators to compare the radiation doses that patient receive from different imaging protocols. $CTDI_{vol}$ can also be used in turn to determine DLP.

Dose-length product

The dose-length product (DLP) is an indicator of the integrated radiation dose of an entire CT examination. The DLP is an approximation of the total energy a patient absorbs from the scan. It incorporates the number of scans and the scan width, *e.g.* the total scan length, while in contrast $CTDI_w$ and $CTDI_{vol}$ represent the radiation dose of an individual slice or scan. Therefore, DLP increases with an increase in total scan length or variables that affect the $CTDI_w$ (*e.g.* tube voltage or tube current) or the $CTDI_{vol}$ (*e.g.*, pitch). Because scan length is expressed in centimeters, the SI unit for DLP is mGy·cm. Similar to $CTDI_{vol}$, DLP is also available on the operator's console.

Absorbed dose and equivalent dose

Absorbed dose is an amount of energy that is deposited in a unit of mass of matter (tissue). It is measured in gray (Gy) with 1 Gy equivalent to 1 joule per kilogram. Each type of ionizing radiation produces different biological effect. For instance, the biological effect on tissue which is exposed to 1 Gy α radiation is more harmful than 1 Gy of X-rays. This is because α particles are more heavily charged and slower than x-rays. Therefore, α particles lose much more energy along the travel path before reaching the target[7]. However, the quantity of equivalent dose is used to compare all types of ionizing radiation equally on the biological effect. Equivalent dose is measured in Sievert (Sv). Equivalent dose is obtained by multiplying the absorbed dose with the radiation weighting factor (Table 1).

Effective dose

The most important parameter in CT imaging is the effective dose (E), which is valuable in assessment and comparison of the potential biological risk of a specific examination. E is a sum of equivalent doses in organs of the body that are considered radiosensitive. It is a uniform whole-body dose that has the same nominal radiation risk of carcinogenesis and induction of genetic effects as any given non-uniform exposure[8]. Each organ in human body has different radiosensitivity with some organs more sensitive to the risk of damage than the others. E can be estimated by multiplying each equivalent dose by a relative organ with the tissue weighting factor related to the risk associated with that organ and summing overall exposed organ. International Commission on Radiological Protection (ICRP) publication 103 released in 2007 has recommended values for the tissue weighting factors with major changes different from the previously published ICRP publication 60[9,10] (Table 2).

The SI unit of estimating E is the sievert (Sv) or millisievert (mSv). The weighting factors used for individual

Table 1 Radiation weighting factor for various type and energy range

Type and energy range	Radiation weighting factor, W_R (ICRP-60)
Photons, all energy	1
Electrons, muons, all energy	1
Neutrons < 10 keV	5
10 eV-100 keV	10
> 100 keV-2MeV	20
> 2–20 MeV	10
> 20 MeV	5
Protons > 2 MeV	5
Alpha particles, fission fragments and heavy nuclei	20

Adapted from Ng *et al*[7]. ICRP: International Commission on Radiological Protection.

Table 2 Tissue weighting factor comparison between International Commission on Radiological Protection publication-103 and publication-60

Organs	Tissue weighting factor, W_T	
	ICRP-103	ICRP-60
Colon	0.12	0.12
Lung	0.12	0.12
Red bone marrow	0.12	0.12
Stomach	0.12	0.12
Breast	0.12	0.05
Gonads	0.08	0.20
Bladder	0.04	0.05
Liver/Oesophagus	0.04	0.05
Thyroid	0.04	0.05
Bone surface/skin	0.01	0.01
Brain	0.01	-
Salivary glands	0.01	-
Remainder tissues	0.12[1]	0.05[2]

Adapted from Ng *et al*[7]. [1]Remainder tissues in International Commission on Radiological Protection (ICRP)-103: adrenals, kidneys, muscle, small intestine, pancreas, spleen, thymus, uterus/cervix, prostate, extra-thoracic region, gallbladder, heart, lymphatic nodes and oral mucosa; [2]Remainder tissues in ICRP-60: adrenals, kidney, muscle, small intestine, pancreas, spleen, thymus, uterus, upper large intestine and brain.

tissues are based on a statistical analysis of the increase in the long-term incidence and mortality for cancer determined from a life span study of the survivors in Japan during the atomic bomb explosion[11-13]. Usually, tabular data of conversion coefficients are available to estimate E from entrance skin dose for radiography[14,15], from dose area product (DAP) for fluoroscopy[16,17], or from $CTDI_{vol}$ or DLP for CT[18]. The goal is to convert the higher radiation doses delivered to a small portion of the body into an equivalent uniform dose to the entire body that carries the same biological risk for causing radiation-induced fatal and nonfatal cancers.

The *E* can be estimated by multiplying the DLP with a conversion coefficient factor (*E*/DLP), *k* (mSv/mGy per centimetre). The *E*/DLP value of 0.026 or 0.028 mSv/mGy per centimetre was applied for coronary CT study since this value was likely to be more accurate for estimation of radiation dose associated with cardiac CT compared to the chest CT (0.014 or 0.017 mSv/mGy per centimetre)[10,19,20]. If no dose-saving strategy is applied, it is estimated that effective doses of coronary CT angiography may reach up to 30 mSv in patients undergoing cardiac CT imaging, thus, there is potential risk of associated radiation-induced malignancy[21].

Gosling *et al*[20] compared the effective dose using the latest ICRP 103 tissue-weighting factors with that calculated with previously published chest conversion factors. Their results showed that the use of chest conversion factors (0.014-0.017) significantly underestimated the effective dose when compared to the dose calculated using the conversion factor of 0.028. A conversion factor of 0.028 would give a better estimation of the effective dose from prospectively ECG-triggered coronary CT angiography. Appropriate conversion factors are needed to accurately estimate effective dose. A conversion factor of 0.014 or 0.017 is commonly used in many cardiac CT studies to estimate the effective dose associated with coronary CT angiography, thus, this could lead to variations in the reported effective dose. As a result, the DLP or $CTDI_{vol}$ is recommended to compare the radiation exposure of coronary CT angiography[22].

Background equivalent radiation time

Background equivalent radiation time (BERT) is used to explain the dose to the general public without complicated scientific units, terminology or concepts. It converts the radiation dose to an equivalent period of natural background radiation in days, weeks, months or years to which the entire population is exposed every day from natural radioactive substance in the air, internal, terrestrial, cosmic and environment. For example, it is more likely for patient to easily understand that "your chest X-ray dose is about equal to 3 d of background radiation" rather than "you have received 0.02 mSv for your chest X-ray examination"[7]. BERT is not used to provide a high level of diagnostic accuracy, but to relieve anxiety about radiation by giving an understandable and satisfactory answer (Table 3)[23].

Entrance skin dose

Entrance skin dose is an amount of energy imparted per gram of tissue at the entrance surface. It is also known as surface absorbed dose (SAD). About 1 Gy is equal to 1 millijoule per gram of energy deposited by the X-rays. Entrance skin dose can be obtained by multiplying the radiation exposure measured in the air at the skin by a factor, f for the tissue. The f factor is a quantity of radiation dose exposure conversion measured in the air (coulomb per kilogram at the standard temperature and pressure) to an equivalent radiation dose absorbed in tissue (grays) at the same location. However, entrance skin dose is not an indicator to measure radiation risks except for skin erythema, but it is useful for organ dose calculation especially in a computer-based program that is involved with Monte Carlo simulations[14,15].

Table 3 Estimated effective doses for diagnostic medical exposures associated with background equivalent radiation time and lifetime fatal cancer risks from National Radiological Protection Board

X-ray examination	Estimated effective dose (mSv)	BERT[1]	Fatal cancer risk per examination[2]
Limbs and joints (exclude hip)	< 0.01	< 1 d	1 in a few millions
Dental (single bitewing)	< 0.01	< 1.5 d	1 in a few millions
Dental (panoramic)	0.01	1.5 d	1 in 2 million
Chest (single PA)	0.02	3 d	1 in a million
Skull	0.07	1 d	1 in 300000
Cervical spine	0.08	2 wk	1 in 200000
Thoracic spine	0.7	4 mo	1 in 30000
Lumbar spine	1.3	7 mo	1 in 15000
Abdomen	0.7	4 mo	1 in 30000
Hip	0.3	7 wk	1 in 67000
Pelvis	0.7	4 mo	1 in 30000
Intravenous urography	2.5	14 mo	1 in 8000
Barium swallow	1.5	8 mo	1 in 13000
Barium meal	3	16 mo	1 in 6700
Barium follow-through	3	16 mo	1 in 6700
Barium enema	7	3.2 yr	1 in 3000
CT head	2	1 yr	1 in 10000
CT chest	8	3.6 yr	1 in 2500
CT abdomen/pelvis	10	4.5 yr	1 in 2000

Adapted from Ng *et al*[7]. [1]Natural background radiation based on Australia average = 2.4 mSv per year; [2]Appropriate lifetime risk for patients from 16-69 years old: paediatric = 2x; geriatric = 5x. BERT: Background equivalent radiation time.

Critical organ dose

Critical organ dose (COD) is more commonly reported in the literature for radiologic examinations. Critical organ dose refers to the energy deposited per unit mass to individual critical organs for which the radiosensitivity and radiation dose are high. Its unit of measurement is usually milligrays, which is equivalent to millijoules per kilogram. COD can be used to assess the risks of irradiation beyond cancer induction for certain organs; for example, other potential biological effects can include skin erythema, cataracts, fetal abnormalities, haematologic effects, vascular damage, and effects on the central nervous system.

Critical organ dose may be determined by other dose descriptors, such as entrance skin dose or dose area product, by using tables or software programs that are based on Monte Carlo calculations for standard patient sizes[14,15]. Also, the critical organ dose values for various organs, along with their corresponding weighting factors, can be used to calculate the effective dose[9,24]. In clinical practice, knowledge of organ doses and the carcinogenic sensitivity of certain organs can lead to better collimation and patient positioning to reduce the risks from exposure to radiation.

Diagnostic acceptable reference level

Diagnostic acceptable reference level is also known as diagnostic reference level (DRL). DRL values are published based on the nationwide evaluation of X-ray trends surveys[23,25]. The data values can be used as a reference point to ensure that all current clinical practice involving radiation in radiological investigations are safe. However, ESD, DAP, or $CTDI_{vol}$ values that are greater than those of DRL may be attributed to the patient's size, the complexity of the clinical case, equipment malfunctions, or suboptimal protocols. Some of the higher values may be unavoidable; however, many of the higher values can be avoided. When patient doses appear to be above those of DRL, especially when they are consistently higher, investigation and assessment are required. If suboptimal protocols or equipment deficiencies are the cause of the higher dose levels, necessary strategies must be undertaken to reduce the radiation dose.

Radiation dosimeter

Radiation dose in clinical practice can be measured accurately by using a dosimeter. There are a number of dose measurement tools with different methods being used to measure the radiation dose absorption. The value of absorbed dose is determined indirectly by measuring the radiation effect through ionization of air, fogging of photographic emulsion, thermoluminescence, scintillation and ionization of a semiconductor. However, the most commonly used method in radiation dosimetry is thermoluminescence dosimeter (TLD)[26].

Thermoluminescence phenomenon

Thermoluminescence is a condition where the light is emitted from a heated crystalline material which is made up of lithium fluoride (LiF) or calcium fluoride (CaF_2) phosphors. When the crystalline is exposed to the radiation, electrons in the crystal are pulled out from valence band to the conduction band by a small amount of energy. However, without enough energy, some of the electrons are trapped into one of the isolated levels provided by impurities in the crystal. It will remain immobilized at that state until energy is supplied to release it (usually by heat). Thus, the electrons leave a positive hole in the valance band. By heating the crystal, the trapped elec-

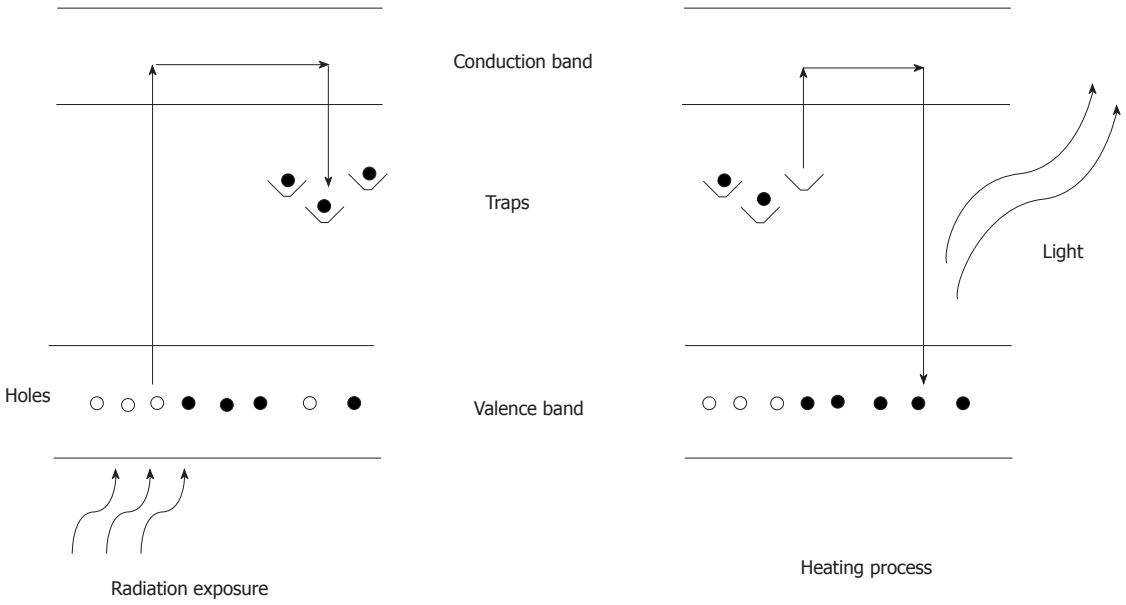

Figure 1 Process of light emission from the radiation exposure in the thermoluminescence phenomenon.

trons will elevate and return to the valence positive hole. A photon of visible light is emitted during the process of returning electrons from the trap to the valence band (Figure 1)[11]. The total light emitted is counted where the measurement for the number of trapped electron indicates the absorbed radiation. Surprisingly, it can be used even after a month of storage.

Several types of TLD are commercially available for a wide range of applications. For instance, LiF: Mg, $Li_2B_4O_7$, $CaSO_4$: Dy, Al_2O_3, CaF_2: Dy and CaF_2: Mn[27]. In diagnostic radiology, LiF: Mg, Ti or usually known as TLD-100 was chosen for dosimetry purposes in clinical radiation measurement. In fact, it was the first material used in diagnostic radiology and one of the most utilised materials when compared to others[28]. TLD with LiF: Mg, Ti material is chosen because of the physical shape which is small, light and convenient for local measurement during the radiological examinations. Apart from physical appearance, it is able to measure entrance surface absorbed dose at the reference point at specific organs without obscuring an image due to the radiolucency specification[27]. Moreover, it has high reproductive capability, thus it can be used repeatedly. The materials are sensitive to detect radiation exposure in a range between 10 μGy and 10 Gy, in addition to having a good linear relationship between thermoluminescence readout value and dose absorption up to 1 mrad.

CT dose measurement

Effective dose in CT can be easily estimated by a simple calculation through multiplying the DLP with a conversion coefficient factor (E/DLP). Huda, Ogden, and Khorasani in their study introduced a new approach to determine the E[8]. They suggested that E can be calculated from DLP by using ImPACT software package which is based on Monte Carlo simulation performed by the National Radiological Protection Board[29]. Yet, the accuracy of this system is undisputable when Huda, Ogden, and Khorasani compared those E calculations with other software packages like CT-expo and ImpactDose. As a result, there were approximately 5% differences between E/DLP values according to each software package and it was not statistically significant[8]. CT-Expo is a program run on Monte Carlo dosimetry data while ImpactDose is a personal computer based-program that calculates ED values for arbitrary scanning parameters and anatomic ranges[30]. However, the E values still can be calculated manually by multiplying the DLP values with the conversion coefficient factor in CT imaging based on individual organs and tissue weighting factors published by the ICRP 103[10,16,31]. Using CT dose reporting packages is an advantage because they are easy to use and produce quick results. However, it must be recognised that there are deviations between the different software packages, and users should understand this and be familiar with different terminologies used in order to provide accurate dose reporting for a consistent comparison[30].

In conclusion, it is important to be aware of the amount of radiation dose produced from cardiac CT scanning. The quantification of the radiation dose is a crucial issue that must be addressed by both practitioners and the operators in determining the correct and accurate dose measurement. With sufficient knowledge of radiation dose terminology and dose quantification, the understanding of radiation dose safety and radiation awareness will be accordingly increased when performing coronary CT angiography examinations. Various dose-saving strategies have been undertaken in the past decade to lower radiation exposure to patients who undergo coronary CT angiography, with effective dose ranging from 10 mSv to as low as 1 mSv. Details of these dose reduction techniques will be discussed in Part Ⅲ of this series.

REFERENCES

1 **Einstein AJ**, Henzlova MJ, Rajagopalan S. Radiation dose to the breast and estimated breast cancer risk in women from 64-slice CT coronary angiography: insights from the Biological Effects of Ionizing Radiation (BEIR) VII report. *J Nucl Cardiol* 2007; **14**: S59

2 **Bogaert E**, Bacher K, Lemmens K, Carlier M, Desmet W, De Wagter X, Djian D, Hanet C, Heyndrickx G, Legrand V, Taeymans Y, Thierens H. A large-scale multicentre study of patient skin doses in interventional cardiology: dose-area product action levels and dose reference levels. *Br J Radiol* 2009; **82**: 303-312 [PMID: 19124567 DOI: 10.1259/bjr/29449648]

3 **Hall EJ**. Radiobiology for the radiologist. New York: Lippincott, 1999

4 **Einstein AJ**, Moser KW, Thompson RC, Cerqueira MD, Henzlova MJ. Radiation dose to patients from cardiac diagnostic imaging. *Circulation* 2007; **116**: 1290-1305 [PMID: 17846343]

5 **Wagner LK**, Eifel PJ, Geise RA. Potential biological effects following high X-ray dose interventional procedures. *J Vasc Interv Radiol* 1994; **5**: 71-84 [PMID: 8136601]

6 **Huda W**. Radiation dosimetry in diagnostic radiology. *AJR Am J Roentgenol* 1997; **169**: 1487-1488 [PMID: 9393150]

7 **Ng KH**. Radiation effect and protection in diagnostic radiology. In: Peh WCG, Hiramatsu Y, editors. Proceedings of the The Asian-Oceanian textbook of radiology. Singapore: TTG Asia Media Pte Ltd, 2003: 175-193

8 **Huda W**, Ogden KM, Khorasani MR. Converting dose-length product to effective dose at CT. *Radiology* 2008; **248**: 995-1003 [PMID: 18710988 DOI: 10.1148/radiol.2483071964]

9 **Task Group on Radiation Quality Effects in Radiological Protection**, Committee 1 on Radiation Effects, International Commission on Radiological Protection. Relative biological effectiveness (RBE), quality factor (Q), and radiation weighting factor (w(R)). A report of the International Commission on Radiological Protection. *Ann ICRP* 2003; **33**: 1-117 [PMID: 14614921]

10 **Huda W**, Magill D, He W. CT effective dose per dose length product using ICRP 103 weighting factors. *Med Phys* 2011; **38**: 1261-1265 [PMID: 21520838]

11 **Martin JE**. Physics for radiation protection. 2nd ed. Weinheim: Wiley-VCH Verlag, 2013

12 **Pierce DA**, Preston DL. Radiation-related cancer risks at low doses among atomic bomb survivors. *Radiat Res* 2000; **154**: 178-186 [PMID: 10931690]

13 **Preston DL**, Shimizu Y, Pierce DA, Suyama A, Mabuchi K. Studies of mortality of atomic bomb survivors. Report 13: solid cancer and noncancer disease mortality: 1950-1997. 2003. *Radiat Res* 2012; **178**: AV146-AV172 [PMID: 22870966]

14 **Rosenstein M**. Handbook of selected tissue doses for projections common in diagnostic radiology. Rockville: HEW Publication (FDA), 1988: 89

15 **Rosenstein M**, Beck TJ, Warner GG. Handbook of selected organ doses for projections common in pediatric radiology. Rockville: HEW Publication (FDA), 1979: 79

16 **Hart D**, Jones DG, Wall BF. Estimation of effective dose in diagnostic radiology from entrance surface dose and dose-area product measurements. NRPB-R262. Oxford: National Radiological Protection Board Oxon, 1994

17 **Le Heron JC**. Estimation of effective dose to the patient during medical x-ray examinations from measurements of the dose-area product. *Phys Med Biol* 1992; **37**: 2117-2126 [PMID: 1438564]

18 **European Commission**. European guidelines on quality criteria for computed tomography. Report EUR 16262 EN. Luxemburg, European Commission, 1999: 69-78

19 **Sabarudin A**, Sun Z, Yusof AK. Coronary CT angiography with single-source and dual-source CT: comparison of image quality and radiation dose between prospective ECG-triggered and retrospective ECG-gated protocols. *Int J Cardiol* 2013; **168**: 746-753 [PMID: 23098849 DOI: 10.1016/j.ijcard.2012.09.217]

20 **Gosling O**, Loader R, Venables P, Rowles N, Morgan-Hughes G, Roobottom C. Cardiac CT: are we underestimating the dose? A radiation dose study utilizing the 2007 ICRP tissue weighting factors and a cardiac specific scan volume. *Clin Radiol* 2010; **65**: 1013-1017 [PMID: 21070906]

21 **Xu L**, Zhang Z. Coronary CT angiography with low radiation dose. *Int J Cardiovasc Imaging* 2010; **26** Suppl 1: 17-25 [PMID: 20058080]

22 **Sun Z**, Ng KH. Prospective versus retrospective ECG-gated multislice CT coronary angiography: a systematic review of radiation dose and diagnostic accuracy. *Eur J Radiol* 2012; **81**: e94-100 [PMID: 21316887]

23 **Nickoloff EL**, Lu ZF, Dutta AK, So JC. Radiation dose descriptors: BERT, COD, DAP, and other strange creatures. *Radiographics* 2008; **28**: 1439-1450 [PMID: 18794317 DOI: 10.1148/rg.285075748]

24 National Council of Radiation Potection and Measurements. Use of personal monitors to estimate effective dose equivalent and effective dose to workers for external exposure to low-LET radiation. Bethesda: NCRP Publications, 1995

25 **Gray JE**, Archer BR, Butler PF, Hobbs BB, Mettler FA, Pizzutiello RJ, Schueler BA, Strauss KJ, Suleiman OH, Yaffe MJ. Reference values for diagnostic radiology: application and impact. *Radiology* 2005; **235**: 354-358 [PMID: 15758190]

26 **Ball J**, Moore AD, Turner S. Essential physics for radiographers. 4th ed. West Sussex: Blackwell Publishing, 2008

27 **Maia AF**, Caldas LV. Response of TL materials to diagnostic radiology X radiation beams. *Appl Radiat Isot* 2010; **68**: 780-783 [PMID: 20097569 DOI: 10.1016/j.apradiso.2010.01.002]

28 **Berni D**, Gori C, Lazzari B, Mazzocchi S, Rossi F, Zatelli G. Use of TLD in evaluating diagnostic reference levels for some radiological examinations. *Radiat Prot Dosimetry* 2002; **101**: 411-413 [PMID: 12382779]

29 National Radiological Protection Board. Living with radiation. London: HMSO, 1998

30 **Abdullah A**, Sun Z, Pongnapang N, Ng KH. Comparison of computed tomography dose reporting software. *Radiat Prot Dosimetry* 2012; **151**: 153-157 [PMID: 22155753]

31 **Kalender WA**, Schmidt B, Zankl M, Schmidt M. A PC program for estimating organ dose and effective dose values in computed tomography. *Eur Radiol* 1999; **9**: 555-562 [PMID: 10087133]

P- Reviewers: Firstenberg MS, Takatoshi K
S- Editor: Zhai HH **L- Editor**: A **E- Editor**: Liu XM

World Journal of Cardiology

Online Submissions: http://www.wjgnet.com/esps/
bpgoffice@wjgnet.com
doi:10.4330/wjc.v5.i12.465

World J Cardiol 2013 December 26; 5(12): 465-472
ISSN 1949-8462 (online)

TOPIC HIGHLIGHT

Zhonghua Sun, PhD, Associate Professor, *Series Editor*

Coronary CT angiography: Dose reduction strategies

Akmal Sabarudin, Zhonghua Sun

Akmal Sabarudin, Diagnostic Imaging and Radiotherapy Program, School of Diagnostic and Applied Health Sciences, Faculty of Health Sciences, Universiti Kebangsaan Malaysia, Kuala Lumpur 50300, Malaysia
Zhonghua Sun, Discipline of Medical Imaging, Department of Imaging and Applied Physics, Curtin University, Perth 6845, Western Australia, Australia
Author contributions: Both authors wrote the paper.
Correspondence to: Zhonghua Sun, PhD, Associate Professor, Discipline of Medical Imaging, Department of Imaging and Applied Physics, Curtin University, GPO Box U1987, Perth 6845, Western Australia, Australia. z.sun@curtin.edu.au
Telephone: +61-8-9266 7509 Fax: +61-8-9266 2377
Received: July 3, 2013 Revised: July 24, 2013
Accepted: August 20, 2013
Published online: December 26, 2013

Abstract

With the introduction of 64- and post-64 slice computed tomography (CT) technology, coronary CT angiography has been increasingly used as a less invasive modality for the diagnosis of coronary artery disease. Despite its high diagnostic value and promising results compared to invasive coronary angiography, coronary CT angiography is associated with high radiation dose, leading to potential risk of radiation-induced cancer. A variety of dose-reduction strategies have been reported recently to reduce radiation dose with effective outcomes having been achieved. This article presents an overview of the various methods currently used for radiation dose reduction.

Key words: Coronary artery disease; Coronary computed tomography angiography; Multislice computed tomography; Radiation dose; Dose reduction

Core tip: Various dose-reduction strategies of coronary computed tomography angiography have been discussed in this article with the aim of providing readers with a comprehensive summary of the effectiveness of these radiation reduction approaches.

Sabarudin A, Sun Z. Coronary CT angiography: Dose reduction strategies. *World J Cardiol* 2013; 5(12): 465-472 Available from: URL: http://www.wjgnet.com/1949-8462/full/v5/i12/465.htm DOI: http://dx.doi.org/10.4330/wjc.v5.i12.465

INTRODUCTION

Coronary computed tomography angiography (CCTA) procedure has been known as an effective technique in non-invasive coronary artery assessment. With high accuracy in the detection of coronary artery disease, this makes CCTA accepted as a widely used diagnostic tool in cardiac imaging[1-4]. However, radiation dose of CCTA that has been reported in the literature is the greatest concern and varies a great deal depending on the scanning parameter settings. There are many factors influencing the overall radiation exposure including tube voltage, tube current, scan range, scanner geometry, the electrocardiogram (ECG)-gating application either prospective or retrospective ECG-gating, slice thickness and pitch value selection (for helical scan mode).

Most of the parameters are controlled, monitored and modulated by the computed tomography (CT) operator during the procedure in order to obtain an optimum image quality. Therefore, all factors need to be taken into consideration in minimizing the radiation exposure to achieve the goal of "as low as reasonably possible". Previous studies have also reported that standard CCTA procedure with the use of retrospective ECG-gated technique results in very high radiation dose, which ranged from 13.4 to 31.4 mSv[5-7]. This has raised serious concerns in the literature due to the potential risk of radiation-induced malignancy resulting from CCTA. Therefore, several dose-saving strategies have been introduced to deal with radiation dose issues, and

these techniques include anatomy-based tube current modulation[8,9], ECG-controlled tube current modulation[10,11], tube voltage reduction[12,13], a high-pitch scanning[14,15] and prospective ECG-triggered CCTA[16,17]. This article is written purposely to provide information about the strategies that could be used to further reduce the radiation dose to patient during CCTA procedure.

STRATEGIES FOR RADIATION DOSE REDUCTION IN CCTA

Anatomy-based tube current modulation

Tube current is an important element that is directly related to radiation dose and image quality. With rapid developments of CT technology, implementation of automatic tube current modulation allows significant reduction in radiation dose for CT examinations. In CT examination, automatic tube current modulation can be defined as a series of techniques that enable automatic adjustment of the tube current in *x*-, *y*-plane (angular modulation) or *z*-plane (*z*-axis modulation), according to the size and attenuation characteristics of the human body. The purpose of these adjustments is to achieve optimum image quality with low radiation dose. The term automatic tube current modulation is similar to automatic exposure-control that is commonly used in conventional radiography[18,19]. Anatomy-based tube current modulation is then divided into two modes namely angular modulation and z-axis modulation.

Angular modulation (x-y plane)

Since the shape of patients body is not symmetrical [anteroposterior (AP) *vs* lateral], angular-modulation techniques automatically adjust the tube current for each projection angle to the appropriate attenuation according to patient's anatomical structures. Without angular modulation, the tube current is held constant over the 360° rotation, regardless of the patient attenuation profile. The angular-modulation technique reduces tube current as a function of projection angles for low-attenuation projections (AP *vs* lateral projections). This technique calculates the modulation function from the online attenuation profile of the patient. The modulation function data are processed and sent to the generator control for further tube current modulation with a delay of 180° from the X-ray generation angle. In asymmetrical regions being scanned such as the shoulders in chest CT, the X-ray attenuation is substantially less in the AP than in the lateral direction. The radiation dose reduction could be achieved up to 90% with application of the angular-modulation technique[20]. Therefore, the technique of angular modulation helps in improving dose efficiency in the *x*- and *y*-axis by reducing radiation exposure in a particular scanning plane.

Z-axis modulation

The principle of z-axis-modulation technique is different from that of angular modulation. Unlike angular modulation, the *z*-axis modulation technique adjusts the tube current automatically to maintain a user-specified quantum noise level in the image data. It provides a noise index to allow users to select the amount of X-ray noise that will be presented in the reconstructed images. Using a localizer radiograph, the scanner computes the tube current required obtaining images with a selected noise level. Hence, *z*-axis modulation attempts to make all images have a similar noise irrespective of patient size and anatomy. The noise index value is approximately equal to the image noise (standard deviation) in the central region of an image of a uniform phantom. However, the actual noise measured on the image by drawing a region of interest that will differ from the noise index selected for scanning. This is due to the fact that noise index settings only adjust the tube current, whereas the standard deviation is also affected by other parameters, including the reconstruction algorithm, the reconstructed section thickness (if different from the prospective thickness), the use of image space filters, variations in patient anatomy and patient motion, and the presence of beam-hardening artifacts.

The CARE Dose 4D protocol (Siemens, Medical Solutions, Erlangen, Germany) was then introduced in order to adapt the tube current to the patient's individual anatomy and modulate the tube current in the section with the lowest dose levels. Previous studies have shown that 20%-60% dose reduction was achieved depending on the anatomic region and patient habitus, with improved image quality[21]. Another study combining angular and z-axis modulation (3D Auto mA; GE Yokogowa Medical Systems, Tokyo, Japan) reported significant dose reductions (60%) in abdominal-pelvic CT examinations[22]. This technique uses a single localizer radiograph to determine patient asymmetry and appropriate angular and z-axis modulation for the patient. The investigators added noise (computer modification of original raw scan data to simulate lower tube current noise levels) to patients' scan data to produce images and calculate the radiation dose reduction.

A lower minimum tube current may result in reduced exposure to patients, which occasionally increases image noise in smaller patients scanned with a substantially reduced tube current. Generally, larger patients receive higher tube current with z-axis modulation if a fixed-tube-current technique used in order to maintain the selected image noise. In contrast, with automatic tube current modulation, the tube current is inconsistent throughout the scan and thus results in the diagnostic image quality with reduced radiation dose. The main limitation of automatic tube current modulation is the lack of uniformity between techniques developed by different vendors.

ECG-CONTROLLED TUBE CURRENT MODULATION

The idea of decreasing radiation doses associated with tube current modulation in CT stimulates manufacturers to improve the CCTA examinations. One of the most recently developed methods, CARE dose 4D by Siemens Medical Solutions, which combining the effects of angular and *z*-axis modulation techniques[23]. Virtually all ana-

tomic regions in the thorax, abdomen, and pelvis have benefited from these sophisticated techniques that result in considerable significant dose reduction[10,24].

However, the *z*-axis modulation principle in CARE dose 4D was not compatible with ECG pulsing. ECG-pulsed tube current modulation is the most significant improvement in minimizing radiation from CT technology and it is the only technique dedicated to cardiac imaging. ECG pulsing is performed online during cardiac CT examination which allows a decrease in radiation exposure of between 30% and 50%. The radiation dose is reduced by modulating the tube current output during the systolic phase[25]. Moreover, the algorithm for ECG-dependent dose modulation also represents a very effective tool for limiting radiation dose in the vast majority of patients undergoing cardiac CT studies.

In ECG-controlled tube current modulation technique, a high tube current with optimal image quality is applied only during the diastolic phase of the cardiac cycle, in which images are most likely to be reconstructed with minimal artifacts, while in the systolic phase, a low tube current (50% of normal tube current) is applied. Image reconstruction during cardiac CT examinations is usually performed in ventricular mid-diastole phase due to less cardiac motion that causes blurring of cardiac structures. Thus, high quality diagnostic images can be acquired during the diastolic phase[26]. However, this method totally depends on the patient's heart rate and requires a regular sinus rhythm in order to prevent poor image quality. Unfortunately, the ECG-controlled tube current modulation algorithm cannot be performed in the presence of arrhythmias such as premature extra beats. Thus, this algorithm may not be useful in patients with arrhythmias.

LOW TUBE VOLTAGE

Since radiation dose varies with the square of tube voltage, an application of lower tube voltage during CT data acquisition is another approach for radiation dose reduction. A previous study by Huda *et al*[27] showed that reducing the X-ray tube potential from 140 to 80 kVp at constant tube current decreased the radiation dose by a factor of about 3.4. Consequently, image contrast and image noise will definitely be increased because of fewer numbers of photons produced[27-29]. However, since the contrast-to-noise ratio (CNR) and signal-to-noise ratio are the key factor of CT image quality, noise is rather irrelevant if the level of contrast or amount of signals are too high[28]. The change in image contrast is dependent on the anatomic number (*Z*) of the structures being investigated. The image structure with high-anatomic-number becomes significantly more prominent than image of low-anatomic-number structures (soft tissue) in the application of low tube voltages[27].

It has been confirmed that diagnostic image quality was not affected by lower tube voltages in pediatric CT investigations. Similarly, in a phantom study by Siegel *et al*[29] showed that reduced beam energy in contrast-enhanced pediatric CT decreased the radiation dose without affecting image contrast and image noise. Moreover, the interrelationship between beam energy and tube output has been described by Boone *et al*[30] in the context of image noise characterization in CT techniques by using tube voltages of 80-140 kVp and tube currents of 10-300 mA. Provided the tube current-time product was appropriately adapted, radiation dose can be significantly reduced at lower tube voltage while CNR remained at a constant level. Cody *et al*[31] reported that the use of 80-kVp tube voltage resulted in beam-hardening artifacts and thus recommended the use of 100- to 120-kVp settings in pediatric patients. For non-cardiac CT studies with kilovoltage reduction, an increase of the tube current by 50% has been proposed to maintain image quality and to reduce the dose estimation concurrently[31]. However, a further increase in tube current is limited with the available standard protocols for cardiac CT scanning on the studied CT scanners. Therefore, a trade-off between dose saving and increased image noise has to be considered with current cardiac CT protocols.

Previous study compared the diagnostic image quality of the coronary artery segments in order to detect stenosis in various scan protocols[32]. In this qualitative analysis, no deterioration of image quality was detected in most of the scan protocols inclusive of the ECG-dose modulation and the 100-kVp tube voltage for both 16- and 64-slice CT scanners. The value of this analysis is only limited by a potential selection bias of the scanning protocols. Image obtained with 120-kVp scan protocol without ECG modulation (on patients with arrhythmia) are likely to present with more non-diagnostic coronary segments, even when no dose-saving algorithms were applied. However, the impact of dose-saving algorithms on the detection of calcified and non-calcified plaques remains unknown. Therefore, further studies are needed to investigate the balance between dose savings and maintained diagnostic image quality for CCTA investigations.

HIGH PITCH VALUE

With the recent advent of second-generation of dual-source, another low-dose technique has been introduced for cardiac CT which is high-pitch scanning mode[33]. This technique was successfully tested with dual-source 128-slice CT in retrospective ECG-gating protocol. In this technique, the data are acquired in a spiral mode while the X-ray table runs with a very high pitch of 3.4 equaling to a table feed of 46 cm/s. When this high-pitch mode is used, the entire heart is scanned within one single cardiac cycle, generally during the diastolic phase (75% R-R interval). The temporal resolution for this system is 75 ms, with the gantry rotation time of 280 ms and only quarter rotations for data reconstruction. Early reports on phantom studies have shown that the purpose of this scan mode is to deliver images of diagnostic quality at a low radiation dose. Moreover, two studies have successfully proved that feasibility of this high-pitch mode technique also in

patients by using the remodeled first generation of dual-source 64-slice CT scanners with effective dose less than 1 mSv[15,34]. Then, several recent studies also have reported similar results[35-37]. In addition to low dose aspect, high diagnostic accuracy has been achieved with the high-pitch dual-source CT[38].

In order to apply the high-pitch mode, several requirements must be fulfilled. Firstly, dual-source geometry is necessary in order to obtain the projection data by the second detector for gaps fill-up due to rapid table movement. In this way, the pitch can be increased up to 3.4 while allowing image reconstruction, although the limited field of view is covered by both detectors. A quarter rotation of data per measurement is used for image reconstruction, and each of the individual axial images has a temporal resolution of a quarter of the rotation time $t_{rot}/4$. Thus, the overlapping of radiation exposure can be avoided with the application of high pitch resulting in radiation dose reduction to the minimum level[39]. Secondly, a higher temporal resolution is essential to enable single cardiac cycle reconstruction without image distortion due to motion artifacts. Thirdly, patient's heart rate must be regular and consistent in order to obtain a good image quality. With used of high pitch mode, the examination table is accelerated to the maximum speed during data acquisition which is triggered by the R-peak of the heartbeat. The examination table could not be accelerated in an infinitely small time period; therefore, it has to be set in motion sufficiently earlier prior to scanning acquisition. Inconstant heart rates lead to inaccurate positioning of the data acquisition window, with data being acquired either too early (if heart rate decreases) or too late (if heart rate increases) in the cardiac cycle. Inconsistent heart rates would compromise image quality by stair-step artifacts.

Finally, high pitch mode requires patient with low heart rates (< 65 bpm). In order to obtain a motion-free artifact, CT data acquisition can possibly be performed during a single diastolic period if the patient heart rate is constantly lower than 65 bpm[39]. On the other hand, patients with high heart rates may not yield diagnostic image quality of the coronary arteries due to a narrow diastolic exposure of R-R interval window and therefore, tube current modulation is required for adjustment accordingly[35].

ITERATIVE RECONSTRUCTION METHODS

Alternative image reconstruction techniques such as iterative reconstruction have been used mainly in nuclear medicine studies[40,41]. In CCTA, iterative reconstruction such as adaptive statistical iterative reconstruction (ASIR) (GE Healthcare) has been introduced as a new reconstruction algorithm[42]. Iterative reconstruction is a method to reconstruct 2D and 3D images from measured projections of an object. However, unlike filtered back projection, iterative reconstruction starts with an initial estimate of the object which is subsequently improved in a stepwise fashion by comparing the synthesized image to the one acquired with projection data and improving the previous estimation.

Moreover, iterative reconstruction reduces image noise by iteratively comparing the acquired image to a modeled projection. This reconstruction algorithm is used to help deal with one of the primary issues of dose and tube current reduction for CCTA. Since iterative reconstruction has been consistently associated with image quality improvement, especially improving CNR, it has the possibility of improving spatial resolution[43,44]. With faster computer technologies and adapted techniques, the use of iterative reconstruction for cardiac CT imaging has been increasingly studied and the reconstruction speed now allows its use in clinical practice. Iterative reconstruction has been shown to reduce noise, improve image quality and reduce radiation dose not only in body CT but in coronary CT. The ASIR technique was reported to provide about 27% of radiation dose reduction compared to that standard filtered back projection reconstruction[43]. In addition, image quality and the proportion of interpretable segments were also improved with the application of 40% or 60% ASIR in CCTA reconstruction compared to that filtered back projection reconstruction[43]. Another study using the similar reconstruction method with different nomenclature, namely iterative reconstruction in image space (IRIS) also resulted in significant reduction of image noise and improved subjective image quality[45]. However, the main limitation to its routine use is the high computational cost, which can be 100-1000 times higher than for filtered back projection[46].

Moreover, iterative reconstruction does not assume that the measured signal is free of noise due to x-ray photon statistics or electronic noise but rather uses more accurate statistical modeling during the reconstruction process[42]. This enables improved noise properties in the reconstructed images, while maintaining spatial resolution and other image quality parameters. The use of iterative reconstruction techniques is expected to increase in CT as computational processing improves and algorithms become more robust and easy to apply. Owing to more powerful iterative reconstruction algorithms are emerging, the impact of these techniques may show greater noise reduction and thereby permit further reductions in radiation exposure to patients.

PROSPECTIVELY ECG-TRIGGERED CORONARY CT ANGIOGRAPHY

Various strategies have been developed to reduce radiation exposure to patients, and prospectively ECG-gated CT coronary angiography is remained as the most important and effective in reducing the radiation dose which also called step-and-shoot mode. The step-and-shoot mode is characterized by turning on the x-ray tube only at a predefined time point of the cardiac cycle, usually in mid-diastole, while keeping the patient table stationary. The x-ray exposure time of this technique is short,

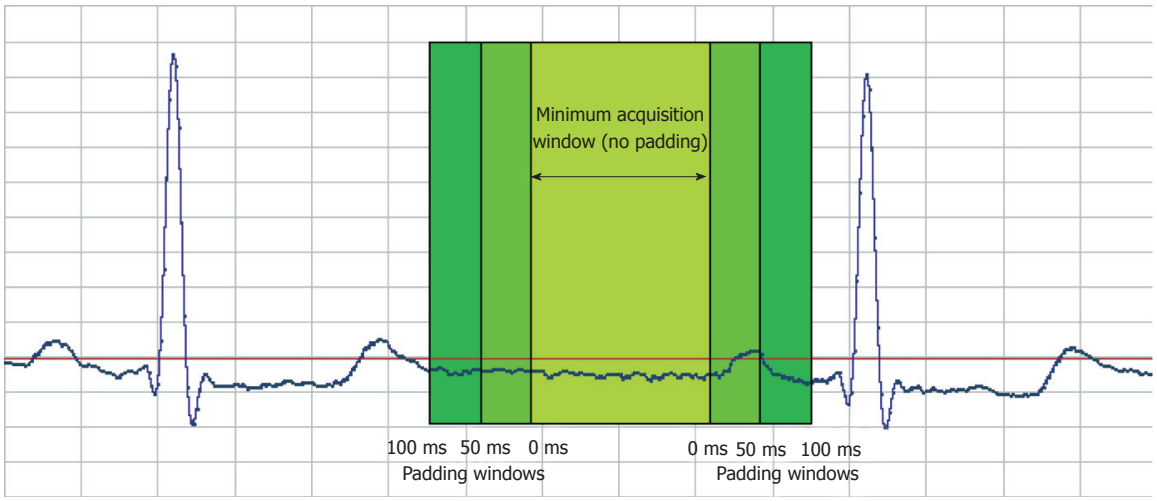

Figure 1 Use of extra tube-on time to acquire image data during additional cardiac phases. Padding turns tube on prior to minimum half-scan time and leaves it on afterwards. It is recommended in cases when heart rate varies during examination.

and thus, low radiation doses ranging between 1.2 and 4.3 mSv have been reported using various 64-slice and first-generation of dual-source 64-slice CT[32,47]. Most importantly, this low-dose step-and-shoot method is still being able to produce high diagnostic accuracy for the detection of coronary stenosis[32,48].

Unlike standard retrospective ECG-gating, where the tube output (in mA) is constant throughout the data acquisition during spiral CT which results in high radiation dose, prospective triggering is performed with sequential scans. In prospective triggering, the tube current is turned off for most of the scan period and is triggered by the ECG to be "on" only for a short period during diastole. Thus, this results in remarkable reduction in radiation dose[49]. With application of prospective ECG triggering, the radiation dose of CCTA can be reduced by up to 83% when compared to that standard retrospective ECG gating technique[47,49].

Prospectively ECG-triggered technique uses axial images and an incrementally moving table to cover the heart with minimal overlap of axial slices. Cardiac imaging with electron beam CT also uses prospective data acquisition triggered by ECG. Prospective triggered technique in cardiac CT is not new and it was actually being used in early 1980 by Dr. Godfrey Hounsfield with conventional single-slice CT[50]. It was recognized that CT image synchronization with heart diastolic phase was optimal for imaging the heart. Unfortunately, the findings were not being achieved when the patient heart rate increases.

When a 64-slice system is used, the scan is prescribed by using 3-5 incremental of 64 mm × 0.625 mm (40 mm) image groups which requires 2-4 incremental table translations of 35 mm. Thus, allow for 5 mm of overlap. The minimum interscan delay is approximately between 0.6 and 1.0 second which normally requires skipping a cardiac cycle between data acquisitions which results in one image acquisition per 2 cardiac R-R cycles[49]. However, the process will be faster with larger detectors (128-, 256- or 320-slice CT) being used. The detector width determines the number of steps/scans to cover the entire heart and complete an examination. For instance, the dual-source 64-slice CT has a narrower detector array (32 mm × 2 mm × 0.6 mm = 38.4 mm per acquisition); thus, it takes more incremental steps (normally 4-5 cardiac cycles) to cover the heart and complete an examination than with the 320-row system (320 × 0.5 mm = 160 mm) which covers the heart in a single acquisition[51].

Prospectively ECG-triggered technique has a limited number of cardiac phases available for reconstruction. Therefore, mid-diastolic phase (75% of R-R interval) was always being selected for data acquisition for all subjects. In addition, by using add-on 'padding' will allow more cardiac phases for reconstruction. Padding technique is described as prolonging the acquisition window in order to allow the reconstruction to adapt with minor heart rate variations and to produce consistent image quality. Padding turns the X-ray tube on before and after the minimum or actual acquisition time (milliseconds) required. Available padding options with current software ranges from 0 to 200 ms (Figure 1). No padding is required for patient with stable heart rates and minimal heart rate variability. However, radiation dose also will increase with application of padding window due to expense of radiation exposure on the particular windows phase[24,49].

Other than adjusting prospective triggering parameters in order to adapt with high heart rates, application of β-blockade for heart rate control is also commonly used in CCTA to produce better results. However, precautions have to be taken in patients who are contraindicated to β-blockage agent. Alternatively, calcium channel blocker could be used in order to reduce the heart rate. The maximum of 15 mg of intravenous metoprolol (β-blocker) or 40 mg of intravenous diltiazem (calcium channel blocker) is recommended prior to the scan in order to control the heart rat[49,52].

The major drawback of prospective ECG triggering is that cardiac functional analysis is unavailable. Since pro-

Table 1 Dose reduction strategies and corresponding effectiveness in dose reduction in coronary computer tomography angiography

Techniques	Advantages	Pitfalls	Dose reduction
Tube current modulation: anatomy-based	Suitable for unsymmetrical body habitus	No apparent reduction in CCTA procedure due to homogeneity of the body thickness in the cardiac region	20%-60%[1]
Tube current modulation: ECG- controlled	Dedicated for cardiac imaging Modulates tube current output during systolic phase	Heart rate must be regular	30%-50%
Low tube voltage (kVp)	Image structure with high-atomic number becomes more prominent than that with low-atomic number	Beam hardening artifacts may occur May increase image noise which leads to suboptimal image quality	Up to 30%
High pitch value	Fast image acquisition Reduce motion artifacts	Patient heart rate must at < 65 bpm and regular Can only be performed on second generation of dual-source CT scanner	Up to 80%
Iterative reconstruction algorithms	Improve contrast-to-noise ratio and spatial resolution Reduce image noise	High computational cost	Up to 40%
Prospectively ECG- triggered CCTA	High sensitivity in the detection of CAD Tube current is only 'on' in a short period during diastolic phase	Limited number for cardiac reconstruction phases No cardiac functional analysis	Up to 83%

[1]Applied to the abdominal-pelvic region. CT: Computed tomography; CCTA: Coronary CT angiography; CAD: Coronary artery disease; ECG: Electrocardiogram.

spective technique acquires data during a limited portion of the cardiac cycle, it cannot be used to evaluate cardiac function. Both quantitative and qualitative functions, either global or regional, require images to be reconstructed throughout the entire cardiac cycle. If the clinical scenario or referring physician requires information about cardiac function, then retrospective gating must be undertaken. Heart rate variability is another limitation for the prospective ECG triggered technique. Heart rate variability of > 5 beat/min is considered not applicable for prospective triggering. Therefore, the scan has to be reverted into retrospective ECG gating technique if patients' heart rate elevated or heart rate variability does not meet the requirement after β-blocker has been given[49]. However, the prospective ECG triggered technique in patients with higher heart rates still produces diagnostic images. CT scanner with higher detector arrays is an alternative to obtain CCTA in patients with high or irregular heart rates. It has been reported that high diagnostic value could be achieved with 320-slice CT angiography in the diagnosis of CAD, with image quality independent of heart rate[51]. The improved temporal resolution (175 ms) and increased coverage scan value (160 mm) of 320-slice CT results in robust image quality within a wide range of heart rates; thus providing the opportunity to image patients with higher heart rates without requiring pre-examination beta-blockage[51].

CONCLUSION

Recent technological developments have led coronary CT to be used widely and the acceptable indications for CCTA imaging become broaden. However, despite the strength of CCTA, the potential risk of radiation- induced malignancy has received attention in scientific publications although it may be unproven. Therefore, appropriate referral of CT studies, lowering tube voltage, using tube current modulation, increasing the pitch value, applying iterative reconstruction technique and implementation of prospective ECG-triggering CCTA enable CCTA to be performed at a low dose while preserving good image quality and diagnostic accuracy. Table 1 summarises above-mentioned dose-reduction strategies and corresponding effectiveness in the reduction of radiation dose associated with CCTA.

REFERENCES

1 **Buth J**, Disselhoff B, Sommeling C, Stam L. Color-flow duplex criteria for grading stenosis in infrainguinal vein grafts. *J Vasc Surg* 1991; **14**: 716-726; discussion 726-728 [PMID: 1960803 DOI: 10.1016/j.jacc.2009.04.027]

2 **Sun Z**, Ng KH. Diagnostic value of coronary CT angiography with prospective ECG-gating in the diagnosis of coronary artery disease: a systematic review and meta-analysis. *Int J Cardiovasc Imaging* 2012; **28**: 2109-2119 [PMID: 22212661 DOI: 10.1007/s10554-011-0006-0]

3 **Sun Z**, Choo GH, Ng KH. Coronary CT angiography: current status and continuing challenges. *Br J Radiol* 2012; **85**: 495-510 [PMID: 22253353]

4 **Sun Z**. Multislice CT angiography in coronary artery disease: Technical developments, radiation dose and diagnostic value. *World J Cardiol* 2010; **2**: 333-343 [PMID: 21160611]

5 **d'Agostino AG**, Remy-Jardin M, Khalil C, Delannoy-Deken V, Flohr T, Duhamel A, Remy J. Low-dose ECG-gated 64-slices helical CT angiography of the chest: evaluation of image quality in 105 patients. *Eur Radiol* 2006; **16**: 2137-2146 [PMID: 16609862]

6 **Johnson TR**, Nikolaou K, Wintersperger BJ, Leber AW, von Ziegler F, Rist C, Buhmann S, Knez A, Reiser MF, Becker CR. Dual-source CT cardiac imaging: initial experience. *Eur Radiol* 2006; **16**: 1409-1415 [PMID: 16770652]

7 **Poll LW**, Cohnen M, Brachten S, Ewen K, Mödder U. Dose reduction in multi-slice CT of the heart by use of ECG-controlled tube current modulation ("ECG pulsing"): phantom measurements. *Rofo* 2002; **174**: 1500-1505 [PMID: 12471520]

8 **Jung B**, Mahnken AH, Stargardt A, Simon J, Flohr TG, Schaller S, Koos R, Günther RW, Wildberger JE. **Individually weight-adapted** examination protocol in retrospectively ECG-gated MSCT of the heart. *Eur Radiol* 2003; **13**: 2560-2566 [PMID: 14569412]

9 **Starck G**, Lönn L, Cederblad A, Forssell-Aronsson E, Sjöström L, Alpsten M. A method to obtain the same levels of CT image

noise for patients of various sizes, to minimize radiation dose. *Br J Radiol* 2002; **75**: 140-150 [PMID: 11893638]
10 **Abada HT**, Larchez C, Daoud B, Sigal-Cinqualbre A, Paul JF. MDCT of the coronary arteries: feasibility of low-dose CT with ECG-pulsed tube current modulation to reduce radiation dose. *AJR Am J Roentgenol* 2006; **186**: S387-S390 [PMID: 16714613]
11 **Wintersperger B**, Jakobs T, Herzog P, Schaller S, Nikolaou K, Suess C, Weber C, Reiser M, Becker C. Aorto-iliac multidetector-row CT angiography with low kV settings: improved vessel enhancement and simultaneous reduction of radiation dose. *Eur Radiol* 2005; **15**: 334-341 [PMID: 15611872]
12 **Geleijns J**, Salvadó Artells M, Veldkamp WJ, López Tortosa M, Calzado Cantera A. Quantitative assessment of selective in-plane shielding of tissues in computed tomography through evaluation of absorbed dose and image quality. *Eur Radiol* 2006; **16**: 2334-2340 [PMID: 16604323]
13 **Hohl C**, Mühlenbruch G, Wildberger JE, Leidecker C, Süss C, Schmidt T, Günther RW, Mahnken AH. Estimation of radiation exposure in low-dose multislice computed tomography of the heart and comparison with a calculation program. *Eur Radiol* 2006; **16**: 1841-1846 [PMID: 16456650]
14 **Achenbach S**, Marwan M, Ropers D, Schepis T, Pflederer T, Anders K, Kuettner A, Daniel WG, Uder M, Lell MM. Coronary computed tomography angiography with a consistent dose below 1 mSv using prospectively electrocardiogram-triggered high-pitch spiral acquisition. *Eur Heart J* 2010; **31**: 340-346 [PMID: 19897497 DOI: 10.1093/eurheartj/ehp470]
15 **Achenbach S**, Marwan M, Schepis T, Pflederer T, Bruder H, Allmendinger T, Petersilka M, Anders K, Lell M, Kuettner A, Ropers D, Daniel WG, Flohr T. High-pitch spiral acquisition: a new scan mode for coronary CT angiography. *J Cardiovasc Comput Tomogr* 2009; **3**: 117-121 [PMID: 19332343 DOI: 10.1016/j.jcct.2009.02.008]
16 **Paul JF**, Abada HT. Strategies for reduction of radiation dose in cardiac multislice CT. *Eur Radiol* 2007; **17**: 2028-2037 [PMID: 17318604]
17 **Sun Z**, Ng KH. Prospective versus retrospective ECG-gated multislice CT coronary angiography: a systematic review of radiation dose and diagnostic accuracy. *Eur J Radiol* 2012; **81**: e94-100 [PMID: 21316887]
18 **Deetjen A**, Möllmann S, Conradi G, Rolf A, Schmermund A, Hamm CW, Dill T. Use of automatic exposure control in multislice computed tomography of the coronaries: comparison of 16-slice and 64-slice scanner data with conventional coronary angiography. *Heart* 2007; **93**: 1040-1043 [PMID: 17395667]
19 **Kalra MK**, Maher MM, Toth TL, Schmidt B, Westerman BL, Morgan HT, Saini S. Techniques and applications of automatic tube current modulation for CT. *Radiology* 2004; **233**: 649-657 [PMID: 15498896]
20 **Greess H**, Nömayr A, Wolf H, Baum U, Lell M, Böwing B, Kalender W, Bautz WA. Dose reduction in CT examination of children by an attenuation-based on-line modulation of tube current (CARE Dose). *Eur Radiol* 2002; **12**: 1571-1576 [PMID: 12042970]
21 **Suess C**, Chen X. Dose optimization in pediatric CT: current technology and future innovations. *Pediatr Radiol* 2002; **32**: 729-734; discussion 751-754 [PMID: 12244463]
22 **Horiuchi T**. Study on 3D modulation auto mA. *Jpn Soc Radiol Technol* 2002; **78**: 166
23 **Schwartzman D**, Lacomis J, Wigginton WG. Characterization of left atrium and distal pulmonary vein morphology using multidimensional computed tomography. *J Am Coll Cardiol* 2003; **41**: 1349-1357 [PMID: 12706931]
24 **Hausleiter J**, Meyer T, Hadamitzky M, Huber E, Zankl M, Martinoff S, Kastrati A, Schömig A. Radiation dose estimates from cardiac multislice computed tomography in daily practice: impact of different scanning protocols on effective dose estimates. *Circulation* 2006; **113**: 1305-1310 [PMID: 16520411]
25 **Leber AW**, Knez A, von Ziegler F, Becker A, Nikolaou K, Paul S, Wintersperger B, Reiser M, Becker CR, Steinbeck G, Boekstegers P. Quantification of obstructive and nonobstructive coronary lesions by 64-slice computed tomography: a comparative study with quantitative coronary angiography and intravascular ultrasound. *J Am Coll Cardiol* 2005; **46**: 147-154 [PMID: 15992649]
26 **Earls JP**, Berman EL, Urban BA, Curry CA, Lane JL, Jennings RS, McCulloch CC, Hsieh J, Londt JH. Prospectively gated transverse coronary CT angiography versus retrospectively gated helical technique: improved image quality and reduced radiation dose. *Radiology* 2008; **246**: 742-753 [PMID: 18195386 DOI: 10.1148/radiol.2463070989]
27 **Huda W**, Scalzetti EM, Levin G. Technique factors and image quality as functions of patient weight at abdominal CT. *Radiology* 2000; **217**: 430-435 [PMID: 11058640]
28 **Huda W**. Dose and image quality in CT. *Pediatr Radiol* 2002; **32**: 709-713; discussion 751-754 [PMID: 12244459]
29 **Siegel MJ**, Schmidt B, Bradley D, Suess C, Hildebolt C. Radiation dose and image quality in pediatric CT: effect of technical factors and phantom size and shape. *Radiology* 2004; **233**: 515-522 [PMID: 15358847]
30 **Boone JM**, Geraghty EM, Seibert JA, Wootton-Gorges SL. Dose reduction in pediatric CT: a rational approach. *Radiology* 2003; **228**: 352-360 [PMID: 12893897]
31 **Cody DD**, Moxley DM, Krugh KT, O'Daniel JC, Wagner LK, Eftekhari F. Strategies for formulating appropriate MDCT techniques when imaging the chest, abdomen, and pelvis in pediatric patients. *AJR Am J Roentgenol* 2004; **182**: 849-859 [PMID: 15039151]
32 **Herzog BA**, Husmann L, Burkhard N, Gaemperli O, Valenta I, Tatsugami F, Wyss CA, Landmesser U, Kaufmann PA. Accuracy of low-dose computed tomography coronary angiography using prospective electrocardiogram-triggering: first clinical experience. *Eur Heart J* 2008; **29**: 3037-3042 [PMID: 18996954 DOI: 10.1093/eurheartj/ehn485]
33 **Ertel D**, Lell MM, Harig F, Flohr T, Schmidt B, Kalender WA. Cardiac spiral dual-source CT with high pitch: a feasibility study. *Eur Radiol* 2009; **19**: 2357-2362 [PMID: 19565245 DOI: 10.1007/s00330-009-1503-6]
34 **Hausleiter J**, Bischoff B, Hein F, Meyer T, Hadamitzky M, Thierfelder C, Allmendinger T, Flohr TG, Schömig A, Martinoff S. Feasibility of dual-source cardiac CT angiography with high-pitch scan protocols. *J Cardiovasc Comput Tomogr* 2009; **3**: 236-242 [PMID: 19577211 DOI: 10.1016/j.jcct.2009.05.012]
35 **Goetti R**, Leschka S, Baumüller S, Plass A, Wieser M, Desbiolles L, Stolzmann P, Falk V, Marincek B, Alkadhi H, Feuchtner G. Low dose high-pitch spiral acquisition 128-slice dual-source computed tomography for the evaluation of coronary artery bypass graft patency. *Invest Radiol* 2010; **45**: 324-330 [PMID: 20404735 DOI: 10.1097/RLI.0b013e3181dfa47e]
36 **Lell M**, Hinkmann F, Anders K, Deak P, Kalender WA, Uder M, Achenbach S. High-pitch electrocardiogram-triggered computed tomography of the chest: initial results. *Invest Radiol* 2009; **44**: 728-733 [PMID: 19809339 DOI: 10.1097/RLI.0b013e3181b9df7e]
37 **Lell M**, Marwan M, Schepis T, Pflederer T, Anders K, Flohr T, Allmendinger T, Kalender W, Ertel D, Thierfelder C, Kuettner A, Ropers D, Daniel WG, Achenbach S. Prospectively ECG-triggered high-pitch spiral acquisition for coronary CT angiography using dual source CT: technique and initial experience. *Eur Radiol* 2009; **19**: 2576-2583 [PMID: 19760421 DOI: 10.1007/s00330-009-1558-4]
38 **Leschka S**, Stolzmann P, Desbiolles L, Baumueller S, Goetti R, Schertler T, Scheffel H, Plass A, Falk V, Feuchtner G, Marincek B, Alkadhi H. Diagnostic accuracy of high-pitch dual-source CT for the assessment of coronary stenoses: first experience. *Eur Radiol* 2009; **19**: 2896-2903 [PMID: 19760229 DOI: 10.1007/s00330-009-1618-9]
39 **Alkadhi H**, Stolzmann P, Desbiolles L, Baumueller S, Goetti R, Plass A, Scheffel H, Feuchtner G, Falk V, Marincek B, Leschka S. Low-dose, 128-slice, dual-source CT coronary angiography: accuracy and radiation dose of the high-pitch and the step-and-shoot mode. *Heart* 2010; **96**: 933-938 [PMID: 20538669 DOI: 10.1136/hrt.2009.189100]
40 **Knesaurek K**, Machac J, Vallabhajosula S, Buchsbaum MS. A

new iterative reconstruction technique for attenuation correction in high-resolution positron emission tomography. *Eur J Nucl Med* 1996; **23**: 656-661 [PMID: 8662099]
41 **Liow JS**, Strother SC, Rehm K, Rottenberg DA. Improved resolution for PET volume imaging through three-dimensional iterative reconstruction. *J Nucl Med* 1997; **38**: 1623-1631 [PMID: 9379203]
42 **Cheng LCY**, Fang T, Tyan J. Fast iterative adaptive reconstruction in low-dose CT imaging. In: Proceedings of the Proceedings of the IEEE International Conference on Image Processing. Sep 1996; Lausanne, 1996: 889-892
43 **Leipsic J**, Labounty TM, Heilbron B, Min JK, Mancini GB, Lin FY, Taylor C, Dunning A, Earls JP. Adaptive statistical iterative reconstruction: assessment of image noise and image quality in coronary CT angiography. *AJR Am J Roentgenol* 2010; **195**: 649-654 [PMID: 20729442 DOI: 10.2214/AJR.10.4285]
44 **Thibault JB**, Sauer KD, Bouman CA, Hsieh J. A three-dimensional statistical approach to improved image quality for multislice helical CT. *Med Phys* 2007; **34**: 4526-4544 [PMID: 18072519]
45 **Bittencourt MS**, Schmidt B, Seltmann M, Muschiol G, Ropers D, Daniel WG, Achenbach S. Iterative reconstruction in image space (IRIS) in cardiac computed tomography: initial experience. *Int J Cardiovasc Imaging* 2011; **27**: 1081-1087 [PMID: 21120612 DOI: 10.1007/s10554-010-9756-3]
46 **Wang G**, Yu H, De Man B. An outlook on x-ray CT research and development. *Med Phys* 2008; **35**: 1051-1064 [PMID: 18404940]
47 **Shuman WP**, Branch KR, May JM, Mitsumori LM, Lockhart DW, Dubinsky TJ, Warren BH, Caldwell JH. Prospective versus retrospective ECG gating for 64-detector CT of the coronary arteries: comparison of image quality and patient radiation dose. *Radiology* 2008; **248**: 431-437 [PMID: 18552312 DOI: 10.1148/radiol.2482072192]
48 **Scheffel H**, Alkadhi H, Leschka S, Plass A, Desbiolles L, Guber I, Krauss T, Gruenenfelder J, Genoni M, Luescher TF, Marincek B, Stolzmann P. Low-dose CT coronary angiography in the step-and-shoot mode: diagnostic performance. *Heart* 2008; **94**: 1132-1137 [PMID: 18519548 DOI: 10.1136/hrt.2008.149971]
49 **Earls JP**. How to use a prospective gated technique for cardiac CT. *J Cardiovasc Comput Tomogr* 2009; **3**: 45-51 [PMID: 19201376 DOI: 10.1016/j.jcct.2008.10.013]
50 **Hounsfield GN**. Computed medical imaging. *Science* 1980; **210**: 22-28 [PMID: 6997993]
51 **Hoe J**, Toh KH. First experience with 320-row multidetector CT coronary angiography scanning with prospective electrocardiogram gating to reduce radiation dose. *J Cardiovasc Comput Tomogr* 2009; **3**: 257-261 [PMID: 19577215 DOI: 10.1016/j.jcct.2009.05.013]
52 **Pannu HK**, Alvarez W, Fishman EK. Beta-blockers for cardiac CT: a primer for the radiologist. *AJR Am J Roentgenol* 2006; **186**: S341-S345 [PMID: 16714607]

P- Reviewers: Peteiro J, Ueda H
S- Editor: Zhai HH **L- Editor**: A **E- Editor**: Liu XM

World Journal of Cardiology

Online Submissions: http://www.wjgnet.com/esps/
bpgoffice@wjgnet.com
doi:10.4330/wjc.v5.i12.473

World J Cardiol 2013 December 26; 5(12): 473-483
ISSN 1949-8462 (online)

TOPIC HIGHLIGHT

Zhonghua Sun, PhD, Associate Professor, *Series Editor*

Coronary CT angiography: Diagnostic value and clinical challenges

Akmal Sabarudin, Zhonghua Sun

Akmal Sabarudin, Diagnostic Imaging and Radiotherapy Program, School of Diagnostic and Applied Health Sciences, Faculty of Health Sciences, Universiti Kebangsaan Malaysia, Kuala Lumpur 50300, Malaysia
Zhonghua Sun, Discipline of Medical Imaging, Department of Imaging and Applied Physics, Curtin University, Western Australia 6845, Australia
Author contributions: Both authors contributed equally to this paper.
Correspondence to: Zhonghua Sun, Associate Professor, Discipline of Medical Imaging, Department of Imaging and Applied Physics, Curtin University, GPO Box, U1987 Perth, Western Australia 6845, Australia. z.sun@curtin.edu.au
Telephone: +61-8-92667509 Fax: +61-8-92662377
Received: July 24, 2013 Revised: September 25, 2013
Accepted: October 11, 2013
Published online: December 26, 2013

Abstract

Coronary computed tomography (CT) angiography has been increasingly used in the diagnosis of coronary artery disease due to improved spatial and temporal resolution with high diagnostic value being reported when compared to invasive coronary angiography. Diagnostic performance of coronary CT angiography has been significantly improved with the technological developments in multislice CT scanners from the early generation of 4-slice CT to the latest 320- slice CT scanners. Despite the promising diagnostic value, coronary CT angiography is still limited in some areas, such as inferior temporal resolution, motion-related artifacts and high false positive results due to severe calcification. The aim of this review is to present an overview of the technical developments of multislice CT and diagnostic value of coronary CT angiography in coronary artery disease based on different generations of multislice CT scanners. Prognostic value of coronary CT angiography in coronary artery disease is also discussed, while limitations and challenges of coronary CT angiography are highlighted.

Key words: Coronary artery disease; Coronary CT angiography; Diagnostic value; Multislice CT; Artifacts

Core tip: Coronary Computed tomography (CT) angiography represents the technical evolution in cardiac imaging due to its high diagnostic value in coronary artery disease as a less invasive technique. Diagnostic performance of coronary CT angiography is significantly enhanced with the development of multislice CT scanners, ranging from 4-slice to 64- and post-64 slice scanners. This article provides readers with a comprehensive review of the diagnostic value of coronary CT angiography according to different generations of multislice CT, with limitations and challenges being addressed.

Sabarudin A, Sun Z. Coronary CT angiography: Diagnostic value and clinical challenges. *World J Cardiol* 2013; 5(12): 473-483 Available from: URL: http://www.wjgnet.com/1949-8462/full/v5/i12/473.htm DOI: http://dx.doi.org/10.4330/wjc.v5.i12.473

INTRODUCTION

Computed tomography (CT) scanner has rapidly evolved from single slice to multislice CT (MSCT) which started from 4-slice systems in 1998 to the latest 256-slice and 320-slice CT systems. With smaller detector size and faster gantry rotation speed, spatial and temporal resolutions of the 64- and post-64 MSCT scanners have enabled coronary artery imaging a feasible and reliable clinical test. The technological advancements from 16- to 320-slice systems have progressed in a relatively uniform fashion with improved longitudinal (z-axis) volume cov-

erage, decreased gantry rotation time, and smaller detector elements[1,2]. With the ability to acquire volume data, technological improvements in CT scanning also enable generation of 3D image processing such as multiplanar reformation, maximum intensity projection, surface-shaded display, and volume-rendering techniques, and these reconstructed visualizations have made coronary CT angiography (CCTA) an important component of medical imaging visualization in daily practice[3].

The purpose of this paper is to provide an overview of CCTA with a focus on the diagnostic accuracy and prognostic value in coronary artery disease. Technological developments of MSCT scanners are briefly discussed, while limitations and challenges of CCTA are highlighted.

TECHNOLOGICAL DEVELOPMENTS IN CCTA

Diagnostic performance of CCTA is closely related to technological improvements that occurred with each successive generation of MSCT scanners. The spatial and temporal resolution of MSCT scanners determine the diagnostic value of CCTA in coronary artery disease (CAD).

4-slice CT

In 1998, a 4-slice CT scanner was introduced by several manufacturers representing an obvious quantum leap in clinical performance[4,5]. Four detector "rows"corresponding to the 4 simultaneously collected slices fed data into four parallel data "channels", so that these 4-slice scanners were said to possess four data channels. These 4-slice scanners, however, were quite flexible with regard to how detector rows could be configured; groups of detector elements in the z-direction could be electronically linked to function as a single, longer detector, thus providing more flexibility in the section thickness of the four acquired slices[6,7]. Fundamental advantages of MSCT include substantially shorter acquisition times, retrospective creation of thinner or thicker sections from the same raw data, and improved three-dimensional rendering with diminished helical artifacts[4].

The main advantage is the increased volume coverage per unit time at high axial resolution and subsequent improved temporal resolution[4]. Four-slice scanners are the basic system for CCTA examination. With only 250 ms of temporal resolution from a gantry rotation of 500 ms CCTA with use of 4-slice CT requires longer longitudinal scan to cover the entire cardiac chamber and coronary arteries, thus, this may result in long breath-hold between 30 and 40 s which leads to breathing and motion artifacts, and also limits to patients with low heart rates[8].

16-slice CT

The installation of 16-slice CT scanners in 2002 provides 16 detector channels enabling simultaneously acquisition of 16 slices per gantry rotation[9]. In addition to simultaneously acquiring up to 16 slices, the detector arrays associated with 16-slice scanners were redesigned to allow thinner slices to be obtained as well. Note that in all of the models, the innermost 16 detector elements along the z-axis are half the size of the outermost elements, allowing simultaneous acquisition of 16 thin slices (from 0.5 mm to 0.75 mm thick, depending on the model and manufacturer). When the inner detectors were used to acquire submillimeter slices, the total acquired z-axis length and therefore the total width of the x-ray beam ranged from 8 mm for the Toshiba model to 12 mm for the Philips and Siemens scanners. Alternatively, the inner 16 elements could be linked in pairs for the acquisition of up to 16 thicker slices[10].

Sixteen-slice scanners have a slightly better spatial resolution and faster gantry rotation (420 ms) than that in 4-slice CT[11]. The major advantage of 16-slice scanners over 4-slice CT is the longer z-axis coverage (16 mm × 0.75 mm *vs* 4 mm × 1.0 mm), resulting in significantly shorter breath- hold and fewer motion artifacts[12-14]. The rotational speed of 16-slice scanners is only marginally faster, and adaptive multi-cycle reconstructions, which require a high number of detectors, cannot be applied because of heart rate variations. As a consequence of these factors, image quality with the 16-slice scanner is significantly improved, reducing the number of coronary segments with poor image quality[12-15].

CCTA became more clinically practical with 16-slice CT scanners using retrospective electrocardiogram (ECG) gating to capture cardiac motion plus the z-axis coverage[16]. However, cardiac motion and stair-step artifacts are the main challenge for this system. Therefore, there are a few steps that are suggested to overcome these problems, which include increasing the number of detector elements and the volume coverage along the z-axis of detector block. Moreover, increase in the sensitivity of detector material and application of iterative image reconstruction algorithms represents another approach to improve cardiac image quality[17,18]. During 2003 and 2004, manufacturers introduced different types of MSCT models with less than 16-slice scanners, but most commonly the introduction of more than 16-slice scanners represented the main direction for improving MSCT systems[9].

64-slice CT

The 64-slice CT was first introduced with a single x-ray source mounted opposite to a 64-detector-array in the gantry unit. With gantry rotation times down to 0.33 s for 64-slice CT (0.375 s for 16-slice CT), temporal resolution for ECG-gated cardiac imaging is again markedly improved. The increased temporal resolution of 64-slice CT has the potential to improve the clinical strength of ECG-gated cardiac examinations at higher heart rates, thereby reducing the number of patients requiring heart rate control. In contrast to previous studies, high diagnostic accuracy has been achieved despite the presence of calcified coronary plaques. In addition, using 64-slice

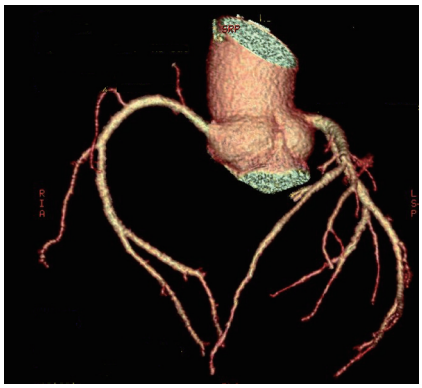

Figure 1 Three-dimensional volume rendering image acquired with 64-slice coronary computed tomography angiography demonstrates right and left coronary arteries without lumen stenosis.

CT the scanning time is reduced to less than 15 s, allowing a decreased breath-hold time, better utilization of contrast medium with fewer enhancements of adjacent structures and a lower dose of applied contrast medium. Improvement of image quality has also been reported in the visualization of all coronary artery branches with high sensitivity and specificity achieved (Figure 1).

The new-generation dual-source MSCT (Somatom Definition FLASH; Siemens Medical Solution, Forchheim, Germany) which was introduced in late 2008 is equipped with two 64-detector row units, each with an alternating focal spot. The 360° gantry rotation time is 280 ms, translating to a temporal resolution of approximately 75 ms when the scanner operates with both x-ray tubes collecting data at the same energy (Figure 2). The vendor has proposed a high-pitch prospectively ECG-triggered scanning acquisition[19,20]. In single-source 64-slice CT, the maximum pitch used in CCTA is roughly between 0.2 and 0.5 for gapless image reconstruction. The pitch can be increased up to 3.4 in dual-source Siemens Definition Flash systems. For CCTA, the typical phase window required for a diagnostic quality examination regarding motion artifact is 10% of the R-R interval. The pitch required for multiphase acquisition ranges from 0.2 to 0.5, depending on the heart rate[21].

With the high-pitch acquisition mode, only one phase is acquired, which gradually increases with the z-axis table translation. The influence on image quality for different clinical scenarios and heart rates is evaluated with the second generation dual-source CT. Achenbach *et al*[22] demonstrated the feasibility of this new scanning method using second-generation dual-source CT. However, slow and regular heart rates are the prerequisite for this acquisition protocol that is prospectively triggered by ECG signal and is anticipated to scan the entire heart in 270 ms, with a pitch of up to 3.4[22]. Another potential advantage of dual-source CT is tissue characterization with both detector systems operating at different tube voltages known as dual-energy CT (DECT). Although this has not been extensively studied to date, the two x-ray beams of different energy spectra in theory could better demonstrate

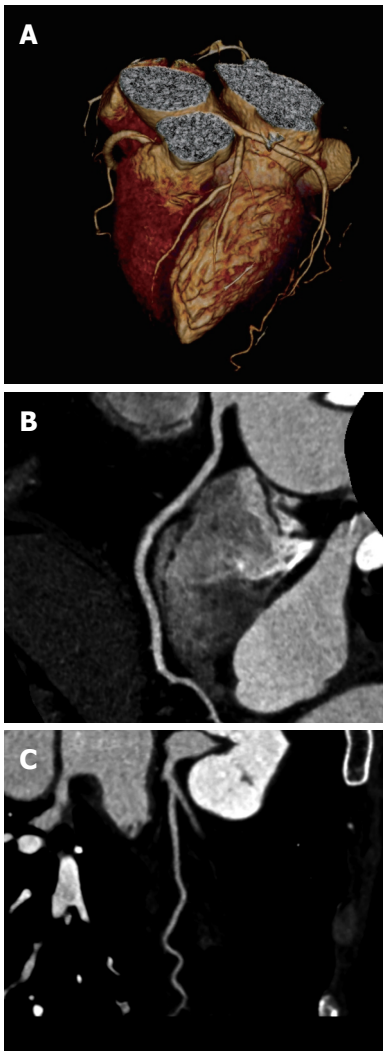

Figure 2 New-generation dual-source multislice computed tomography. A: 3D volume rendering image acquired with dual-source coronary computed tomography angiography shows excellent visualisation of normal left coronary artery and its side branches; B, C: Curved planar reformation clearly shows the anatomical structure of right and left coronary arteries.

varying attenuation characteristics of different tissues[23,24]. Studies have shown the feasibility of using DECT for myocardial perfusion imaging of CAD. Ruzsics *et al*[23] compared DECT with SPECT to evaluate the diagnostic performance of DECT for imaging coronary artery morphology and assessing myocardial blood supply. In a group of 36 patients with suspected or known CAD, over 90% diagnostic accuracy was achieved with DECT for detecting any type of myocardial perfusion defect observed on SPECT. Nagao *et al*[25] used iodine map that is available with DECT to detect alterations in coronary flow during adenosine stress and rest. This is the first non-invasive method to provide a functional assessment of coronary artery flow using cardiac CT, although further studies are needed to confirm these early results.

DECT cardiac imaging can also be achieved with a single X-ray tube. GE Healthcare's Discovery CT750 HD spectral imaging is based on fast kV switching-dynamic

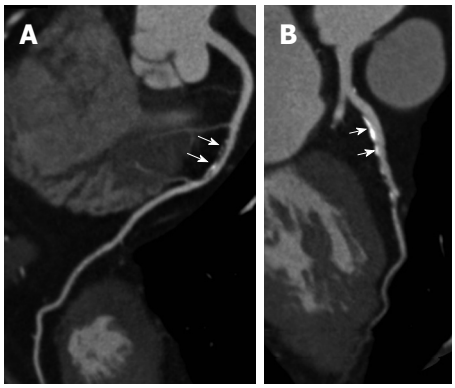

Figure 3 Electrocardiogram-triggered coronary computed tomography angiography. Prospectively ECG-triggered coronary computed tomography angiography shows a mixed plaque at the mid-segment of right coronary artery (A, arrows), and calcified plaques at the proximal segment of left anterior descending branch (B, arrows). ECG: Electrocardiogram.

switching between 2 different energy levels of X-rays from view to view during a single rotation[26]. This allows for demonstration of different material densities as scatter plots, histograms and region of interest, thus, enabling myocardial perfusion analysis of cardiac function. Despite these promising results, however, large patient cohorts are needed to confirm the potential application of a single protocol for anatomic and myocardial perfusion assessment of CAD. The diagnostic accuracy of CCTA has been reported extensively in the literature ranging from the earlier studies using retrospectively ECG-gated protocols to the recent reports comparing prospective ECG-triggering and retrospective ECG-gating. In retrospectively ECG-gated CCTA, several studies on different types and generations of MSCT scanners were carried out with overall results showing that CCTA had moderate to high sensitivity of 86%-99% and high specificity of 89%-100% in patients with suspected CAD. Image quality of coronary artery visualization was impaired and suboptimal in a number of cases with 4-slice CT as the unassessable coronary segments could be as high as more than 20%[27]. With 16-and 64-slice CT, thinner detector rows increased the spatial resolution and further shortened the total scan time, resulting in improved diagnostic value of CCTA[12,14,15]. In particular, a very high negative predictive value of over 95% (96%-99%) has been reported in these studies indicating that CCTA can be used as a reliable screening tool for CAD[28,29]. Moreover, multicenter studies were also conducted on 64-slice CT scanner to investigate the diagnostic accuracy of CCTA with different risks of CAD prevalence. The results showed that high sensitivity (94%), specificity (83%) and negative predictive value (99%) was achieved in high risk patients with CAD (68%). Similarly, high diagnostic accuracy was also presented in low risk of CAD with sensitivity, specificity and negative predictive value being 94%, 83% and 99% in 25% of CAD prevalence; 85%, 90% and 83% in 56% of CAD prevalence, respectively[30-32]. A study on the high-pitch mode with dual source CT also resulted in high sensitivity, specificity and negative predictive value of 94%, 91% and 97% respectively[33]. Over the last few years, prospectively ECG-triggered CCTA is increasingly used in the diagnosis of CAD with promising results reported. The sensitivity (93.7%-100%), specificity (82.7%-97%) and negative predictive value (95%-98%) in the assessment of CAD were reported in multiple studies confirming the feasibility of this fast developing technique[28,29] (Figure 3).

128- and 256-slice CT

In late 2007, the 128-slice CT (Brilliance iCT; Philips Healthcare, Cleveland, OH) was introduced with a 128 mm × 0.625 mm detector row system with dual focal spot positions to double the number of slices within the 8-cm (width) z-axis gantry coverage. The iCT has a gantry rotation time of 270 ms, which translates to an approximate temporal resolution of 135 ms. Prospectively ECG-triggered CCTA typically covers the entire heart in two axial acquisitions over three heartbeats. During the diastole of the first heartbeat, the upper half of the heart is imaged. During the second heartbeat, the X-ray table translates 62.4 mm. Subsequently, the lower half of the heart is acquired during the diastole of the third heartbeat. The scanner is equipped with several radiation reduction capabilities, including a dynamic helical collimator and an adaptive axial collimator to reduce z-over scanning[34,35].

Second generation of 128-slice CT was introduced with dual-source which uses two x-ray tubes with opposing 64 detector arrays mounted 90° from each other. The main advantage of this system is that the temporal resolution is effectively halved because each x-ray tube/detector array system only needs to rotate half of the angle that would otherwise be required by a single-source system. The number of detector rows in the longitudinal axis (z-axis) and the number of slices of CT system are not interchangeable terms because multiple systems with an alternating focal spot allow the same z-axis coverage to be sampled twice, and thus the number of image slices generated is double the number of detector rows[20]. However, the volume coverage remains the same; for example, a 128-detector row scanner with two alternating z-focal spot positions can be referred to as 256-slice CT. It is important to specify the number of detector rows in z-axis, with or without alternating focal spot positions, and single versus dual source. A 128-slice dual-source CT also demonstrated high diagnostic accuracy of 93%, 94% and 97% corresponding to sensitivity, specificity and negative predictive value, respectively[33].

Most of the current studies using 128- and 256-slice CCTA focus on image quality and radiation dose reduction, while reports on the diagnostic performance are scarce[34-36]. Two recent studies have reported that 256-slice CCTA have high sensitivity (> 90% patient- and segment-based) and high diagnostic accuracy in patients with suspected CAD, with resultant very low radiation dose[37,38], althoughfurther research is needed to investigate the di-

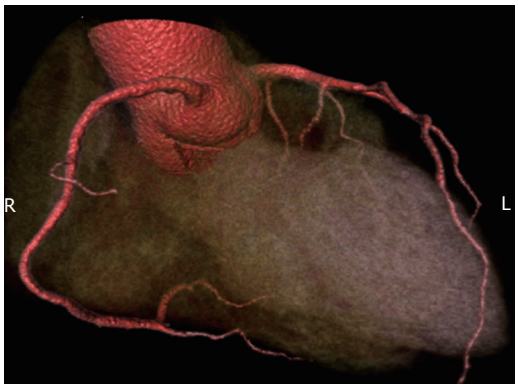

Figure 4 3D volume rendering image acquired with 320-slice coronary computed tomography angiography in a single heartbeat shows excellent visualisation of coronary arteries and side branches without artifacts.

agnostic performance of CCTA with use of these recent models based on a large cohort and multi-centre studies.

320-slice CT

This hardware (Aquilion One Dynamic Volume CT; Toshiba Medical System, Japan) currently has the largest z-axis detector coverage. It was released shortly after experiments with a 256-detector row CT prototype[39-41]. Each detector element is 0.5 mm wide, yielding a maximum of 16-cm z-axis coverage (Figure 4). This configuration allows three-dimensional volumetric entire heart imaging during the diastole of one R-R interval. In 320-detector row CT, the entire heart is imaged with temporal uniformity. Furthermore, if the x-ray beam is turned on for a longer period, the scanner can capture the heart over one or more cardiac cycles. This has been described as four-dimensional CT or volumetric cine imaging[42]. The temporal resolution of CT scanner reflects the ability to freeze cardiac motion, thus producing motion-free images. The 320-detector scanner has a standard temporal resolution of approximately 175 ms, half of the gantry rotation times. For patients with higher heart rate (> 65 bpm) and contraindications to β-blockers, multi-segment reconstruction can be used at the expense of higher radiation dose. For example, in two-segment reconstruction, data required for image reconstruction are acquired over two cardiac cycles. Therefore, only data from 90° rotation during each of the two cardiac cycles are used, improving the effective temporal resolution by a factor of 2[43].

Results using 320-slice CCTA are compared favourably to the studies using 64-slice and DSCT coronary angiography[44,45]. van Velzen *et al*[44] in their recent study reported sensitivity and specificity of 100% and 85% for 320-slice CCTA in 106 patients with acute chest pain admitted to the Emergency Department. Pellicia *et al*[45] in their prospective study consisting of 118 unselected consecutive patients with suspected CAD demonstrated the excellent results with 320-slice CT, with more than 90% of sensitivity, specificity, positive predictive value and negative predictive value achieved at the per-patient, per-vessel and per-segment analysis. These results indicate that 320-slice CT has the potential to broaden the use of CCTA to more patients, such as patients with atrial fibrillation.

Two recently reported systematic reviews and meta-analyses further confirmed the high diagnostic accuracy of 320-slice CCTA[46,47]. These results also revealed that negative predictive value of CCTA was close to 100%, indicating the high value of 320-slice CCTA for excluding coronary artery stenosis. However, it has to be recognized that diagnostic performance of 320-slice CCTA is similar to that of 64- and 128-slice for the determination of ⩾ 50% coronary artery stenosis due to its limited temporal resolution, despite improved extended z-axis coverage.

DIAGNOSTIC VALUE OF CCTA: CURRENT STATUS AND CHALLENGES

Despite promising results having been achieved with CCTA in coronary artery disease, it suffers from some limitations which affect its diagnostic performance to some extent. Artifacts (motion-related or due to severe calcification) represent one of the common limitations, although this is less commonly seen in CCTA performed with latest post-64 slice CT. Heart rate comprises another issue which needs to be addressed in the cardiac imaging, and temporal resolution of CCTA is still inferior to that of invasive coronary angiography.

Artifacts

Imaging coronary arteries using coronary CT angiography requires high spatial and temporal resolution, good low-contrast resolution, intravascular contrast enhancement and a short scanning time. Image artifacts are always associated with the limitations of either temporal resolution, or noise or the reconstruction algorithm in the scanner system. Images artifacts are mainly demonstrated as blooming, streaks, partial volume and motion artifacts. All these artifacts can arise from technical, operator, and patient errors[48].

Stair-step artifact is the most common artifact that occurs in CCTA. Stair-step artifact occurs especially in patients with high heart rates, heart rate variability, and the presence of irregular or ectopic heart beats such as premature ventricular contractions and atrial fibrillation during image acquisition (Figure 5). It can be best recognized in a sagittal or coronal view. Therefore, beta-blockers should be used to lower the heart rate prior to the scan. Reducing this artifact is achieved by reconstructing the dataset at different phases of the cardiac cycle. In general, reconstructions for CCTA are performed in mid-diastole to late diastole (60%-70% of the R-R interval). However, because the duration of diastole decreases as the heart rate increases, an end-systolic phase reconstruction at 25%-35% of the R-R interval might be considered for image processing[48].

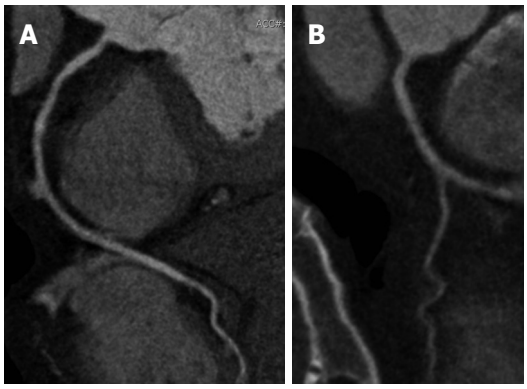

Figure 5 Prospectively electrocardiogram-triggered coronary computed tomography angiography and coronary arteries. Prospectively ECG-triggered coronary computed tomography angiography curved planar reformatted images show right (A) and left (B) coronary arteries with blurred borders due to motion artifacts. ECG: Electrocardiogram.

Heart rate

Heart rate variability is another limitation for the prospectively ECG-triggered technique. Heart rate variability of > 5 beats/minute is considered not applicable for prospective triggering. Therefore, the scan has to be reverted into retrospective ECG gating technique if patients' heart rate elevated or heart rate variability does not meet the requirement after β-blocker has been given[49]. However, precautions have to be taken in patients who are contraindicated to β-blockage agent. Alternatively, calcium channel blocker could be used in order to reduce the heart rate. The maximum of 15 mg of intravenous *metoprolol* (β-blocker) or 40 mg of intravenous diltiazem (calcium channel blocker) is recommended prior to the scan in order to control the heart rate[50,51].

However, the prospectively ECG-triggered technique in patients with higher heart rates still produces diagnostic images. CT scanner with higher detector arrays is an alternative option in patients with high or irregular heart rates. It has been reported that high diagnostic value could be achieved with 320-slice CCTA in the diagnosis of CAD, with image quality independent of heart rate[42]. The increased longitudinal coverage scan value (up to 160 mm) of 320-slice CT results in improved image quality within a wide range of heart rates; thus providing the opportunity to image patients with higher heart rates without requiring pre-examination beta-blockage[42,44,45].

Coronary CT angiography is most commonly performed in the spiral acquisition mode with continuous acquisition of data throughout the cardiac cycle. Multiple reconstruction parameters determine the quality of the reconstructed axial images. Images are usually reconstructed with a slice thickness of 0.5-0.6 mm, 50% overlap between images (0.4 mm increment), and a pixel matrix of 512 × 512. Although a thinner slice improves the resolution of the 3D dataset and the quality of reconstructed images, it comes at the cost of increased image noise, which can significantly limit the diagnostic assessment of the coronary arteries in patients with body mass index of greater than 30 kg/m^2[52].

Temporal resolution

In single-source CT, improved temporal resolution is obtained at the expense of limited spiral pitch and correspondingly increased radiation dose to the patient. For a single segment reconstruction, the table has to travel slowly in order to ensure that each z-position of the heart is visualized by a detector slice during each phase of cardiac cycle. Therefore, the patient's heart rate would determine the spiral pitch (if the heart rate goes up, the spiral pitch can be increased). Moreover, if multi-segment reconstructions are applied at higher heart rates to improve temporal resolution, the spiral pitch has to be reduced again. For example, each z-position of the heart has to be visualized by a detector slice during two consecutive heart beats in a 2-segment reconstruction; and three consecutive heart beats for a 3-segment reconstruction; and so on. In general, manufacturers of single-source CT scanners recommend an adaptive approach for ECG-gated cardiac scanning which the pitch of the ECG-gated spiral scan is kept constant at a relatively low value between 0.2 and 0.25. Therefore, more segments are used for image reconstruction at higher heart rates to improve temporal resolution[53,54].

Using a DSCT system, a temporal resolution of a quarter of the gantry rotation time is achieved, resulting in high temporal resolution of 75 ms, independent of the patient's heart rate.This shows a significant improvement in cardiac imaging. However, the temporal resolution is still inferior to that of invasive coronary angiography, which is 10 ms, therefore, aggressive approaches such as heart rate control with the use of beta-blockers are necessary in CCTA examinations.

Excellent spatial resolution of 0.4 to 0.5 mm is achieved with latest CT models, however, this is still not comparable to that of invasive coronary angiography, with spatial resolution being 0.1 and 02 mm. Although CCTA enables excellent visualization of main and side coronary arteries, identification and characterization of coronary plaques[55,56], differentiation of lipid-rich content from fibrous component with CCTA remains difficult and challenging due to overlap in the attenuation values of lipid and fibrous tissue[57].

Severe calcifications

Vessel calcification poses a serious challenge to the accurate assessment of coronary artery lumen. Calcium deposits have CT attenuation which is similar to metal density and thus overwhelm the density of other tissues in the same voxel. Beam hardening is due to the attenuation of low-energy X-ray by very dense structures such as calcium. A higher energy beam, causing a darker appearance that can be mistaken for plaque, therefore penetrates adjacent pixels. All these effects can be modified, but not eliminated, by the smaller voxel size produced by the 64-slice scanner. The efficacy of this scanner in ameliorating imaging difficulties is shown in an overall sensitivity of 95% and specificity of 90% for the detection of angiographically significant stenosis even in the

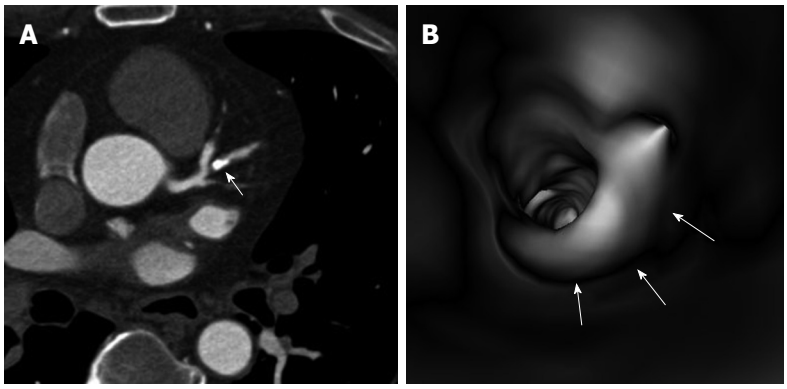

Figure 6 A severely calcified plaque is present in the left coronary artery (ramus intermedius) (A, arrow), with impression of more than 90% lumen stenosis on a 2D axial image. Corresponding 3D virtual endoscopy views shows the intraluminal protrusion sign due to presence of plaque (B, arrows), but with less than 60% lumen stenosis.

presence of high coronary calcium scores (Agatston score of > 400)[58] (Figure 6).

A study by Brodoefel *et al*[58] compared overall calcium burden and studies the effects of calcium on image quality and diagnostic accuracy. Their results showed that dual-source CCTA was affected by calcification in terms of image quality and diagnostic value. Furthermore, a total of 100 (8.1%) segments that were considered non-diagnostic because of abundant calcification suggest that calcium burden remains a fundamental problem of coronary CT angiography and is certainly not addressed by exclusive increase of temporal resolution. In fact, from the linear regression analysis[59], there is a persistent threshold for adequate image quality at an Agatston score around 400. This is supported by reports from Diederichsen *et al*[59] and Chen *et al*[60] who also concluded that the specificity of CCTA was decreased significantly in patients with high calcium score > 400. However, Stolzmann *et al*[61] stated in their study that CCTA had high diagnostic accuracy despite the presence of heavy calcifications with sensitivity and specificity being 99% and 99% in patients with median CAC score < 316, and 98% and 99% in patients with median CAC score > 316. Despite these promising results, further studies on 256- and 320-slice CT are needed to evaluate the diagnostic performance of CCTA in patients with high coronary calcium score.

PROGNOSTIC VALUE OF CCTA

CCTA allows for visualization and characterization of coronary plaques, thus, it can detect non-obstructive and non-calcified plaques as well as plaques with positive modelling, both of which play an important role in the pathophysiology of acute myocardial infarction and may be indicative of vulnerable plaques. Studies based on single centre experiences have demonstrated that CCTA provides prognostic information for predictive adverse cardiac events in patients with known or suspected CAD[62-65]. Ostrom *et al*[66] demonstrated a correlation between mortality and the number of involved vessels for both nonobstructive and obstructive coronary lesions. Min *et al*[67] reported that coronary segments with presence of plaque, regardless of stenosis severity, had a particularly good correlation with patient survival.

Prospective large and multi-centre trials evaluating patients presenting to the emergency department with acute chest pain symptoms further confirmed the prognostic value of CCTA. In a 2-year follow-up of the ROMICAT trial, Schlett *et al*[68] evaluated the prognostic value of CCTA for major adverse cardiac events in 333 patients with a mean follow-up of 23 mo. Their results showed that in acute chest pain emergency patients, CCTA provided incremental prognostic value beyond clinical risk score in predicting major adverse cardiac events with absence of CAD leading to a 2-year cardiac events free warranty period, while coronary stenosis with regional wall motion abnormalities associated with highest risk of major cardiac events. Results from the international Coronary CT Angiography Evaluation For Clinical Outcomes: An International Multicenter Registry consisting of 20299 patients have further reaffirmed the predictive value of segmental plaque burden above and beyond the degree of stenosis[69]. A predictive score combining CCTA parameters with clinical information has been demonstrated to significantly improve prediction compared with well-established clinical risk scores.

CCTA REFERRAL

Identification of the exact role of CCTA in patients from different risk groups is clinically significant as this could lead to unnecessary examinations due to the fact that CT is an imaging modality with high radiation dose[70-72]. In addition, appropriate selection of CCTA is of paramount importance for physicians to choose CCTA as a gatekeeper for further diagnostic testing. Performing CCTA before invasive coronary angiography is a cost-effective strategy in the management of patients without symptoms who have positive stress rest results. Halpern *et al*[73] in their study reported that when a patient with an expected CAD prevalence of less than 85% is found to have a positive test result, CCTA is a less expensive alternative

to invasive coronary angiography. Thus, the use of CCTA in asymptomatic patients can avoid unnecessary invasive coronary angiography procedures. CCTA is considered to be of limited clinical value in the evaluation of symptomatic patients or the high pre-test probability group as the majority of these patients are likely to proceed to invasive coronary angiography, despite the negative CCTA findings[74,75]. In patients with a high pre-test likelihood for significant stenosis, functional evaluation, such as myocardial perfusion imaging, may be more relevant than CCTA to determine the need for revascularization.

SUMMARY AND CONCLUSION

There is increasing evidence to show that coronary CT angiography represents the most rapidly developed imaging modality in cardiac imaging. Coronary CT angiography has high diagnostic value in the diagnosis of coronary artery disease due to rapid advances in multislice CT scanners. Furthermore, coronary CT angiography has demonstrated incremental prognostic value beyond clinical risk factors and allows for a quantification of the risk associated with coronary plaque in coronary CT angiography. The current challenges in performing coronary CT angiography have made the imaging technique to improve by using latest CT technology which provides an attractive alternative to invasive coronary angiography in routine clinical practice. With further developments in CT technology, coronary CT angiography will continue to play an important role in the diagnostic evaluation of coronary artery disease and prediction of major adverse cardiac events.

REFERENCES

1 **Paul JF**, Dambrin G, Caussin C, Lancelin B, Angel C. Sixteen-slice computed tomography after acute myocardial infarction: from perfusion defect to the culprit lesion. *Circulation* 2003; **108**: 373-374 [PMID: 12876136 DOI: 10.1161/01.CIR.0000075092.94870.57]

2 **Ropers D**, Baum U, Pohle K, Anders K, Ulzheimer S, Ohnesorge B, Schlundt C, Bautz W, Daniel WG, Achenbach S. Detection of coronary artery stenoses with thin-slice multi-detector row spiral computed tomography and multiplanar reconstruction. *Circulation* 2003; **107**: 664-666 [PMID: 12578863 DOI: 10.1161/01.CIR.0000055738.31551.A9]

3 **Sun Z**, Choo GH, Ng KH. Coronary CT angiography: current status and continuing challenges. *Br J Radiol* 2012; **85**: 495-510 [PMID: 22253353 DOI: 10.1259/bjr/15296170]

4 **Costello P**, Lobree S. Subsecond scanning makes CT even faster. *Diag Imaging* 1996; **18**: 76-79

5 **Taguchi K**, Aradate H. Algorithm for image reconstruction in multi-slice helical CT. *Med Phys* 1998; **25**: 550-561 [PMID: 9571623 DOI: 10.1118/1.598230]

6 **Flohr TG**, Schaller S, Stierstorfer K, Bruder H, Ohnesorge BM, Schoepf UJ. Multi-detector row CT systems and image-reconstruction techniques. *Radiology* 2005; **235**: 756-773 [PMID: 15833981 DOI: 10.1148/radiol.2353040037]

7 **McCollough CH**, Zink FE. Performance evaluation of a multi-slice CT system. *Med Phys* 1999; **26**: 2223-2230 [PMID: 10587202 DOI: 10.1118/1.598777]

8 **Haberl R**, Tittus J, Böhme E, Czernik A, Richartz BM, Buck J, Steinbigler P. Multislice spiral computed tomographic angiography of coronary arteries in patients with suspected coronary artery disease: an effective filter before catheter angiography? *Am Heart J* 2005; **149**: 1112-1119 [PMID: 15976796 DOI: 10.1016/j.ahj.2005.02.048]

9 **Goldman LW**. Principles of CT: multislice CT. *J Nucl Med Technol* 2008; **36**: 57-68; quiz 75-76 [PMID: 18483143 DOI: 10.2967/jnmt.107.044826]

10 **Lewis M**, Keat N, Edyvean S. 16 Slice CT scanner comparison report version 14, 2006. Available from: URL: http://www.impactscan.org/reports/Report06012.htm

11 **Kopp AF**, Schroeder S, Kuettner A, Baumbach A, Georg C, Kuzo R, Heuschmid M, Ohnesorge B, Karsch KR, Claussen CD. Non-invasive coronary angiography with high resolution multidetector-row computed tomography. Results in 102 patients. *Eur Heart J* 2002; **23**: 1714-1725 [PMID: 12398830 DOI: 10.1016/S0195-668X(02)93264-1]

12 **Achenbach S**, Ropers D, Pohle FK, Raaz D, von Erffa J, Yilmaz A, Muschiol G, Daniel WG. Detection of coronary artery stenoses using multi-detector CT with 16 x 0.75 collimation and 375 ms rotation. *Eur Heart J* 2005; **26**: 1978-1986 [PMID: 15923203 DOI: 10.1093/eurheartj/ehi326]

13 **Gibbons RJ**, Balady GJ, Beasley JW, Bricker JT, Duvernoy WF, Froelicher VF, Mark DB, Marwick TH, McCallister BD, Thompson PD, Winters WL, Yanowitz FG, Ritchie JL, Gibbons RJ, Cheitlin MD, Eagle KA, Gardner TJ, Garson A, Lewis RP, O'Rourke RA, Ryan TJ. ACC/AHA Guidelines for Exercise Testing. A report of the American College of Cardiology/American Heart Association Task Force on Practice Guidelines (Committee on Exercise Testing). *J Am Coll Cardiol* 1997; **30**: 260-311 [PMID: 9207652 DOI: 10.1161/01.CIR.0000034670.06526.15]

14 **Kuettner A**, Beck T, Drosch T, Kettering K, Heuschmid M, Burgstahler C, Claussen CD, Kopp AF, Schroeder S. Image quality and diagnostic accuracy of non-invasive coronary imaging with 16 detector slice spiral computed tomography with 188 ms temporal resolution. *Heart* 2005; **91**: 938-941 [PMID: 15958366 DOI: 10.1136/hrt.2004.044735]

15 **Garcia MJ**, Lessick J, Hoffmann MH. Accuracy of 16-row multidetector computed tomography for the assessment of coronary artery stenosis. *JAMA* 2006; **296**: 403-411 [PMID: 16868298 DOI: 10.1001/jama.296.4.403]

16 **Kalender WA**, Seissler W, Klotz E, Vock P. Spiral volumetric CT with single-breath-hold technique, continuous transport, and continuous scanner rotation. *Radiology* 1990; **176**: 181-183 [PMID: 2353088]

17 **Klingenbeck-Regn K**, Schaller S, Flohr T, Ohnesorge B, Kopp AF, Baum U. Subsecond multi-slice computed tomography: basics and applications. *Eur J Radiol* 1999; **31**: 110-124 [PMID: 10565510 DOI: 10.1016/S0720-048X(99)00086-8]

18 **Liang Y**, Kruger RA. Dual-slice spiral versus single-slice spiral scanning: comparison of the physical performance of two computed tomography scanners. *Med Phys* 1996; **23**: 205-220 [PMID: 8668101 DOI: 10.1118/1.597705]

19 **Achenbach S**, Ropers D, Kuettner A, Flohr T, Ohnesorge B, Bruder H, Theessen H, Karakaya M, Daniel WG, Bautz W, Kalender WA, Anders K. Contrast-enhanced coronary artery visualization by dual-source computed tomography--initial experience. *Eur J Radiol* 2006; **57**: 331-335 [PMID: 16426789 DOI: 10.1016/j.ejrad.2005.12.017]

20 **Flohr TG**, McCollough CH, Bruder H, Petersilka M, Gruber K, Süss C, Grasruck M, Stierstorfer K, Krauss B, Raupach R, Primak AN, Küttner A, Achenbach S, Becker C, Kopp A, Ohnesorge BM. First performance evaluation of a dual-source CT (DSCT) system. *Eur Radiol* 2006; **16**: 256-268 [PMID: 16341833 DOI: 10.1007/s00330-005-2919-2]

21 **Steigner ML**, Otero HJ, Cai T, Mitsouras D, Nallamshetty L, Whitmore AG, Ersoy H, Levit NA, Di Carli MF, Rybicki FJ. Narrowing the phase window width in prospectively ECG-gated single heart beat 320-detector row coronary CT angiography. *Int J Cardiovasc Imaging* 2009; **25**: 85-90 [PMID: 18663599

DOI: 10.1007/s10554-008-9347-8]
22 **Achenbach S**, Marwan M, Schepis T, Pflederer T, Bruder H, Allmendinger T, Petersilka M, Anders K, Lell M, Kuettner A, Ropers D, Daniel WG, Flohr T. High-pitch spiral acquisition: a new scan mode for coronary CT angiography. *J Cardiovasc Comput Tomogr* 2009; **3**: 117-121 [PMID: 19332343 DOI: 10.1016/j.jcct.2009.02.008]
23 **Ruzsics B**, Lee H, Zwerner PL, Gebregziabher M, Costello P, Schoepf UJ. Dual-energy CT of the heart for diagnosing coronary artery stenosis and myocardial ischemia-initial experience. *Eur Radiol* 2008; **18**: 2414-2424 [PMID: 18523782 DOI: 10.1007/s00330-008-1022-x]
24 **Schwarz F**, Ruzsics B, Schoepf UJ, Bastarrika G, Chiaramida SA, Abro JA, Brothers RL, Vogt S, Schmidt B, Costello P, Zwerner PL. Dual-energy CT of the heart--principles and protocols. *Eur J Radiol* 2008; **68**: 423-433 [PMID: 19008064 DOI: 10.1016/j.ejrad.2008.09.010]
25 **Nagao M**, Kido T, Watanabe K, Saeki H, Okayama H, Kurata A, Hosokawa K, Higashino H, Mochizuki T. Functional assessment of coronary artery flow using adenosine stress dual-energy CT: a preliminary study. *Int J Cardiovasc Imaging* 2011; **27**: 471-481 [PMID: 20686853]
26 **Jiang HC**, Vartuli J, Vess C. Gemstone-the ultimatum scintillator for computed tomography. Gemstone detector white paper. London: GE Healthcare, 2008: 1-8
27 **Sun Z**, Jiang W. Diagnostic value of multislice computed tomography angiography in coronary artery disease: a meta-analysis. *Eur J Radiol* 2006; **60**: 279-286 [PMID: 16887313 DOI: 10.1016/j.ejrad.2006.06.009]
28 **Pontone G**, Andreini D, Bartorelli AL, Cortinovis S, Mushtaq S, Bertella E, Annoni A, Formenti A, Nobili E, Trabattoni D, Montorsi P, Ballerini G, Agostoni P, Pepi M. Diagnostic accuracy of coronary computed tomography angiography: a comparison between prospective and retrospective electrocardiogram triggering. *J Am Coll Cardiol* 2009; **54**: 346-355 [PMID: 19608033 DOI: 10.1016/j.jacc.2009.04.027]
29 **Sun Z**, Ng KH. Diagnostic value of coronary CT angiography with prospective ECG-gating in the diagnosis of coronary artery disease: a systematic review and meta-analysis. *Int J Cardiovasc Imaging* 2012; **28**: 2109-2119 [PMID: 22212661 DOI: 10.1007/s10554-011-0006-0]
30 **Budoff MJ**, Dowe D, Jollis JG, Gitter M, Sutherland J, Halamert E, Scherer M, Bellinger R, Martin A, Benton R, Delago A, Min JK. Diagnostic performance of 64-multidetector row coronary computed tomographic angiography for evaluation of coronary artery stenosis in individuals without known coronary artery disease: results from the prospective multicenter ACCURACY (Assessment by Coronary Computed Tomographic Angiography of Individuals Undergoing Invasive Coronary Angiography) trial. *J Am Coll Cardiol* 2008; **52**: 1724-1732 [PMID: 19007693 DOI: 10.1016/j.jacc.2008.07.031]
31 **Meijboom WB**, Meijs MF, Schuijf JD, Cramer MJ, Mollet NR, van Mieghem CA, Nieman K, van Werkhoven JM, Pundziute G, Weustink AC, de Vos AM, Pugliese F, Rensing B, Jukema JW, Bax JJ, Prokop M, Doevendans PA, Hunink MG, Krestin GP, de Feyter PJ. Diagnostic accuracy of 64-slice computed tomography coronary angiography: a prospective, multicenter, multivendor study. *J Am Coll Cardiol* 2008; **52**: 2135-2144 [PMID: 19095130 DOI: 10.1016/j.jacc.2008.08.058]
32 **Miller JM**, Rochitte CE, Dewey M, Arbab-Zadeh A, Niinuma H, Gottlieb I, Paul N, Clouse ME, Shapiro EP, Hoe J, Lardo AC, Bush DE, de Roos A, Cox C, Brinker J, Lima JA. Diagnostic performance of coronary angiography by 64-row CT. *N Engl J Med* 2008; **359**: 2324-2336 [PMID: 19038879 DOI: 10.1056/NEJMoa0806576]
33 **Alkadhi H**, Stolzmann P, Desbiolles L, Baumueller S, Goetti R, Plass A, Scheffel H, Feuchtner G, Falk V, Marincek B, Leschka S. Low-dose, 128-slice, dual-source CT coronary angiography: accuracy and radiation dose of the high-pitch and the step-and-shoot mode. *Heart* 2010; **96**: 933-938 [PMID: 20538669 DOI: 10.1136/hrt.2009.189100]
34 **Hou Y**, Yue Y, Guo W, Feng G, Yu T, Li G, Vembar M, Olszewski ME, Guo Q. Prospectively versus retrospectively ECG-gated 256-slice coronary CT angiography: image quality and radiation dose over expanded heart rates. *Int J Cardiovasc Imaging* 2012; **28**: 153-162 [PMID: 21153709 DOI: 10.1007/s10554-010-9760-7]
35 **Rajiah P**, Schoenhagen P, Mehta D, Ivanc T, Lieber M, Soufan K, Desai M, Flamm SD, Halliburton S. Low-dose, wide-detector array thoracic aortic CT angiography using an iterative reconstruction technique results in improved image quality with lower noise and fewer artifacts. *J Cardiovasc Comput Tomogr* 2012; **6**: 205-213 [PMID: 22612906 DOI: 10.1016/j.jcct.2012.04.009]
36 **Kido T**, Kurata A, Higashino H, Sugawara Y, Okayama H, Higaki J, Anno H, Katada K, Mori S, Tanada S, Endo M, Mochizuki T. Cardiac imaging using 256-detector row four-dimensional CT: preliminary clinical report. *Radiat Med* 2007; **25**: 38-44 [PMID: 17225052 DOI: 10.1007/s11604-006-0097-z]
37 **Hou Y**, Ma Y, Fan W, Wang Y, Yu M, Vembar M, Guo Q. Diagnostic accuracy of low-dose 256-slice multi-detector coronary CT angiography using iterative reconstruction in patients with suspected coronary artery disease. *Eur Radiol* 2014; **24**: 3-11 [PMID: 23887663 DOI: 10.1007/s00330-013-2969-9]
38 **Petcherski O**, Gaspar T, Halon DA, Peled N, Jaffe R, Molnar R, Lewis BS, Rubinshtein R. Diagnostic accuracy of 256-row computed tomographic angiography for detection of obstructive coronary artery disease using invasive quantitative coronary angiography as reference standard. *Am J Cardiol* 2013; **111**: 510-515 [PMID: 23206926 DOI: 10.1016/j.amjcard.2012.10.036]
39 **Mori S**, Endo M, Obata T, Murase K, Fujiwara H, Susumu K, Tanada S. Clinical potentials of the prototype 256-detector row CT-scanner. *Acad Radiol* 2005; **12**: 148-154 [PMID: 15721591 DOI: 10.1016/j.acra.2004.11.011]
40 **Mori S**, Endo M, Obata T, Tsunoo T, Susumu K, Tanada S. Properties of the prototype 256-row (cone beam) CT scanner. *Eur Radiol* 2006; **16**: 2100-2108 [PMID: 16568264 DOI: 10.1007/s00330-006-0213-6]
41 **Mori S**, Kondo C, Suzuki N, Yamashita H, Hattori A, Kusakabe M, Endo M. Volumetric cine imaging for cardiovascular circulation using prototype 256-detector row computed tomography scanner (4-dimensional computed tomography): a preliminary study with a porcine model. *J Comput Assist Tomogr* 2005; **29**: 26-30 [PMID: 15665678 DOI: 10.1097/01.rct.0000151189.80473.2e]
42 **Hoe J**, Toh KH. First experience with 320-row multidetector CT coronary angiography scanning with prospective electrocardiogram gating to reduce radiation dose. *J Cardiovasc Comput Tomogr* 2009; **3**: 257-261 [PMID: 19577215 DOI: 10.1016/j.jcct.2009.05.013]
43 **de Graaf FR**, Schuijf JD, van Velzen JE, Kroft LJ, de Roos A, Reiber JH, Boersma E, Schalij MJ, Spanó F, Jukema JW, van der Wall EE, Bax JJ. Diagnostic accuracy of 320-row multidetector computed tomography coronary angiography in the non-invasive evaluation of significant coronary artery disease. *Eur Heart J* 2010; **31**: 1908-1915 [PMID: 20047991 DOI: 10.1093/eurheartj/ehp571]
44 **van Velzen JE**, de Graaf FR, Kroft LJ, de Roos A, Reiber JH, Bax JJ, Jukema JW, Schuijf JD, Schalij MJ, van der Wall EE. Performance and efficacy of 320-row computed tomography coronary angiography in patients presenting with acute chest pain: results from a clinical registry. *Int J Cardiovasc Imaging* 2012; **28**: 865-876 [PMID: 21614485 DOI: 10.1007/s10554-011-9889-z]
45 **Pelliccia F**, Pasceri V, Evangelista A, Pergolini A, Barillà F, Viceconte N, Tanzilli G, Schiariti M, Greco C, Gaudio C. Diagnostic accuracy of 320-row computed tomography as compared with invasive coronary angiography in unselected, consecutive patients with suspected coronary artery disease. *Int J Cardiovasc Imaging* 2013; **29**: 443-452 [PMID: 22806317 DOI: 10.1007/s10554-012-0095-4]

46 **Gaudio C**, Pelliccia F, Evangelista A, Tanzilli G, Paravati V, Pannarale G, Pannitteri G, Barillà F, Greco C, Franzoni F, Speziale G, Pasceri V. 320-row computed tomography coronary angiography vs. conventional coronary angiography in patients with suspected coronary artery disease: a systematic review and meta-analysis. *Int J Cardiol* 2013; **168**: 1562-1564 [PMID: 23347611 DOI: 10.1016/j.ijcard.2012.12.067]

47 **Li S**, Ni Q, Wu H, Peng L, Dong R, Chen L, Liu J. Diagnostic accuracy of 320-slice computed tomography angiography for detection of coronary artery stenosis: meta-analysis. *Int J Cardiol* 2013; **168**: 2699-2705 [PMID: 23566493 DOI: 10.1016/j.ijcard.2013.03.023]

48 **Barrett JF**, Keat N. Artifacts in CT: recognition and avoidance. *Radiographics* 2004; **24**: 1679-1691 [PMID: 15537976 DOI: 10.1148/rg.246045065]

49 **Earls JP**. How to use a prospective gated technique for cardiac CT. *J Cardiovasc Comput Tomogr* 2009; **3**: 45-51 [PMID: 19201376 DOI: 10.1016/j.jcct.2008.10.013]

50 **Pannu HK**, Alvarez W, Fishman EK. Beta-blockers for cardiac CT: a primer for the radiologist. *AJR Am J Roentgenol* 2006; **186**: S341-S345 [PMID: 16714607 DOI: 10.2214/AJR.04.1944]

51 **Pannu HK**, Sullivan C, Lai S, Fishman EK. Evaluation of the effectiveness of oral Beta-blockade in patients for coronary computed tomographic angiography. *J Comput Assist Tomogr* 2008; **32**: 247-251 [PMID: 18379311 DOI: 10.1097/RCT.0b013e318075e759]

52 **Leschka S**, Stolzmann P, Schmid FT, Scheffel H, Stinn B, Marincek B, Alkadhi H, Wildermuth S. Low kilovoltage cardiac dual-source CT: attenuation, noise, and radiation dose. *Eur Radiol* 2008; **18**: 1809-1817 [PMID: 18392829 DOI: 10.1007/s00330-008-0966-1]

53 **Ketelsen D**, Thomas C, Werner M, Luetkhoff MH, Buchgeister M, Tsiflikas I, Reimann A, Burgstahler C, Brodoefel H, Kopp AF, Claussen CD, Heuschmid M. Dual-source computed tomography: estimation of radiation exposure of ECG-gated and ECG-triggered coronary angiography. *Eur J Radiol* 2010; **73**: 274-279 [PMID: 19097836 DOI: 10.1016/j.ejrad.2008.10.033]

54 **Dikkers R**, Greuter MJ, Kristanto W, van Ooijen PM, Sijens PE, Willems TP, Oudkerk M. Assessment of image quality of 64-row Dual Source versus Single Source CT coronary angiography on heart rate: a phantom study. *Eur J Radiol* 2009; **70**: 61-68 [PMID: 18308496]

55 **Sun Z**, Dimpudus FJ, Nugroho J, Adipranoto JD. CT virtual intravascular endoscopy assessment of coronary artery plaques: a preliminary study. *Eur J Radiol* 2010; **75**: e112-e119 [PMID: 19781885 DOI: 10.1016/j.ejrad.2009.09.007]

56 **Sun Z**, Cao Y. Multislice CT angiography assessment of left coronary artery: correlation between bifurcation angle and dimensions and development of coronary artery disease. *Eur J Radiol* 2011; **79**: e90-e95 [PMID: 21543178 DOI: 10.1016/j.ejrad.2011.04.015]

57 **Hoffmann U**, Moselewski F, Nieman K, Jang IK, Ferencik M, Rahman AM, Cury RC, Abbara S, Joneidi-Jafari H, Achenbach S, Brady TJ. Noninvasive assessment of plaque morphology and composition in culprit and stable lesions in acute coronary syndrome and stable lesions in stable angina by multidetector computed tomography. *J Am Coll Cardiol* 2006; **47**: 1655-1662 [PMID: 16631006 DOI: 10.1016/j.jacc.2006.01.041]

58 **Brodoefel H**, Burgstahler C, Tsiflikas I, Reimann A, Schroeder S, Claussen CD, Heuschmid M, Kopp AF. **Dual-source** CT: effect of heart rate, heart rate variability, and calcification on image quality and diagnostic accuracy. *Radiology* 2008; **247**: 346-355 [PMID: 18372455 DOI: 10.1148/radiol.2472070906]

59 **Diederichsen AC**, Petersen H, Jensen LO, Thayssen P, Gerke O, Sandgaard NC, Høilund-Carlsen PF, Mickley H. Diagnostic value of cardiac 64-slice computed tomography: importance of coronary calcium. *Scand Cardiovasc J* 2009; **43**: 337-344 [PMID: 19266395 DOI: 10.1080/14017430902785501]

60 **Chen CC**, Chen CC, Hsieh IC, Liu YC, Liu CY, Chan T, Wen MS, Wan YL. The effect of calcium score on the diagnostic accuracy of coronary computed tomography angiography. *Int J Cardiovasc Imaging* 2011; **27** Suppl 1: 37-42 [PMID: 21993896 DOI: 10.1007/s10554-011-9955-6]

61 **Stolzmann P**, Scheffel H, Leschka S, Plass A, Baumüller S, Marincek B, Alkadhi H. Influence of calcifications on diagnostic accuracy of coronary CT angiography using prospective ECG triggering. *AJR Am J Roentgenol* 2008; **191**: 1684-1689 [PMID: 19020236 DOI: 10.2214/AJR.07.4040]

62 **Gaemperli O**, Valenta I, Schepis T, Husmann L, Scheffel H, Desbiolles L, Leschka S, Alkadhi H, Kaufmann PA. Coronary 64-slice CT angiography predicts outcome in patients with known or suspected coronary artery disease. *Eur Radiol* 2008; **18**: 1162-1173 [PMID: 18286291 DOI: 10.1007/s00330-008-0871-7]

63 **Carrigan TP**, Nair D, Schoenhagen P, Curtin RJ, Popovic ZB, Halliburton S, Kuzmiak S, White RD, Flamm SD, Desai MY. Prognostic utility of 64-slice computed tomography in patients with suspected but no documented coronary artery disease. *Eur Heart J* 2009; **30**: 362-371 [PMID: 19153177 DOI: 10.1093/eurheartj/ehn605]

64 **Chow BJ**, Wells GA, Chen L, Yam Y, Galiwango P, Abraham A, Sheth T, Dennie C, Beanlands RS, Ruddy TD. Prognostic value of 64-slice cardiac computed tomography severity of coronary artery disease, coronary atherosclerosis, and left ventricular ejection fraction. *J Am Coll Cardiol* 2010; **55**: 1017-1028 [PMID: 20202518 DOI: 10.1016/j.jacc.2009.10.039]

65 **Miszalski-Jamka T**, Klimeczek P, Banyś R, Krupiński M, Nycz K, Bury K, Lada M, Pelberg R, Kereiakes D, Mazur W. The composition and extent of coronary artery plaque detected by multislice computed tomographic angiography provides incremental prognostic value in patients with suspected coronary artery disease. *Int J Cardiovasc Imaging* 2012; **28**: 621-631 [PMID: 21369735 DOI: 10.1007/s10554-011-9799-0]

66 **Ostrom MP**, Gopal A, Ahmadi N, Nasir K, Yang E, Kakadiaris I, Flores F, Mao SS, Budoff MJ. Mortality incidence and the severity of coronary atherosclerosis assessed by computed tomography angiography. *J Am Coll Cardiol* 2008; **52**: 1335-1343 [PMID: 18929245 DOI: 10.1016/j.jacc.2008.07.027]

67 **Min JK**, Feignoux J, Treutenaere J, Laperche T, Sablayrolles J. The prognostic value of multidetector coronary CT angiography for the prediction of major adverse cardiovascular events: a multicenter observational cohort study. *Int J Cardiovasc Imaging* 2010; **26**: 721-728 [PMID: 20349139 DOI: 10.1007/s10554-010-9613-4]

68 **Schlett CL**, Banerji D, Siegel E, Bamberg F, Lehman SJ, Ferencik M, Brady TJ, Nagurney JT, Hoffmann U, Truong QA. Prognostic value of CT angiography for major adverse cardiac events in patients with acute chest pain from the emergency department: 2-year outcomes of the ROMICAT trial. *JACC Cardiovasc Imaging* 2011; **4**: 481-491 [PMID: 21565735 DOI: 10.1016/j.jcmg.2010.12.008]

69 **Hadamitzky M**, Achenbach S, Al-Mallah M, Berman D, Budoff M, Cademartiri F, Callister T, Chang HJ, Cheng V, Chinnaiyan K, Chow BJ, Cury R, Delago A, Dunning A, Feuchtner G, Gomez M, Kaufmann P, Kim YJ, Leipsic J, Lin FY, Maffei E, Min JK, Raff G, Shaw LJ, Villines TC, Hausleiter J. Optimized prognostic score for coronary computed tomographic angiography: results from the CONFIRM registry (COronary CT Angiography EvaluatioN For Clinical Outcomes: An InteRnational Multicenter Registry). *J Am Coll Cardiol* 2013; **62**: 468-476 [PMID: 23727215 DOI: 10.1016/j.jacc.2013.04.064]

70 **Sun Z**, Ng KH. Coronary computed tomography angiography in coronary artery disease. *World J Cardiol* 2011; **3**: 303-310 [PMID: 21949572 DOI: 10.4330/wjc.v3.i9.303]

71 **Sun Z**. Multislice CT angiography in coronary artery disease: Technical developments, radiation dose and diagnostic value. *World J Cardiol* 2010; **2**: 333-343 [PMID: 21160611 DOI: 10.4330/wjc.v2.i10.333]

72 **Sun Z**. Cardiac CT imaging in coronary artery disease: Current status and future directions. *Quant Imaging Med Surg* 2012; **2**: 98-105 [PMID: 23256066 DOI: 10.3978/j.issn.2223-4292.2012.05.02]
73 **Halpern EJ**, Savage MP, Fischman DL, Levin DC. Cost-effectiveness of coronary CT angiography in evaluation of patients without symptoms who have positive stress test results. *AJR Am J Roentgenol* 2010; **194**: 1257-1262 [PMID: 20410412 DOI: 10.2214/AJR.09.3209]
74 **Meijboom WB**, van Mieghem CA, Mollet NR, Pugliese F, Weustink AC, van Pelt N, Cademartiri F, Nieman K, Boersma E, de Jaegere P, Krestin GP, de Feyter PJ. 64-slice computed tomography coronary angiography in patients with high, intermediate, or low pretest probability of significant coronary artery disease. *J Am Coll Cardiol* 2007; **50**: 1469-1475 [PMID: 17919567 DOI: 10.1016/j.jacc.2007.07.007]
75 **Sun Z**, Aziz YF, Ng KH. Coronary CT angiography: how should physicians use it wisely and when do physicians request it appropriately? *Eur J Radiol* 2012; **81**: e684-e687 [PMID: 21724353 DOI: 10.1016/j.ejrad.2011.06.040]

P- Reviewers: Chattipakorn N, Fazio S, Goldhammer E, Hardt SE
S- Editor: Cui XM **L- Editor**: A **E- Editor**: Liu XM

World Journal of Cardiology

Online Submissions: http://www.wjgnet.com/esps/
bpgoffice@wjgnet.com
doi:10.4330/wjc.v5.i12.484

World J Cardiol 2013 December 26; 5(12): 484-494
ISSN 1949-8462 (online)

REVIEW

Coronary-cameral fistulas in adults: Acquired types (second of two parts)

Salah AM Said, Rikke HM Schiphorst, Richard Derksen, Lodewijk J Wagenaar

Salah AM Said, Department of Cardiology, Hospital Group Twente, 7555 DL Hengelo, The Netherlands
Rikke HM Schiphorst, Department of Cardiology, Thoraxcentrum Twente, Medisch Spectrum Twente, 7513 ER Enschede, The Netherlands
Richard Derksen, Department of Cardiology, Rijnstate Hospital, 6815 AD Arnhem, The Netherlands
Lodewijk J Wagenaar, Department of Cardiology, Thoraxcentrum Twente, Medisch Spectrum Twente, 7513 ER Enschede, The Netherlands
Author contributions: Said SAM, Schiphorst RHM, Derksen R contributed to this paper. Schiphorst RHM collected the data; Derksen R provided the case with the congenital coronary cameral fistula described in part Ⅰ; Said SAM prepared the manuscript and the literature review; Wagenaar LJ revised the manuscript; all the authors approved the final version of the paper.
Correspondence to: Salah AM Said, MD, PhD, FESC, Department of Cardiology, Hospital Group Twente,f Geerdinksweg 141, 7555 DL Hengelo, The Netherlands. samsaid@home.nl
Telephone: +31-74-2905286 Fax: +31-74-2905289
Received: May 24, 2013 Revised: August 25, 2013
Accepted: October 17, 2013
Published online: December 26, 2013

Abstract

Acquired coronary artery fistulas (CCFs) are infrequently detected during conventional coronary angiography. To delineate the characteristics of congenital (first part) and acquired (second part) CCFs in adults, a PubMed search was conducted for papers dealing with congenital or acquired CCFs. None of the publications describing patients with coronary-vascular fistulas were included. Papers dealing with pediatric subjects were excluded. From the world literature, a total of 243 adult patients were selected who had congenital (*n* = 159/243, 65%) and acquired (*n* = 84/243, 35%) CCFs. Among the acquired types (*n* = 72, 85.7%) were traumatic (iatrogenic (*n* = 65/72, 90%), accidental (*n* = 7/72, 10%) and (*n* = 12, 14.3%) spontaneously developing in relation to severe coronary atherosclerosis or myocardial infarction. A high incidence of spontaneous resolution of iatrogenic CCFs resulting from endomyocardial biopsy or following post-septal myectomy was reported. Spontaneous CCFs associated with myocardial ischemia or infarction resolved completely in 8% of the subjects. Early surgical intervention was the treatment of choice in acquired traumatic accidental CCFs. The congenital types are addressed in a previous issue of this journal (first part). In this review (second of two parts, part Ⅱ), we describe the acquired coronary-cameral fistulas.

Key words: Acquired coronary-cameral fistulas; Accidental coronary-cameral fistulas; Iatrogenic coronary-cameral fistulas; Spontaneous coronary-cameral fistulas; Coronary angiography, Spontaneous resolution; Surgical treatment

Core tip: The literature addressing acquired coronary artery fistulas (CCFs) is reviewed. A detailed classification of acquired CCFs is attempted. Acquired coronary artery fistulas are subdivided into spontaneous and traumatic types. The traumatic fistulas encounter iatrogenic and accidental subtypes. The iatrogenic fistulas are secondary to non-surgical interventions (endomyocardial biopsy, permanent pacing and implantable cardioverter-defibrillator leads, radiofrequency cardioablation, baro-trauma and transseptal puncture) and cardiac surgical procedures (septal myectomy and other cardiac surgical procedures). Diagnosis of acquired CCFs is suspected by clinical history and recurrence of symptoms, occurrence of a new continuous machinery cardiac murmur and a palpable thrill. Watchful waiting and supportive medical management may be advocated in the majority of acquired CCFs. Acquired traumatic accidental CCFs are indications for emergent surgical procedures. Within this entity of CCFs, each subtype has its own specific characteristics such as age of the subjects, origin, termination of fistulas or mechanism

of injury and its specific treatment modality.

Said SAM, Schiphorst RHM, Derksen R, Wagenaar LJ. Coronary-cameral fistulas in adults: Acquired types (second of two parts). *World J Cardiol* 2013; 5(12): 484-494 Available from: URL: http://www.wjgnet.com/1949-8462/full/v5/i12/484.htm DOI: http://dx.doi.org/10.4330/wjc.v5.i12.484

INTRODUCTION

Congenital coronary-cameral fistulas (CCFs) include solitary and coronary-ventricular multiple micro-fistulas. Congenital CCFs have been described in the first part of this review[1]. Acquired CCFs are rare disorders. In this part (second of two parts), we present the acquired traumatic iatrogenic, acquired traumatic accidental and spontaneously occurring CCFs[2-4]. The acquired types are defined as single or multiple, direct communications arising from one or more coronary arteries entering into one of the four cardiac chambers (right atrium (RA) and ventricle (RV) and left atrium (LA) and ventricle (LV)) elucidating arterio-venous or arterio-arterial connection, giving rise to left-right or left-left shunt, respectively. Acquired traumatic accidental CCFs as a result of penetrating chest injuries have been reported since 1935[5]. Acquired traumatic accidental fistulas usually occur when the continuity or the vicinity of a coronary artery is lacerated subsequent to severe blunt or sharp chest trauma.

Acquired traumatic accidental fistulas may develop secondary to exogenous injuries such as deceleration traumas[6] or sharp chest injuries[7] in civilian practice due to violence and physical assault[8-10] and warfare[11] situations during military combat[12]. On the other hand, acquired traumatic iatrogenic fistulas may occur following endogenous (intravascular or extra-vascular) diagnostic[13,14] or therapeutic interventions[15-17].

Furthermore, iatrogenic fistulas may be acquired secondary to surgical[3,18] or non-surgical interventions[19,20]. Rarely, CCFs may occur spontaneously in association with severe obstructive atherosclerotic lesions or myocardial infarction[21,4]. Diagnosis of acquired CCFs is suspected by clinical history and recurrence of symptoms, occurrence of a new continuous machinery cardiac murmur and a palpable thrill[8].

The entity of CCFs characterized by various manifestations and etiologies, congenital (first part) and acquired (second part), are discussed and the international literature is briefly reviewed. The acquired traumatic iatrogenic, acquired traumatic accidental and spontaneously developing types are presented.

LITERATURE RESEARCH

PubMed and Google Scholar were searched for the terms "coronary-cameral fistulas (CCFs)", "congenital" and "acquired" combined with "adult". The English and non-English medical literature were screened for both types of congenital (first of two parts, part 1) and acquired (second of two parts, part 2) CCFs in an adult population. The related articles shown on the side page were explored and references were checked for relevant papers, as illustrated in the flow diagram (Figure 1). The definition used for acquired traumatic iatrogenic acquired and traumatic accidental CCFs was adopted from a previous publication[22]. The following criteria were stipulated to include homogenous subsets for analysis: acquired traumatic accidental, acquired traumatic iatrogenic and spontaneous CCFs. Manuscripts were checked for completeness and a meticulous search was performed for recognition of fistula termination into any of the four cardiac chambers. Patients were tabulated according to the etiology, age, gender, clinical presentations, complications and management (Table 1 and Figure 2). Publications dealing with adult patients with congenital or acquired coronary-vascular fistulas were not included. Publications considering a pediatric population were excluded.

Definitions

Acquired traumatic (accidental or iatrogenic) coronary-cameral fistulas are secondary to exogenous or endogenous thoracic trauma, accidental (penetrating or non-penetrating) or iatrogenic (intravascular or extravascular, surgical or non-surgical diagnostic or therapeutic procedures). Furthermore, a direct communication occurs between one or more epicardial coronary arteries and a cardiac chamber, bypassing the myocardial capillary network, which was not present on a prior coronary angiographic study (when available) and not congenital in origin[22].

Iatrogenic coronary-cameral fistulas (surgical and non-surgical procedures) (Figure 3A) develop subsequent to surgical septal myectomy[3] or other cardiac surgical procedures (bypass grafting, valvular repair and surgery for congenital anomalies)[2,23,24]. The varieties of non-surgical interventions are caused by repeated endomyocardial biopsy[15,13], permanent pacing and ICD implantation[16,20] or electrophysiological procedures[17,25] and following barotrauma[19,26] or subsequent to vessel rupture after coronary stent placement[27].

Accidental coronary-cameral fistulas (penetrating and non-penetrating injuries) (Figure 3B) may occur due to sharp chest wounds such as shrapnel[11], stab wound[7] or gunshot[8], and blunt thoracic injury due to deceleration trauma (car and motorcycle accidents)[6,28].

Spontaneous CCFs are coronary-cameral fistulas, spontaneously emerging, associated with severe atherosclerotic lesions[29] or develop following myocardial infarction[4,21], resulting in direct communication between the culprit coronary artery and an adjacent cardiac chamber.

Descriptive analyses

Descriptive analyses were expressed as means and ranges and categorical data were presented as percentages.

RESEARCH

From the world literature, 243 adult patients were selected

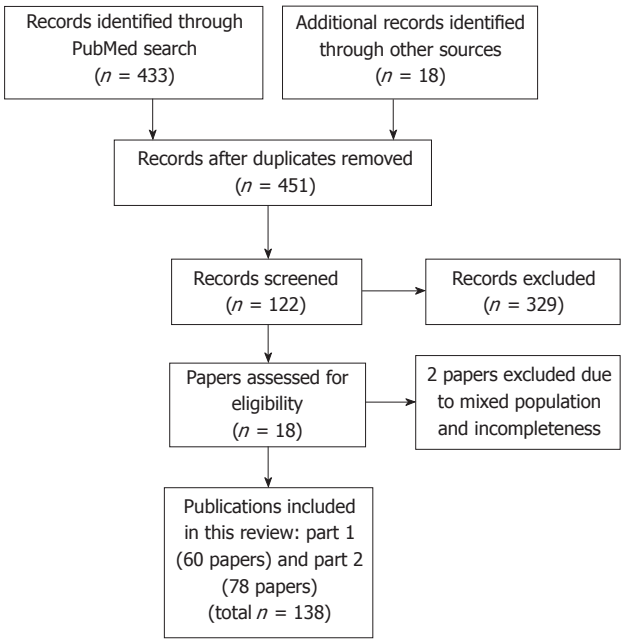

Figure 1 Flow diagram of literature search of coronary cameral fistulas in adult population.

with congenital (*n* = 159/243, 65%) or acquired (*n* = 84/243, 35%) CCFs. Among the reviewed subjects with acquired fistulas, (*n* = 65/84, 77.4%) were traumatic iatrogenic of origin, (*n* = 7/84, 8.3%) were traumatic accidental and (*n* = 12/84, 14.3%) presented with spontaneous occurrence of fistulas developing post-MI.

This review focuses on the different aspects with regard to etiology, clinical presentation and management of congenital (first part)[1] or acquired (second part) coronary-cameral fistulas (Table 1).

Summary of literature review (Figure 1): Acquired coronary artery fistulas are subdivided into spontaneous (*n* = 12/84, 14.3%) and traumatic (*n* = 72/84, 85.7%). The traumatic fistulas encounter iatrogenic (*n* = 65/72, 90%) and accidental (*n* = 7/72, 10%) subtypes. The iatrogenic fistulas are secondary to non-surgical interventions (endomyocardial biopsy, permanent pacing and implantable cardioverter-defibrillator (ICD) leads and radiofrequency cardio-ablation) and cardiac surgical procedures (septal myectomy and other cardiac surgical procedures).

Traumatic fistulas: (*n* = 72/84, 85.7%), acquired traumatic iatrogenic (*n* = 65/72, 90%), non-surgical interventions: (*n* = 40/65, 61%).

Acquired traumatic iatrogenic: Electrophysiological procedures (permanent pacing and ICD leads, transseptal puncture and percutaneous cardio-ablation procedures): These CCFs involve complications of permanent pacing and implantable cardioverter-defibrillator leads, transseptal puncture and electro-physiological procedures (*n* = 8/65, 12%)[14,16,17,20,23,25,30]. The data of 8 patients (5 male and 3 female) were analyzed. The mean age was 55.8 years (range 46-73). The termination sites were RA[14], LA[23], RV[16,20] and LV[17]. Regardless of their termination site, conservative medical management was sufficient to relieve symptoms in these acquired fistulas and spontaneous resolution occurring following RF cardio-ablation after 9-10 mo was observed[17,23].

Acquired traumatic iatrogenic (baro-trauma): These CCFs occur subsequent to non-surgical therapeutic interventions *e.g.*, baro-trauma. Subsequent to percutaneous coronary intervention (PCI) procedures, fistulous communications between the native left coronary artery and RV[19] or LV[26] were reported in 7 (*n* = 7/65, 11%) patients (5 males and 2 females) with a mean age of 66.6 (range 58-75). Moreover, these complications were described after PTCA of a distal anastomosis of a totally occluded venous graft[31]. The donor artery was the left anterior descending coronary artery (LAD) in most of the cases. As the shunt magnitude was trivial without hemodynamic consequences and spontaneous closure was observed, conservative medical management (CMM) was commonly employed.

Post-endomyocardial biopsy (EMB) following heart transplantation (*n* = 25/65, 38%): The iatrogenic fistulas occurred after repeated EMB[32] or interrelated[33] with the applied surgical procedure. The mean age was 50.8 years (range 43-64) with 22% female subjects.

Surgical procedures: 25/65 = 38%

Acquired traumatic iatrogenic after bypass surgery, valvular repair and surgical procedures for congenital heart anomalies: These CCFs occur subsequent to surgical procedures[2,18,34-36]. Five adult patients were selected (*n* = 5/65, 8%) with a mean age of 61 years (range 40-78). CCFs occurring after heart surgery were reported post-aortic valve[36] and mitral valve[35] replacement.

Acquired CCFs have been observed after surgical septal myectomy **(**SM**)** for hypertrophic cardiomyopathy (HCMP)(*n* = 20/65, 31%)[3,18,37-40]. Twenty patients were selected with a mean age of 45 years (range 32-74). Acquired CCFs following surgical intervention may occur after SM alone[39] or after combined aortic valve replacement and SM for hypertrophic cardiomyopathy[18]. The drainage site was always the LV. The majority were asymptomatic and disappeared spontaneously (78%). The management is usually a conservative medical strategy and percutaneous therapeutic embolization (PTE) was rarely needed to close the acquired fistula in a symptomatic patient[3].

Acquired traumatic accidental CCFs (*n* = 7/72, 10%)[6-8,28,41-43]: The mean age of the 7 reviewed male subjects was 24.1 years (range 17-38). CCFs occurred following penetrating (*n* = 3) or non-penetrating chest injuries (*n* = 4). They presented with chest pain, angina pectoris, palpitation, dyspnea, congestive heart failure and hemoptysis. The origin was the LAD (*n* = 4) and the right coronary artery (RCA) (*n* = 3). The CCFs terminated into the RA (*n* = 1), RV (*n* = 4) and LV (*n* = 2). All 7 reviewed patients were treated surgically. The surgical procedures included ligation and coronary artery bypass grafting, valvular repair and closure of ventricular septal defects. In three patients, reoperation was necessary for a complete repair.

Spontaneous fistulas

Spontaneously occurring: These are CCFs associated with

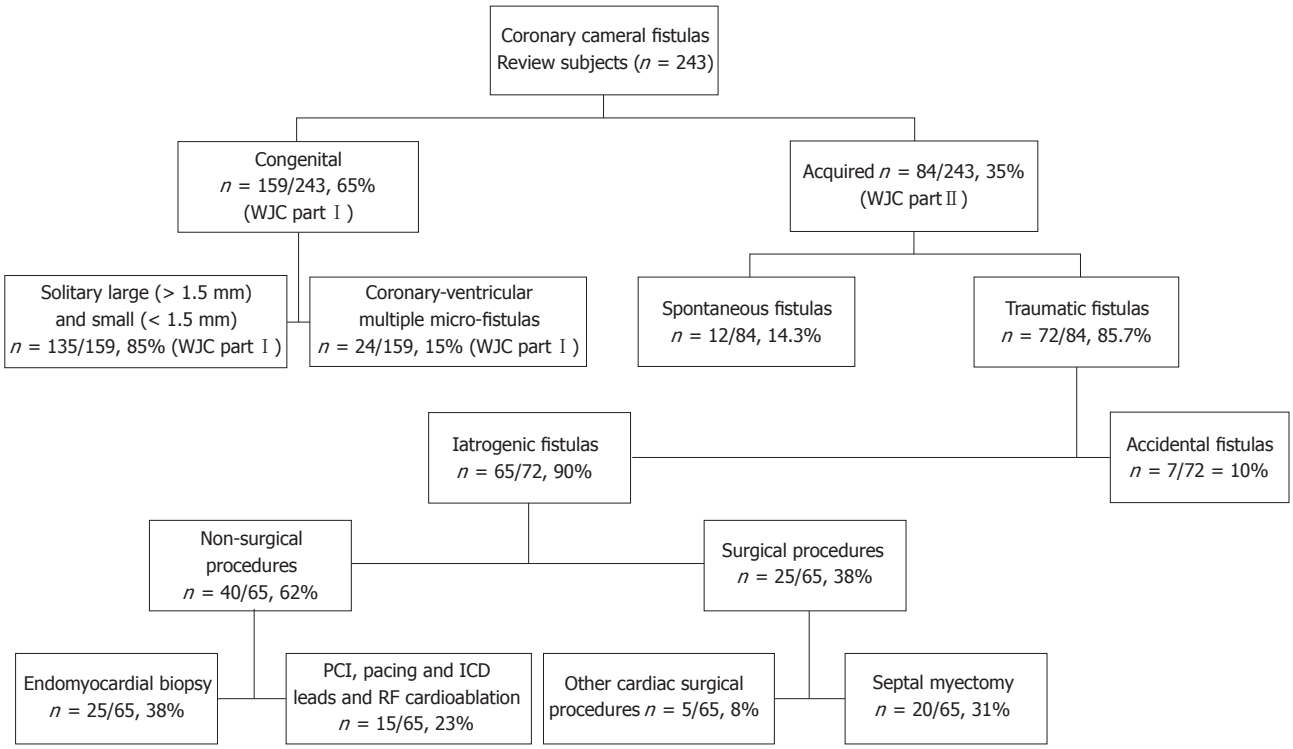

Figure 2 Schematic representation of review subjects with congenital and acquired coronary-cameral fistulas. ICD: Implantable cardioverter-defibrillator; PCI: Percutaneous coronary intervention; RF: Radiofrequency.

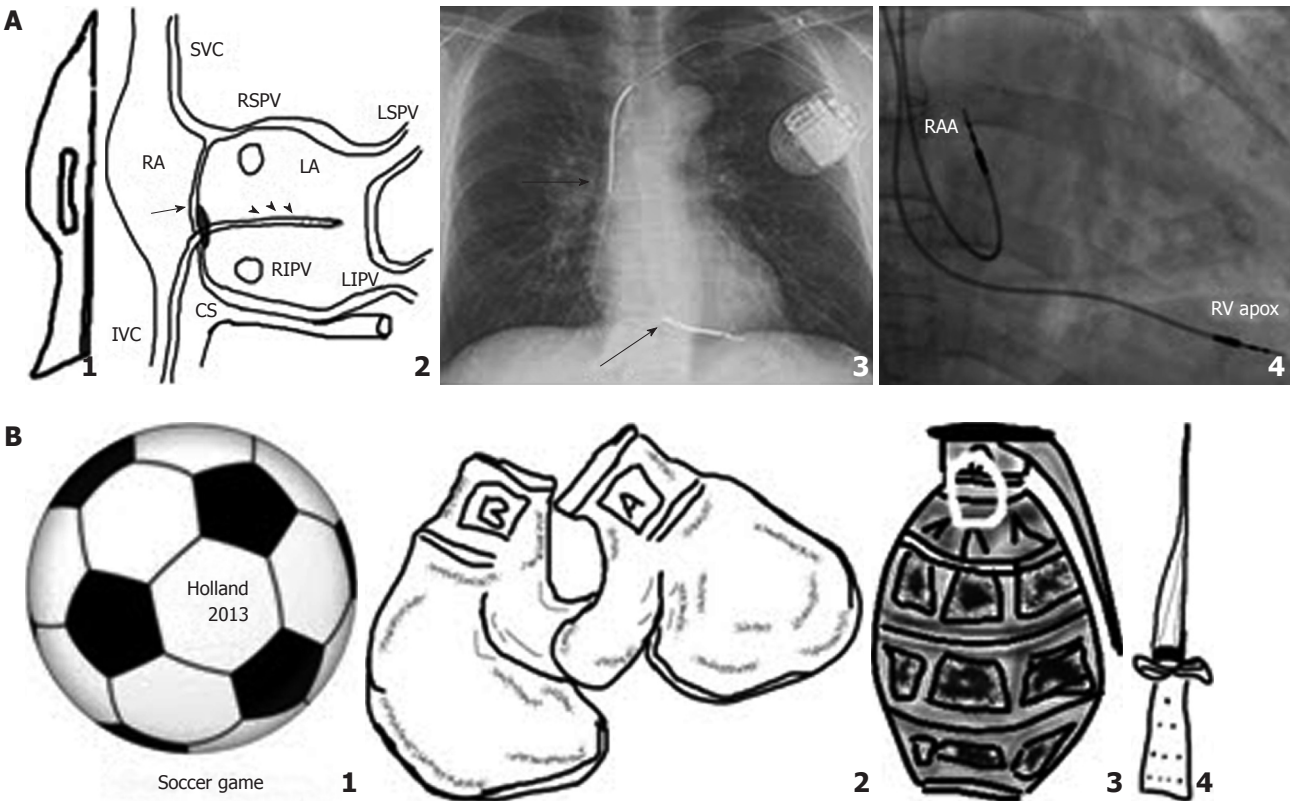

Figure 3 Schematic examples of some of the conditions, procedures and attributes involved in the development of (A) acquired traumatic iatrogenic and (B) acquired traumatic accidental coronary-cameral fistulas. A: 1: Surgical scalpel; 2: Radiofrequency cardio-ablation (arrow heads), and transseptal puncture (arrow); 3: ICD lead (arrows); and 4: Pacing leads; B: 1 Soccer game; 2 Boxing; 3: Shrapnel; and 4: Knife. CS: Coronary sinus; ICD: Internal cardioverter defibrillator; IVC: Inferior vena cava; LA: Left atrium; LIPV: Left inferior pulmonary vein; LSPV: Left superior pulmonary vein; RA: Right atrium; RAA: Right atrial appendage; RIPV: Right inferior pulmonary vein; RSPV: Right superior pulmonary vein; RV: Right ventricular; SVC: Superior vena cava.

Table 1 Fistula characteristics in congenital and acquired coronary cameral fistulas of 243 reviewed subjects

Congenital CCFs n = 159 (65%)			Acquired n = 84 (35%)					
Solitary CCFs and coronary artery-ventricular multiple micro-fistulas[1]			Traumatic CCFs n = 72 (85.7%)					Spontaneous n = 12 (14.3%)
Sub-classification	Solitary 85%	MMFs 15%	Iatrogenic CCFs n = 65/72 (90%)				Accidental CCFs n = 7/72 (10%)	
Aetiology	Congenital 65%		Post-SM	After other cardiac surgery	Post-EMB	EP and PCI	Blunt or sharp chest trauma	post-MI or associated with severe coronary artery disease
Female percentage	50%	63%	Unknown	20%	22%	33%	0%	0%
Mean age	46.2 (18-85)	62.7 (39-85)	45 (32-74)	61 (40-78)	50.8 (43-64)	60.8 (46-75)	24.1 (17-38)	61 (29-75)
Prevalence/incidence	135/159 (85%)	24/159 (15%)	20/65 (31%)	5/65 (8%)	25/65 (38%)	15/65 (23%)	10%	14.30%
Management	CMM 22%, SL 56%, PTE 22%	CMM 100%, incidentally ICD	CMM 11%, PTE 11%	WW 40%, CMM 40%, PTE 20%	CMM 73%	CMM	Surgical repair 100%	CMM 17%, SL 58%
Fistula characteristics								
Origin	Proximal segment	Mid- or distal segment	Septal perforators	LCA or RCA	RCA > LAD > Cx	LCA	RCA or LAD	RCA or LAD
Termination	Any cardiac chambers	LV > RV	LV	Any cardiac chambers	RV	Any cardiac chambers	RV or LV	RV or LV
Spontaneous resolution	Occasionally	Not reported	High rate	Not reported	High rate	Occasionally	Not reported	8%

CCFs: Coronary cameral fistulas; CMM: Conservative medical management; EMB: Endomyocardial biopsy; EP: Electrophysiological procedures; ICD: Implantable cardioverter-defibrillator; LA: Left atrium; LAD: Left anterior descending artery; LCA: Left coronary artery; LV: Left ventricle; MI: Myocardial infarction; MMFs: Coronary artery-ventricular multiple micro-fistulas; PCI: Percutaneous coronary intervention; PTE: Percutaneous therapeutic embolization; RA: Right atrium; RCA: Right coronary artery; RV: Right ventricle; SL: Surgical ligation; SM: Septal myectomy; WW: Watchful waiting follow-up.

severe atherosclerotic stenotic lesions or myocardial infarction (n = 12/84, 14.3%)[4,21,44-51]. Twelve male subjects with a mean age of 61 years (range 29-75) were selected. The RCA[21] (n =4) and LCA[44] (n =8) participated in the formation of the acquired CCFs. Acquired CCFs (LAD-LV fistula) were noticed following anterior MI[46] and complicating neovascularization of mural thrombus formation[51]. The right[47] (n = 3), left ventricular[48] (n = 5) lumen, right atrium (n = 1) and left atrium (n = 3) may be the site of cameral termination. Among these patients, spontaneous resolution occurred in (n = 1/12, 8%)[47], surgical ligation of the fistula was conducted in (n = 7/12, 58%) and CMM was implemented in (n = 2/12, 17%). Death was reported in one case[45] and the management was not reported in another[44].

COMMENTS

CCFs encompass a group of infrequently detected solitary or multiple *micro* or *macro* coronary cameral communications, either congenital[1] or acquired traumatic subsequent to accidental injuries[43], and iatrogenic secondary to surgical[3] or non-surgical interventions[15,16] that are increasingly recognized due to material sophistication and wide spread application of non-invasive and invasive angiographic imaging modalities[2,16,52]. CCFs may rarely also occur spontaneously after MI[44]. CCFs may be subdivided into congenital and acquired types, the former making up the vast majority.

As was found in the current review, 35% of the subjects presented with an acquired type. In 1997, on reviewing the world literature 36% of the fistulas were found to have an acquired etiology[22].

Within this entity of CCFs, each subtype has its own specific characteristics, such as age of the subjects, origin, termination of fistulas or mechanism of injury and its specific treatment modality.

The precise incidence of acquired traumatic accidental CCFs is unknown due to a lack of data and literature has been essentially limited to case reports and small series of patients[43]. Acquired traumatic iatrogenic CCFs may occur due to trans-venous[16,20] or trans-arterial[19,26] endovascular diagnostic (endomyocardial biopsy) or therapeutic procedures (percutaneous coronary intervention and pacemaker implantation)[20,53]. In the current era, it is believed that technical developments, material sophistications, procedural refinements and the enhanced gain in experience have resulted in a great reduction or abolishing of acquired traumatic iatrogenic CCFs post percutaneous coronary intervention (PCI) and spontaneously developing post-MI[53,54].

Acquired iatrogenic CCFs may occur after heterogeneous causes of endogenous or exogenous traumas such as sharp[7,12] and blunt chest injury. Endogenous surgical or non-surgical trauma, such as baro-trauma after PCI[19,26,31,55], and following permanent endocardial ventricular pacing lead placement[20] may cause CCFs. Acquired accidental CCFs develop after non-penetrating[42] or penetrating thoracic injuries[7,56]. They may also occur after surgical septal myectomy[3] and radio-frequency cardio-ablation[17]. They are sometimes characterized by the appearance of a novel continuous cardiac murmur or by recurrence of symptoms[6,9,34].

Traumatic fistulas

Acquired traumatic iatrogenic CCFs (non-surgical): secondary to electrophysiological procedures (permanent pacing and implantable cardioverter-defibrillator (ICD) leads, transseptal puncture and radiofrequency cardio-ablation).

Etiology and incidence: They formed 12% of the traumatic fistulas. These are very rare complications of permanent pacing and ICD leads, transseptal puncture and electrophysiological procedures that have been observed. Only a few cases have been reported in the literature. Recently, Tamura *et al*[14] reported the occurrence of acquired iatrogenic CCFs between the Cx and the RA following transseptal puncture. Surgical[23,30] and non-surgical[17,25] electro-physiological interventions (*e.g.*, radio-frequency cardio-ablation) may lead to acquired CCFs. The potential risk of coronary vessel lesions during the cardio-ablation is associated with the close relationship between the RCA and Cx to the site of ablation on the atrioventricular annulus. After percutaneous radiofrequency ablation, in the majority of reviewed subjects, the origin of CCFs was the Cx[23,30,57].

Mechanism: Acquired traumatic iatrogenic CCFs develop secondary to mechanical and thermal injuries. The application of radiofrequency cardio-ablation may be complicated with the occurrence of a communication between an adjacent coronary artery and a cardiac chamber which is thought to result from thermal and mechanical injury[23,14,25]. Most of the reported acquired CCFs have their exit to the RV, but outflow to the LA[30] and LV[17] have also been described.

Management and prognosis: Pharmacological or supportive therapy is sufficient to relieve symptoms in these acquired fistulas, and spontaneous resolution occurring after 9-10 mo has been reported[23,17]. In the current review, regardless of their termination site, they were all treated medically except two in whom spontaneous resolution occurred. Conservative management was advised for acquired CCFs entering the RV complicating endocardial active fixation of an ICD lead[16] and of permanent ventricular pacing leads[20].

Acquired traumatic iatrogenic CCFs secondary to baro-trauma

Etiology and incidence: They formed 11% of the iatrogenic fistulas. These coronary-cameral fistulas occur subsequent to baro-trauma (non-surgical therapeutic procedures). These complications have infrequently been reported in Asian[31] and Caucasian patients[26]. Subsequent to PTCA procedures, fistulous communications between the native left coronary artery and RV[19] or LV[26] have been reported. Moreover, these complications have been described after PTCA of a distal anastomosis of a totally occluded venous graft[31]. The donor artery was the LAD in most of the cases.

Mechanism: Several mechanisms are responsible, alone or together. It is thought to be based on mechanical injury to the vessel wall in the vicinity of a cardiac chamber, resulting in a direct communication. Moreover, they may occur due to subsequent rupture of a false aneurysm following PTCA, besides inappropriate wire tracking, artery-balloon size mismatch and involvement of calcified lesions with vessel wall cracking and curved segment[19,26,27,31,55].

Earlier reports documented acquired traumatic iatrogenic CCFs caused by baro-trauma that were associated with a high mortality rate (29%, 2 of the 7 reported cases in literature) which were published in the eighties and nineties. In 1996, Karim[55] reported the first case of an acquired iatrogenic fistula between RCA and RA, complicating stent placement in a tight lesion, after which it was rarely reported following vessel rupture after coronary stenting[27] or subsequent to coronary artery pseudo-aneurysm late post-stenting[53]. Not only acquired CCFs could occur between a coronary artery and a cardiac chamber following PCI procedure, but also it may develop after PCI to saphenous vein graft which was treated by a covered stent[58].

Management and prognosis: As the shunt magnitude was trivial without hemodynamic consequences and spontaneous closure was observed, CMM was commonly employed. Complete and spontaneous resolution of an acquired fistula complicating PCI occurring between a branch of the RCA and RV has been documented[59]. In the current era, such complications following PCI proce-

dures are rarely reported[53,54].

Acquired iatrogenic CCFs following endomyocardial biopsy in the heart transplant population

Etiology and incidence: They formed 38% of the iatrogenic fistulas. The reported angiographic prevalence varies from 2.8% to 23.2%[13,15,60-63]. Two decades ago, Sauer *et al*[64] reported an incidence of 80%. The majority of these CCFs have their origin from the RCA (52%), followed by the LAD (43%) and finally by the Cx (5%)[15]. They nearly all terminate into the RV[13,32,60,62,65]. Rarely, repeated endomyocardial biopsy induced a fistula from an atrial branch of the Cx to the LA[61].

Mechanism: They occur subsequent to arterial trauma with neovascularization during the phase of granulation and tissue organization at the biopsy site following frequent and repeated RV endomyocardial biopsies and in relation to the applied surgical techniques of cardiac implantation[13,15,61].

Management and prognosis: Spontaneous disappearance is a more common occurrence in biopsy-related CCFs. Spontaneous closure is reported to occur in post-biopsy CCFs in heart transplant patients with an estimated rate of 27%[15]. The majority demonstrate a benign evolution and non-surgical management is usually the treatment of choice due to lack of severe symptoms and small shunt magnitude[13,15,52]. However, in some symptomatic patients, closure of the fistula may be obtained surgically[32] or achieved by placement of a covered stent[65] or a detachable balloon[66] using percutaneous catheter techniques[65,66].

Surgical procedures

Acquired traumatic iatrogenic CCFs following surgical septal myectomy

Etiology and prevalence: They formed 31% of the iatrogenic fistulas. After surgical septal myectomy for hypertrophic cardiomyopathy, CCFs have been reported[3,18,37-40]. Asymptomatic acquired CCFs draining into the LV following surgical intervention may occur after SM alone[39] or after combined aortic valve replacement with SM for HCMP[18]. The prevalence of acquired post-SM CCFs varies from 19% to 23%[3,37].

Mechanism: The proposed mechanism of fistula formation after surgical SM for treatment of hypertrophic cardiomyopathy: It is postulated that they originate secondary to injury of one or more septal perforator branches of the left anterior descending coronary artery, resulting in a direct communication between the lacerated vessel and the left ventricular cavity[3,37-39].

Management and prognosis: Surgical or percutaneous interventions were rarely needed to close the acquired fistula in a symptomatic patient since spontaneous closure is reported to be very high, accounting for 78%[3]. With the introduction of alcohol septal ablation in 1994, acquired CCFs are currently not seen after percutaneous procedures for treatment of HCMP with an outflow gradient[67-69].

After other cardiac surgical procedures (coronary artery bypass grafting, valvular repair and surgery for congenital heart anomalies)

Etiology and incidence: These CCFs occur after aortic or mitral valvular replacement[34,35] or surgical procedures for congenital cardiac anomalies. Chiu *et al*[2] reported an incidence of 0.44% following surgery for tetralogy of Fallot, ventricular septal defect (VSD), double chamber RV and transposition of the great arteries with VSD. In the current review, the acquired traumatic iatrogenic fistulas (n = 5/65, 8%) developed subsequent to other cardiac surgical procedures.

Clinical presentation: The majority was asymptomatic but recurrence of congestive heart failure was reported. Audible continuous murmur or continuous Doppler flow on echocardiography was prevalent.

Mechanism: The postulated mechanisms were subsequent to right atrial artery injured at the site of access for cardiopulmonary bypass, damage to the precapillary arteriole of the circle of Vieussens[2], injury to the RCA at reoperation[35] or possibly secondary to hypoxia-induced angiogenesis[36]. Chiu *et al*[2] identified risk factors for acquired CCFs as re-do procedures and RV myocardial resection of hypertrophic muscle bundles in ventricular septal defect.

Management and prognosis: Watchful waiting follow-up and CMM were the strategies in all except a case described in 2004, by Mestre Barceló *et al*[34] who performed percutaneous occlusion using coated stent of an acquired iatrogenic CCF between LAD and RV.

Acquired traumatic accidental CCFs

Etiology and incidence: They formed 10% of the acquired traumatic fistulas. They occur secondary to penetrating and non-penetrating thoracic injuries and are infrequently reported[43,10]. The mean age was 24.1 years, which was found to be lower than the patients presented with congenital solitary CCFs (46.2) or congenital coronary artery left ventricular multiple micro-fistulas (62.7)[1].

Clinical presentation: Three presented with sharp and four with blunt chest traumas. Dyspnea, angina pectoris, chest pain, palpitation, congestive heart failure and hemoptysis were reported. Machinery cardiac murmur was audible in four, diastolic in one and holosystolic murmur in two of the patients.

Mechanism: Myocardial contusion, laceration and tissue damage in blunt chest trauma and secondary to transfer

of kinetic energy in case of gunshot wounds associated with penetrating and non-penetrating injuries were the suggested mechanisms.

Management and prognosis: The management of acquired accidental CCFs, whether subsequent to penetrating or non-penetrating injury, is always an emergent surgical intervention. In 1965, Jones and Jahnke described the first surgical repair of a traumatic CCFs[10].

As early as 1975, a few papers were published regarding CCFs, with twelve traumatic CCFs reported in the world' s literature; the penetrating injuries were prevalent[70]. In 2000, Hancock Friesen *et al*[43] reviewed 28 patients, published between 1958-1998, with acquired accidental CCFs and added one of their own. All were surgically repaired. Origin from the RCA was twice as common as origin from the LAD. Five of them had blunt chest trauma and 24 were presented with sharp thoracic injury. Termination into right-sided atrial or ventricular cardiac chambers was prevalent. The first reported successful repair of a traumatic CCF was in 1965 by Jones *et al*[10]. Blunt trauma to the anterior chest wall may cause laceration of the RCA[42] or LAD[6,28], associated with or without myocardial contusion. Regardless of their origin, they usually communicate with the RV or RA due to traumas directed to the anterior chest wall[6,28,42,43] but they sometimes communicate with the LV cavity[41]. These CCFs usually manifest itself by the presentation of a new continuous cardiac murmur[71]. Early intervention was recommended, applying surgical ligation with[72] or without a coronary artery bypass graft (CABG) and direct repair from within a recipient chamber[8,43]. In the review of Haas *et al*[9], surgical repair was performed in all 19 patients with acquired traumatic accidental CCFs resulting from penetrating and non-penetrating chest injuries. Of these, 5 required reoperation due to recurrence of murmur after an interval varying from 24 h to 7 mo[8]. In our current literature review, the origin was equally distributed between the LAD and the RCA. All seven reviewed patients were treated surgically. Reoperation for complete repair was needed in three subjects. No spontaneous closure was observed among the reviewed subjects with acquired traumatic accidental CCFs.

Spontaneous CCFs

Spontaneously acquired CCFs as a result of severe stenotic lesions or myocardial infarction have been reported[4,21,29].

Etiology and incidence: They formed 14.3% (12/84) of the acquired fistulas. In the last century, reports have rarely been published incriminating myocardial ischemia or infarction for the occurrence of spontaneous CCFs[4,21]. Currently, such complications are rarely published. Two reports were cited in the literature of acquired CCFs secondary to anterior MI with a fistula entering into the RV[44] or LV[45]. Acquired CCFs were reported after anterior[44,45,48], inferior[4,21] or posterior MI[47,50]. They may also be associated with inferior[49] or anterior myocardial ischemia[73].

Mechanism: It has been postulated that an aberrant pathway of newly developed collaterals, neo-vascularization of left ventricular mural thrombus formation post-MI, ruptures of localized micro-necrosis subsequent to destruction of the microvasculature or by reopening of the Thebesian vessels probably may lead to the fistula formation into the lumen of a cardiac chamber[4,45,47-50]. Furthermore, it has been suggested that as collaterals lose their way, acquired fistulas may develop following MI or in association with severe atherosclerotic obstructive lesions[74]. In contrast to congenital CCFs between the LAD and LV which may cause angina pectoris secondary to myocardial ischemia documented with myocardial perfusion test[75], acquired CCFs may develop and emerge secondary to MI or severe atherosclerotic lesions. The precise mechanisms by which congenital or acquired CCFs could enhance atherosclerosis are not yet known.

Management and prognosis: In the current review, the majority of patients (58%) were treated surgically. Angiographically documented spontaneous closure was seen in 8% and CMM was the treatment modality in 17% of subjects. One death (8%) secondary to intractable congestive heart failure occurred in a 63 year old Asian patient who developed CCF between LCA and LV following anterior MI.

Patients considered for the potential diagnosis of acquired CCFs: Although acquired CCFs are incidentally detected on routine CAG, the diagnosis should be expected, with a high index of suspicion, in subjects who develop new symptoms or show recurrence of symptoms or develop a novel cardiac murmur. Treatment is reserved for symptomatic patients with a hemodynamically significant shunt. Management of asymptomatic patients is controversial. In contrast to congenital CCFs, high spontaneous disappearance of the acquired CCFs has been reported. Watchful waiting and supportive medical management may be advocated in the majority of acquired CCFs. With amenable fistulous morphological anatomy, percutaneous therapeutic embolization or surgical closure may be applied. Acquired traumatic accidental CCFs are indications for emergent surgical procedures. Furthermore, indications for surgery, as suggested by Konno *et al*[76] and others for congenital types, are: large L-R shunt > 30%, ischemia or volume overload, pulmonary hypertension or congestive heart failure, the presence of an aneurysm, and infective endocarditis[77,78].

CONCLUSION

Acquired CCFs are infrequent coronary artery anomalies which are often asymptomatic and found incidentally on routine coronary catheter angiography. The majority of acquired CCFs are secondary to iatrogenic trauma resulting from various interventional surgical or non-surgical endovascular or extravascular procedures. Acquired traumatic accidental CCFs are associated with a younger age (between second and fourth decade of life) compared with congenital fistulas[1] or acquired iatrogenic

CCFs (fifth decade of life). They usually originate from the RCA or LAD and all end in the RV. Early surgical intervention is always indicated in these subjects. The termination site of acquired iatrogenic CCFs resulting from endomyocardial biopsy in post-heart transplantation subjects is nearly always the RV associated with reported high spontaneous resolution. The prevalence of acquired post-SM CCFs is also high and they possess the highest rate of spontaneous disappearance.

ACKNOWLEDGMENTS

During the preparation of the manuscript, the assistance of the librarian, Mrs. A. Geerdink, and Mr. D. Maas of hospital group Twente is gratefully acknowledged. The authors thank Prof. Dr. Clemens von Birgelen, Department of Cardiology, Thoraxcentrum Twente, Medisch Spectrum Twente, Enschede, the Netherlands for his intellectual suggestions for the manuscript.

REFERENCES

1 **Said SA**, Schiphorst RH, Derksen R, Wagenaar L. Coronary-cameral fistulas in adults (first of two parts). *World J Cardiol* 2013; **5**: 329-336 [PMID: 24109496]
2 **Chiu SN**, Wu MH, Lin MT, Wu ET, Wang JK, Lue HC. Acquired coronary artery fistula after open heart surgery for congenital heart disease. *Int J Cardiol* 2005; **103**: 187-192 [PMID: 16080979 DOI: 10.1016/j.ijcard.2004.09.005]
3 **Sgalambro A**, Olivotto I, Rossi A, Nistri S, Baldini K, Baldi M, Stefano P, Antoniucci D, Garbini F, Cecchi F, Yacoub MH. Prevalence and clinical significance of acquired left coronary artery fistulas after surgical myectomy in patients with hypertrophic cardiomyopathy. *J Thorac Cardiovasc Surg* 2010; **140**: 1046-1052 [PMID: 20471659 DOI: 10.1016/j.jtcvs.2010.02.020]
4 **Ryan C**, Gertz EW. Fistula from coronary arteries to left ventricle after myocardial infarction. *Br Heart J* 1977; **39**: 1147-1149 [PMID: 911568 DOI: 10.1136/hrt.39.10.1147]
5 **Beck CS**. Two cardiac compression triads. *JAMA* 1935; **104**: 714-716 [DOI: 10.1001/jama.1935.02760090018005]
6 **Lowe JE**, Adams DH, Cummings RG, Wesly RL, Phillips HR. The natural history and recommended management of patients with traumatic coronary artery fistulas. *Ann Thorac Surg* 1983; **36**: 295-305 [PMID: 6615068 DOI: 10.1016/S0003-4975(10)60132-4]
7 **Forker AD**, Morgan JR. Acquired coronary artery fistula from nonpenetrating chest injury. *JAMA* 1971; **215**: 289-291 [PMID:4923342 DOI: 10.1001/jama.1971.03180150071018]
8 **Cheng TO**, Adkins PC. Traumatic aneurysm of left anterior descending coronary artery with fistulous opening into left ventricle and left ventricular aneurysm after stab wound of chest. Report of case with successful surgical repair. *Am J Cardiol* 1973; **31**: 384-390 [PMID: 4687853 DOI: 10.1016/0002-9149(73)90273-7]
9 **Haas GE**, Parr GV, Trout RG, Hargrove WC. Traumatic coronary artery fistula. *J Trauma* 1986; **26**: 854-857 [PMID: 3489105 DOI: 10.1097/00005373-198609000-00015]
10 **Jones RC**, Jahnke EJ. Coronary artery-atrioventricular fistula and ventricular septal defect due to penetrating wound of the heart. *Circulation* 1965; **32**: 995-1000 [PMID: 5846104 DOI: 10.1161/01.CIR.32.6.995]
11 **Heller RF**, Rahimtoola SH, Ehsani A, Johnson S, Boyd DR, Tatooles CJ, Loeb HS, Rosen KR. Cardiac complications. Results of penetrating chest wounds involving the heart. *Arch Intern Med* 1974; **134**: 491-496 [PMID: 4850883 DOI: 10.1001/archinte.134.3.491]
12 **Tsagaris TJ**, Bustamante RA. Coronary arteriovenous fistula and myocardial infarction due to trauma. *Am J Cardiol* 1966; **18**: 777-780 [DOI: 10.1016/0002-9149(66)90098-1]
13 **Fitchett DH**, Forbes C, Guerraty AJ. Repeated endomyocardial biopsy causing coronary arterial-right ventricular fistula after cardiac transplantation. *Am J Cardiol* 1988; **62**: 829-831 [PMID: 3048074 DOI: 10.1016/0002-9149(88)91237-4]
14 **Tamura A**, Naono S, Kadota J. A fistula from the coronary artery into the right atrium caused by transseptal puncture. *Eur Heart J* 2008; **29**: 2472 [PMID: 18436558 DOI: 10.1093/eurheartj/ehn175]
15 **Sandhu JS**, Uretsky BF, Zerbe TR, Goldsmith AS, Reddy PS, Kormos RL, Griffith BP, Hardesty RL. Coronary artery fistula in the heart transplant patient. A potential complication of endomyocardial biopsy. *Circulation* 1989; **79**: 350-356 [PMID: 2644055 DOI: 10.1161/01.CIR.79.2.350]
16 **Härle T**, Reimers J, Schaumann A. Coronary artery fistula caused by an endocardial active fixation ICD lead. *Europace* 2008; **10**: 458 [PMID: 18292123 DOI: 10.1093/europace/eun034]
17 **Shalaby A**, Refaat M, Lacomis JM, Amidi M. Iatrogenic coronary-cameral fistula after left ventricular radiofrequency ablation. *Heart Rhythm* 2009; **6**: 720-721 [PMID: 18848504 DOI: 10.1016/j.hrthm.2008.08.013]
18 **López-Candales A**, Kumar V. Coronary artery to left ventricle fistula. *Cardiovasc Ultrasound* 2005; **3**: 35 [PMID: 16277656 DOI: 10.1186/1476-7120-3-35]
19 **Meng RL**, Harlan JL. Left anterior descending coronary artery-right ventricle fistula complicating percutaneous transluminal angioplasty. *J Thorac Cardiovasc Surg* 1985; **90**: 387-390 [PMID: 3162067]
20 **Saeian K**, Vellinga T, Troup P, Wetherbee J. Coronary artery fistula formation secondary to permanent pacemaker placement. *Chest* 1991; **99**: 780-781 [PMID: 1995248 DOI: 10.1378/chest.99.3.780]
21 **Chapman RW**, Watkins J. Rupture of right coronary artery aneurysm into the right atrium. *Br Heart J* 1978; **40**: 938-939 [PMID: 687496 DOI: 10.1136/hrt.40.8.938]
22 **Said SA**, el Gamal MI, van der Werf T. Coronary arteriovenous fistulas: collective review and management of six new cases--changing etiology, presentation, and treatment strategy. *Clin Cardiol* 1997; **20**: 748-752 [PMID: 9294664 DOI: 10.1002/clc.4960200907]
23 **Nguyen-Do P**, Bannon P, Leung DY. Coronary artery to the left atrial fistula after resection of atrial appendages. *Ann Thorac Surg* 2004; **78**: e26-e27 [PMID: 15276584 DOI: 10.1016/j.athoracsur.2003.10.117]
24 **de Marchena E**, Musial B, Wozniak P, Schob A, Chakko S, Kessler KM. Iatrogenic internal mammary artery to coronary vein fistula. *Chest* 1990; **97**: 251-252 [PMID: 2295253 DOI: 10.1378/chest.97.1.251]
25 **Wieczorek M**, Braun P, Schoels W. Acquired arteriovenous fistula and chronic occlusion of the left anterior descending coronary artery in a patient with previous ablation of a left-sided accessory pathway. *Pacing Clin Electrophysiol* 2005; **28**: 874-876 [PMID: 16105019 DOI: 10.1111/j.1540-8159.2005.00170.x]
26 **Iannone LA**, Iannone DP. Iatrogenic left coronary artery fistula-to-left ventricle following PTCA: a previously unreported complication with nonsurgical management. *Am Heart J* 1990; **120**: 1215-1217 [PMID: 2239674 DOI: 10.1016/0002-8703(90)90139-O]
27 **Korpas D**, Acevedo C, Lindsey RL, Gradman AH. Left anterior descending coronary artery to right ventricular fistula complicating coronary stenting. *J Invasive Cardiol* 2002; **14**: 41-43 [PMID: 11773695]
28 **Zamani J**, Amirghofran AA, Moaref AR, Afifi S, Rezaian GR. Posttraumatic coronary artery-right ventricular fistula with multiple ventricular septal defects. *J Card Surg* 2010; **25**: 670-671 [PMID: 20412356 DOI: 10.1111/j.1540-8191.2010.01032.x]
29 **King SB**, Schoonmaker FW. Coronary artery to left atrial fistula in association with severe atherosclerosis and mitral stenosis: report of surgical repair. *Chest* 1975; **67**: 361-363 [PMID: 1112134 DOI: 10.1378/chest.67.3.361]
30 **Wada T**, Ohara T, Nakatani S, Sumita Y, Kobayashi J, Kitakaze M. A case of coronary artery fistula between a coronary artery and the left atrium following maze procedure. *J Am Soc Echo-*

cardiogr 2009; **22**: 323.e3-323.e6 [PMID: 19153027 DOI: 10.1016/j.echo.2008.12.019]
31 **el-Omar MM**, Hargreaves MR, Venkataraman A, Been M. Coronary ventricular fistula as a complication of PTCA: a case report and literature review. *Int J Cardiol* 1995; **51**: 113-116 [PMID: 8522405 DOI: 10.1016/0167-5273(95)02417-U]
32 **Uchida N**, Baudet E, Roques X, Laborde N, Billes MA. **Surgical experience of coronary artery-right ventricular fistula in a heart transplant patient.** *Eur J Cardiothorac Surg* 1995; **9**: 106-108 [PMID: 7748569 DOI: 10.1016/S1010-7940(05)80030-2]
33 **Vermeulen T**, Haine S, Paelinck BP, Rodrigus IE, Vrints CJ, Conraads VM. Coronary artery-pulmonary artery fistula in a heart-transplanted patient. *Eur J Echocardiogr* 2010; **11**: 80-81 [PMID: 19749198 DOI: 10.1093/ejechocard/jep113]
34 **Mestre Barceló JL**, Salido Tahoces L, del Río del Busto A, Camino López A, Moya Mur JL, Pey Illera J. [Closure of an iatrogenic coronary artery fistula with a PTFE-coated stent]. *Rev Esp Cardiol* 2004; **57**: 699-701 [PMID: 15274856]
35 **Lee RT**, Mudge GH, Colucci WS. Coronary artery fistula after mitral valve surgery. *Am Heart J* 1988; **115**: 1128-1130 [PMID:3364344 DOI: 10.1016/0002-8703(88)90089-0]
36 **Rudraiah L**, Dhar G, Thatai D. Acquired coronary cameral fistula--a report of two cases. *Int J Cardiol* 2008; **123**: e40-e42 [PMID: 17303268 DOI: 10.1016/j.ijcard.2006.11.117]
37 **Chenzbraun A**, Pinto FJ, Meyer B, Stinson EB, Popp RL. **Frequency of acquired coronary-cameral fistula after ventricular septal myectomy in hypertrophic cardiomyopathy.** *Am J Cardiol* 1993; **71**: 1244-1246 [PMID:8480661]
38 **Awasthi A**, Wormer D, Heggunje PS, Obeid A. Long-term follow-up of acquired coronary artery fistula after septal myectomy for hypertrophic cardiomyopathy. *J Am Soc Echocardiogr* 2002; **15**: 1104-1107 [PMID: 12373254 DOI: 10.1067/mje.2002.122632]
39 **Choi YJ**, You CW, Park MK, Park JI, Kwon SU, Lee SC, Lee HJ, Park SW. Spontaneous closure of iatrogenic coronary artery fistula to left ventricle after septal myectomy for hypertrophic obstructive cardiomyopathy. *J Korean Med Sci* 2006; **21**: 1111-1114 [PMID: 17179697 DOI: 10.3346/jkms.2006.21.6.1111]
40 **Garber PJ**, Hussain F, Koenig JK, Maycher B, Jassal DS. Multimodality imaging of a coronary artery fistula after septal myomectomy in hypertrophic cardiomyopathy. *J Am Coll Cardiol* 2011; **57**: e95 [PMID: 21349395 DOI: 10.1016/j.jacc.2010.04.077]
41 **Renzulli A**, Wren C, Hilton CJ. Coronary artery-left ventricular fistula and multiple ventricular septal defects due to blunt chest trauma. *Thorax* 1989; **44**: 1055-1056 [PMID: 2617447 DOI: 10.1136/thx.44.12.1055]
42 **Lynn RB**, Fay JE. Post-traumatic cardiocoronary fistula. *Can J Surg* 1971; **14**: 335-336 [PMID: 5113538]
43 **Hancock Friesen C**, Howlett JG, Ross DB. **Traumatic coronary artery fistula management.** *Ann Thorac Surg* 2000; **69**: 1973-1982 [PMID:10892970 DOI: 10.1016/S0003-4975(00)01207-8]
44 **Radomski M**, Kubica J, Sukiennik A, Wojtowicz A, Lewicka-Nowak E, Dorniak W, Skarżyński P, Nowak A, Ciećwierz D, Rynkiewicz A, Świątecka G. Left anterior descending coronary artery to the right ventricle fistula: an unusual complication of myocardial infarction. Case report. *Folia Cardiol* 1999; **6**: 399-403
45 **Shimizu M**, Yoshio H, Ino H, Takeda R, Okada Y. Histopathologic findings of a left coronary artery fistula to the left ventricle after myocardial infarction. *Cardiology Elderly* 1993; **1**: 335-336
46 **Yu R**, Sharma B, Franciosa JA. **Acquired coronary artery fistula to the left ventricle after acute myocardial infarction.** *Am J Cardiol* 1986; **58**: 557-558 [PMID: 3751920 DOI: 10.1016/0002-9149(86)90036-6]
47 **Schanzenbächer P**, Bauersachs J. Acquired right coronary artery fistula draining to the right ventricle: angiographic documentation of first appearance following reperfusion after acute myocardial infarction, with subsequent spontaneous closure. *Heart* 2003; **89**: e22 [PMID: 12860888 DOI: 10.1136/heart.89.8.e22]
48 **Lucca MJ**, Tomlinson GC. Acquired coronary artery fistula: a sign of mural thrombus. *Cathet Cardiovasc Diagn* 1988; **15**: 273-276 [PMID: 2465831 DOI: 10.1002/ccd.1810150413]
49 **Ray SG**, Cowan MD, Kennedy JA. Spontaneously acquired fistula from the right coronary artery to the right ventricular cavity. *Br Heart J* 1992; **67**: 323-324 [PMID: 1389709 DOI: 10.1136/hrt.67.4.323]
50 **Lee KM**, Pichard AD, Lindsay J Jr. **Acquired coronary artery-left ventricular pseudoaneurysm fistula after myocardial infarction.** *Am J Cardiol* 1989; **64**: 824-825 [PMID:2801541 DOI: 10.1016/0002-9149(89)90778-9]
51 **Cipriano PR**, Guthaner DF. **Organized left atrial mural thrombus demonstrated by coronary angiography.** *Am Heart J* 1978; **96**: 166-169 [PMID:676977]
52 **Jacob S**, Feigenbaum H. Acquired coronary-cameral fistula. *Clin Cardiol* 2009; **32**: E70 [PMID: 19610122 DOI: 10.1002/clc.20507]
53 **Hagau AM**, Dudea SM, Hagau R, Hagau N. Large coronary pseudoaneurysm with pulmonary artery fistula, six months after left main trunk stenting with paclitaxel-eluting stent. *Med Ultrason* 2013; **15**: 59-62 [PMID: 23486626 DOI: 10.11152/mu.2013.2066.151.ah1lcp2]
54 **Ahmed TAN**. Innovative therapies for optimizing outcomes of coronary artery disease. Thesis. Leiden: LUMC, 2011
55 **Karim MA**. Coronary artery aneurysmal fistula: a late complication of stent deployment. *Int J Cardiol* 1996; **57**: 207-209 [PMID:9024907 DOI: 10.1016/S0167-5273(96)02809-4]
56 **Lemos AE**, Araújo AL, Belém Lde S, Mejia JA, Cruz A, Evangelista NL, Oliveira LS. Traumatic fistula between the right coronary artery and right atrial chamber. *Arq Bras Cardiol* 2007; **88**: e66-e67 [PMID: 17533462]
57 **Mabo P**, Le Breton H, De Place C, Daubert C. **Asymptomatic pseudoaneurysm of the left ventricle and coronary artery fistula after closed-chest ablation of an accessory pathway.** *Am Heart J* 1992; **124**: 1637-1639 [PMID:1462930 DOI: 10.1016/0002-8703(92)90089-E]
58 **El Hosieny A**, Hui W. Fistula between right coronary artery vein graft and right atrium as an immediate complication of percutaneous coronary intervention. *Catheter Cardiovasc Interv* 2012; **80**: 71-74 [PMID: 22234898 DOI: 10.1002/ccd.23371]
59 **Diego-Nieto A**, Cuellas-Ramón C, Pérez de Prado A, Fernández-Vázquez F. [Iatrogenic coronary-cameral fistula after percutaneous intervention on the right coronary artery]. *Rev Esp Cardiol* 2008; **61**: 434-435 [PMID: 18405529 DOI: 10.1157/13117741]
60 **Martí V**, Bailén JL, Augé JM, Bordes R, Crexells C. [Coronary fistula to the right ventricle in heart transplant patients as a complication of repeated endomyocardial biopsies]. *Rev Esp Cardiol* 1991; **44**: 320-323 [PMID: 1852961]
61 **Gascueña R**, de Lombera F, Fernández S, Santos M, Delgado J, Escribano P, Gómez MA. Left circumflex coronary artery-to-left atrium fistulas detected by transesophageal echocardiography in heart transplant recipients. *Echocardiography* 2000; **17**: 443-445 [PMID: 10979018 DOI: 10.1111/j.1540-8175.2000.tb01161.x]
62 **Saraiva F**, Matos V, Gonçalves L, Antunes M, Providência LA. Complications of endomyocardial biopsy in heart transplant patients: a retrospective study of 2117 consecutive procedures. *Transplant Proc* 2011; **43**: 1908-1912 [PMID: 21693299 DOI: 10.1016/j.transproceed.2011.03.010]
63 **Gasser S**, Gasser R, Bareza N, Klein W. Iatrogenic coronary fistula in post transplant patients: pathogenesis, clinical features and therapy. *J Clin Basic Cardiol* 2003; **6**: 19-21
64 **Sauer HU**, Regitz V, Thierstein T, Schüler S, Warnecke H, Hetzer R, Fleck E. [Coronary fistulas--high prevalence in patients with heart transplantation]. *Herz* 1991; **16**: 46-54 [PMID: 2026383]
65 **Lee CH**, Lemos PA, Serruys PW. Acquired coronary artery fistula leading to acute myocardial infarction after endomyocardial biopsy. *Heart* 2003; **89**: 495 [PMID: 12695449 DOI: 10.1136/heart.89.5.495]
66 **Hartog JM**, van den Brand M, Pieterman H, di Mario C. Closure of a coronary cameral fistula following endomyocardial biopsies in a cardiac transplant patient with a detachable balloon. *Cathet Cardiovasc Diagn* 1993; **30**: 156-159 [PMID: 8221871 DOI: 10.1002/ccd.1810300215]

67 **Khouzam RN**, Naidu SS. Alcohol septal ablation for symptomatic hypertrophic obstructive cardiomyopathy in patients with prior coronary revascularization. *J Invasive Cardiol* 2010; **22**: E220-E224 [PMID: 21127375]

68 **Lyne JC**, Kilpatrick T, Duncan A, Knight CJ, Sigwart U, Fox KM. Long-term follow-up of the first patients to undergo transcatheter alcohol septal ablation. *Cardiology* 2010; **116**: 168-173 [PMID: 20616549 DOI: 10.1159/000318307]

69 **Kovacic JC**, Khanna D, Kaplish D, Karajgikar R, Sharma SK, Kini A. Safety and efficacy of alcohol septal ablation in patients with symptomatic concentric left ventricular hypertrophy and outflow tract obstruction. *J Invasive Cardiol* 2010; **22**: 586-591 [PMID: 21127363]

70 **Sutherland RD**, Gholston DE, Gulde RE, Martinez HE. Traumatic fistula between left anterior descending coronary artery and right ventricle. Case report with successful surgical repair. *J Thorac Cardiovasc Surg* 1975; **70**: 692-695 [PMID: 1177482]

71 **Allen RP**, Liedtke AJ. The role of coronary artery injury and perfusion in the development of cardiac contusion secondary to nonpenetrating chest trauma. *J Trauma* 1979; **19**: 153-156 [PMID: 458879 DOI: 10.1097/00005373-197903000-00004]

72 **Wańczura P**, Stecko W, Kukla P, Kuźniar J. [A continuous murmur in female patient after traffic injury]. *Kardiol Pol* 2012; **70**: 1283-1285 [PMID: 23264249]

73 **Sibille L**, Boudousq V, Soullier C, Rossi M, Mariano-Goulart D. Tc-99m tetrofosmin SPECT in coronary cameral fistula. *Clin Nucl Med* 2009; **34**: 473-474 [PMID: 19542962 DOI: 10.1097/RLU.0b013e3181a7cfa2]

74 **Said SA**, van der Werf T. Acquired coronary cameral fistulas: are these collaterals losing their destination? *Clin Cardiol* 1999; **22**: 297-302 [PMID: 10198740 DOI: 10.1002/clc.4960220409]

75 **Sengul C**, Ciftci R, Ertem FU, Cevik C. Coronary cameral fistula: A rare cause of coronary ischemia. *Ach Iatr* 2012; **31**: 159-161

76 **Konno S**, Endo M. [Congenital coronary artery diseases]. *Kokyu To Junkan* 1973; **21**: 397-409 [PMID: 4580425]

77 **Sethuratnam R**, Srinivasan B, Menon A, Anbarasu M, Pillai RS, Dhruv T, Davidson Y. Unusual presentation of a coronary cameral fistula. *Ind J Thorac Cardiovasc Surg* 2007; **23**: 28-30 [DOI: 10.1007/s12055-007-0006-9]

78 **Chiu CZ**, Shyu KG, Cheng JJ, Lin SC, Lee SH, Hung HF, Liou JY. Angiographic and clinical manifestations of coronary fistulas in Chinese people: 15-year experience. *Circ J* 2008; **72**: 1242-1248 [PMID: 18654007 DOI: 10.1253/circj.72.1242]

P- Reviewers: Kounis GN, Panduranga P, Raja SG, Rognoni A, Ye YC
S- Editor: Wen LL **L- Editor**: Roemmele A **E- Editor**: Liu XM

World Journal of Cardiology

Online Submissions: http://www.wjgnet.com/esps/
bpgoffice@wjgnet.com
www.wjgnet.com

World J Cardiol 2013 December 26; 5(12): I-V
ISSN 1949-8462 (online)

GENERAL INFORMATION

World Journal of Cardiology (*World J Cardiol*, *WJC*, online ISSN 1949-8462, DOI: 10.4330) is a peer-reviewed open access (OA) academic journal that aims to guide clinical practice and improve diagnostic and therapeutic skills of clinicians.

Aim and scope

WJC covers topics concerning arrhythmia, heart failure, vascular disease, stroke, hypertension, prevention and epidemiology, dyslipidemia and metabolic disorders, cardiac imaging, pediatrics, nursing, and health promotion. Priority publication will be given to articles concerning diagnosis and treatment of cardiology diseases. The following aspects are covered: Clinical diagnosis, laboratory diagnosis, differential diagnosis, imaging tests, pathological diagnosis, molecular biological diagnosis, immunological diagnosis, genetic diagnosis, functional diagnostics, and physical diagnosis; and comprehensive therapy, drug therapy, surgical therapy, interventional treatment, minimally invasive therapy, and robot-assisted therapy.

We encourage authors to submit their manuscripts to *WJC*. We will give priority to manuscripts that are supported by major national and international foundations and those that are of great basic and clinical significance.

WJC is edited and published by Baishideng Publishing Group (BPG). BPG has a strong professional editorial team composed of science editors, language editors and electronic editors. BPG currently publishes 42 OA clinical medical journals, including 41 in English, has a total of 15 471 editorial board members or peer reviewers, and is a world first-class publisher.

Columns

The columns in the issues of *WJC* will include: (1) Editorial: The editorial board members are invited to make comments on an important topic in their field in terms of its current research status and future directions to lead the development of this discipline; (2) Frontier: The editorial board members are invited to select a highly cited cutting-edge original paper of his/her own to summarize major findings, the problems that have been resolved and remain to be resolved, and future research directions to help readers understand his/her important academic point of view and future research directions in the field; (3) Diagnostic Advances: The editorial board members are invited to write high-quality diagnostic advances in their field to improve the diagnostic skills of readers. The topic covers general clinical diagnosis, differential diagnosis, pathological diagnosis, laboratory diagnosis, imaging diagnosis, endoscopic diagnosis, biotechnological diagnosis, functional diagnosis, and physical diagnosis; (4) Therapeutics Advances: The editorial board members are invited to write high-quality therapeutic advances in their field to help improve the therapeutic skills of readers. The topic covers medication therapy, psychotherapy, physical therapy, replacement therapy, interventional therapy, minimally invasive therapy, endoscopic therapy, transplantation therapy, and surgical therapy; (5) Field of Vision: The editorial board members are invited to write commentaries on classic articles, hot topic articles, or latest articles to keep readers at the forefront of research and increase their levels of clinical research. Classic articles refer to papers that are included in Web of Knowledge and have received a large number of citations (ranking in the top 1%) after being published for more than years, reflecting the quality and impact of papers. Hot topic articles refer to papers that are included in Web of Knowledge and have received a large number of citations after being published for no more than 2 years, reflecting cutting-edge trends in scientific research. Latest articles refer to the latest published high-quality papers that are included in PubMed, reflecting the latest research trends. These commentary articles should focus on the status quo of research, the most important research topics, the problems that have now been resolved and remain to be resolved, and future research directions. Basic information about the article to be commented (including authors, article title, journal name, year, volume, and inclusive page numbers; (6) Minireviews: The editorial board members are invited to write short reviews on recent advances and trends in research of molecular biology, genomics, and related cutting-edge technologies to provide readers with the latest knowledge and help improve their diagnostic and therapeutic skills; (7) Review: To make a systematic review to focus on the status quo of research, the most important research topics, the problems that have now been resolved and remain to be resolved, and future research directions; (8) Topic Highlight: The editorial board members are invited to write a series of articles (7-10 articles) to comment and discuss a hot topic to help improve the diagnostic and therapeutic skills of readers; (9) Medical Ethics: The editorial board members are invited to write articles about medical ethics to increase readers' knowledge of medical ethics. The topic covers international ethics guidelines, animal studies, clinical trials, organ transplantation, *etc.*; (10) Clinical Case Conference or Clinicopathological Conference: The editorial board members are invited to contribute high-quality clinical case conference; (11) Original Articles: To report innovative and original findings in cardiology; (12) Brief Articles: To briefly report the novel and innovative findings in cardiology; (13) Meta-Analysis: Covers the systematic review, mixedtreatment comparison, meta-regression, and overview of reviews, in order to summarize a given quantitative effect, e.g., the clinical effectiveness and safety of clinical treatments by combining data from two or more randomized controlled trials, thereby providing more precise and externally valid estimates than those which would stem from each individual dataset if analyzed separately from the others; (14) Case Report: To report a rare or typical case; (15) Letters to the Editor: To discuss and make reply to the contributions published in *WJC*, or to introduce and comment on a controversial issue of general interest; (16) Book Reviews: To introduce and comment on quality monographs of cardiology; and (17) Autobiography: The editorial board members are invited to write their autobiography to provide readers with stories of success or failure in their scientific research career. The topic covers their basic personal information and information about when they started doing research work, where and how they did research work, what they have achieved, and their lessons from success or failure.

Name of journal

World Journal of Cardiology

ISSN

ISSN 1949-8462 (online)

Launch date

December 31, 2009

Frequency

Monthly

Editorial office
Jin-Lei Wang, Director
Xiu-Xia Song, Vice Director
World Journal of Cardiology
Room 903, Building D, Ocean International Center,
No. 62 Dongsihuan Zhonglu, Chaoyang District,
Beijing 100025, China
Telephone: +86-10-59080039
Fax: +86-10-85381893
E-mail: bpgoffice@wjgnet.com
http://www.wjgnet.com

Publisher
Baishideng Publishing Group Co., Limited
Flat C, 23/F., Lucky Plaza, 315-321 Lockhart Road,
Wan Chai, Hong Kong, China
Fax: +852-65557188
Telephone: +852-31779906
E-mail: bpgoffice@wjgnet.com
http://www.wjgnet.com

Production center
Beijing Baishideng BioMed Scientific Co., Limited
Room 903, Building D, Ocean International Center,
No. 62 Dongsihuan Zhonglu, Chaoyang District,
Beijing 100025, China
Telephone: +86-10-85381892
Fax: +86-10-85381893

Representative office
USA Office
8226 Regency Drive,
Pleasanton, CA 94588-3144, United States

Instructions to authors
Full instructions are available online at http://www.wjgnet.com/1949-8462/g_info_20100316161927.htm.

Indexed and Abstracted in
PubMed Central, PubMed, Digital Object Identifier, and Directory of Open Access Journals.

SPECIAL STATEMENT

All articles published in this journal represent the viewpoints of the authors except where indicated otherwise.

Biostatistical editing
Statistical review is performed after peer review. We invite an expert in Biomedical Statistics to evaluate the statistical method used in the paper, including *t*-test (group or paired comparisons), chi-squared test, Ridit, probit, logit, regression (linear, curvilinear, or stepwise), correlation, analysis of variance, analysis of covariance, *etc*. The reviewing points include: (1) Statistical methods should be described when they are used to verify the results; (2) Whether the statistical techniques are suitable or correct; (3) Only homogeneous data can be averaged. Standard deviations are preferred to standard errors. Give the number of observations and subjects (*n*). Losses in observations, such as drop-outs from the study should be reported; (4) Values such as ED50, LD50, IC50 should have their 95% confidence limits calculated and compared by weighted probit analysis (Bliss and Finney); and (5) The word 'significantly' should be replaced by its synonyms (if it indicates extent) or the *P* value (if it indicates statistical significance).

Conflict-of-interest statement
In the interests of transparency and to help reviewers assess any potential bias, *WJC* requires authors of all papers to declare any competing commercial, personal, political, intellectual, or religious interests in relation to the submitted work. Referees are also asked to indicate any potential conflict they might have reviewing a particular paper. Before submitting, authors are suggested to read "Uniform Requirements for Manuscripts Submitted to Biomedical Journals: Ethical Considerations in the Conduct and Reporting of Research: Conflicts of Interest" from International Committee of Medical Journal Editors (ICMJE), which is available at: http://www.icmje.org/ethical_4conflicts.html.

Sample wording: [Name of individual] has received fees for serving as a speaker, a consultant and an advisory board member for [names of organizations], and has received research funding from [names of organization]. [Name of individual] is an employee of [name of organization]. [Name of individual] owns stocks and shares in [name of organization]. [Name of individual] owns patent [patent identification and brief description].

Statement of informed consent
Manuscripts should contain a statement to the effect that all human studies have been reviewed by the appropriate ethics committee or it should be stated clearly in the text that all persons gave their informed consent prior to their inclusion in the study. Details that might disclose the identity of the subjects under study should be omitted. Authors should also draw attention to the Code of Ethics of the World Medical Association (Declaration of Helsinki, 1964, as revised in 2004).

Statement of human and animal rights
When reporting the results from experiments, authors should follow the highest standards and the trial should conform to Good Clinical Practice (for example, US Food and Drug Administration Good Clinical Practice in FDA-Regulated Clinical Trials; UK Medicines Research Council Guidelines for Good Clinical Practice in Clinical Trials) and/or the World Medical Association Declaration of Helsinki. Generally, we suggest authors follow the lead investigator's national standard. If doubt exists whether the research was conducted in accordance with the above standards, the authors must explain the rationale for their approach and demonstrate that the institutional review body explicitly approved the doubtful aspects of the study.

Before submitting, authors should make their study approved by the relevant research ethics committee or institutional review board. If human participants were involved, manuscripts must be accompanied by a statement that the experiments were undertaken with the understanding and appropriate informed consent of each. Any personal item or information will not be published without explicit consents from the involved patients. If experimental animals were used, the materials and methods (experimental procedures) section must clearly indicate that appropriate measures were taken to minimize pain or discomfort, and details of animal care should be provided.

SUBMISSION OF MANUSCRIPTS

Manuscripts should be typed in 1.5 line spacing and 12 pt. Book Antiqua with ample margins. Number all pages consecutively, and start each of the following sections on a new page: Title Page, Abstract, Introduction, Materials and Methods, Results, Discussion, Acknowledgements, References, Tables, Figures, and Figure Legends. Neither the editors nor the publisher are responsible for the opinions expressed by contributors. Manuscripts formally accepted for publication become the permanent property of Baishideng Publishing Group Co., Limited, and may not be reproduced by any means, in whole or in part, without the written permission of both the authors and the publisher. We reserve the right to copy-edit and put onto our website accepted manuscripts. Authors should follow the relevant guidelines for the care and use of laboratory animals of their institution or national animal welfare committee. For the sake of transparency in regard to the performance and report-

ing of clinical trials, we endorse the policy of the ICMJE to refuse to publish papers on clinical trial results if the trial was not recorded in a publicly-accessible registry at its outset. The only register now available, to our knowledge, is http://www.clinicaltrials.gov sponsored by the United States National Library of Medicine and we encourage all potential contributors to register with it. However, in the case that other registers become available you will be duly notified. A letter of recommendation from each author's organization should be provided with the contributed article to ensure the privacy and secrecy of research is protected.

Authors should retain one copy of the text, tables, photographs and illustrations because rejected manuscripts will not be returned to the author(s) and the editors will not be responsible for loss or damage to photographs and illustrations sustained during mailing.

Online submissions

Manuscripts should be submitted through the Online Submission System at: http://www.wjgnet.com/esps/. Authors are highly recommended to consult the ONLINE INSTRUCTIONS TO AUTHORS (http://www.wjgnet.com/1949-8462/g_info_20100316161927.htm) before attempting to submit online. For assistance, authors encountering problems with the Online Submission System may send an email describing the problem to bpgoffice@wjgnet.com, or by telephone: +86-10-85381892. If you submit your manuscript online, do not make a postal contribution. Repeated online submission for the same manuscript is strictly prohibited.

MANUSCRIPT PREPARATION

All contributions should be written in English. All articles must be submitted using word-processing software. All submissions must be typed in 1.5 line spacing and 12 pt. Book Antiqua with ample margins. Style should conform to our house format. Required information for each of the manuscript sections is as follows:

Title page

Title: Title should be less than 12 words.

Running title: A short running title of less than 6 words should be provided.

Authorship: Authorship credit should be in accordance with the standard proposed by ICMJE, based on (1) substantial contributions to conception and design, acquisition of data, or analysis and interpretation of data; (2) drafting the article or revising it critically for important intellectual content; and (3) final approval of the version to be published. Authors should meet conditions 1, 2, and 3.

Institution: Author names should be given first, then the complete name of institution, city, province and postcode. For example, Xu-Chen Zhang, Li-Xin Mei, Department of Pathology, Chengde Medical College, Chengde 067000, Hebei Province, China. One author may be represented from two institutions, for example, George Sgourakis, Department of General, Visceral, and Transplantation Surgery, Essen 45122, Germany; George Sgourakis, 2nd Surgical Department, Korgialenio-Benakio Red Cross Hospital, Athens 15451, Greece

Author contributions: The format of this section should be: Author contributions: Wang CL and Liang L contributed equally to this work; Wang CL, Liang L, Fu JF, Zou CC, Hong F and Wu XM designed the research; Wang CL, Zou CC, Hong F and Wu XM performed the research; Xue JZ and Lu JR contributed new reagents/analytic tools; Wang CL, Liang L and Fu JF analyzed the data; and Wang CL, Liang L and Fu JF wrote the paper.

Supportive foundations: The complete name and number of supportive foundations should be provided, *e.g.*, Supported by National Natural Science Foundation of China, No. 30224801

Correspondence to: Only one corresponding address should be provided. Author names should be given first, then author title, affiliation, the complete name of institution, city, postcode, province, country, and email. All the letters in the email should be in lower case. A space interval should be inserted between country name and email address. For example, Montgomery Bissell, MD, Professor of Medicine, Chief, Liver Center, Gastroenterology Division, University of California, Box 0538, San Francisco, CA 94143, United States. montgomery.bissell@ucsf.edu

Telephone and fax: Telephone and fax should consist of +, country number, district number and telephone or fax number, *e.g.*, Telephone: +86-10-85381892 Fax: +86-10-85381893

Peer reviewers: All articles received are subject to peer review. Normally, three experts are invited for each article. Decision on acceptance is made only when at least two experts recommend publication of an article. All peer-reviewers are acknowledged on Express Submission and Peer-review System website.

Abstract

There are unstructured abstracts (no less than 200 words) and structured abstracts. The specific requirements for structured abstracts are as follows:

An informative, structured abstract should accompany each manuscript. Abstracts of original contributions should be structured into the following sections: AIM (no more than 20 words; Only the purpose of the study should be included. Please write the Aim in the form of "To investigate/study/…"), METHODS (no less than 140 words for Original Articles; and no less than 80 words for Brief Articles), RESULTS (no less than 150 words for Original Articles and no less than 120 words for Brief Articles; You should present *P* values where appropriate and must provide relevant data to illustrate how they were obtained, *e.g.*, 6.92 ± 3.86 *vs* 3.61 ± 1.67, $P < 0.001$), and CONCLUSION (no more than 26 words).

Key words

Please list 5-10 key words, selected mainly from *Index Medicus*, which reflect the content of the study.

Core tip

Please write a summary of less than 100 words to outline the most innovative and important arguments and core contents in your paper to attract readers.

Text

For articles of these sections, original articles and brief articles, the main text should be structured into the following sections: INTRODUCTION, MATERIALS AND METHODS, RESULTS and DISCUSSION, and should include appropriate Figures and Tables. Data should be presented in the main text or in Figures and Tables, but not in both.

Illustrations

Figures should be numbered as 1, 2, 3, *etc.*, and mentioned clearly in the main text. Provide a brief title for each figure on a separate page. Detailed legends should not be provided under the figures. This part should be added into the text where the figures are applicable. Keeping all elements compiled is necessary in line-art image. Scale bars should be used rather than magnification factors, with the length of the bar defined in the legend rather than on the bar itself. File names should identify the figure and panel. Avoid layering type directly over shaded or textured areas. Please use uniform legends for the same subjects. For example: Figure 1 Pathological changes in atrophic gastritis after treatment. A: ...; B: ...; C: ...; D: ...; E: ...; F: ...; G: …*etc.* It is our principle to publish high resolution-figures for the E-versions.

Tables

Three-line tables should be numbered 1, 2, 3, *etc.*, and mentioned clearly in the main text. Provide a brief title for each table. Detailed legends should not be included under tables, but rather added into the text where applicable. The information should complement, but not duplicate the text. Use one horizontal line under the title, a

second under column heads, and a third below the Table, above any footnotes. Vertical and italic lines should be omitted.

Notes in tables and illustrations

Data that are not statistically significant should not be noted. $^{a}P <$ 0.05, $^{b}P < 0.01$ should be noted ($P > 0.05$ should not be noted). If there are other series of P values, $^{c}P < 0.05$ and $^{d}P < 0.01$ are used. A third series of P values can be expressed as $^{e}P < 0.05$ and $^{f}P < 0.01$. Other notes in tables or under illustrations should be expressed as ^{1}F, ^{2}F, ^{3}F; or sometimes as other symbols with a superscript (Arabic numerals) in the upper left corner. In a multi-curve illustration, each curve should be labeled with ●, ○, ■, □, ▲, △, *etc.*, in a certain sequence.

Acknowledgments

Brief acknowledgments of persons who have made genuine contributions to the manuscript and who endorse the data and conclusions should be included. Authors are responsible for obtaining written permission to use any copyrighted text and/or illustrations.

REFERENCES

Coding system

The author should number the references in Arabic numerals according to the citation order in the text. Put reference numbers in square brackets in superscript at the end of citation content or after the cited author's name. For citation content which is part of the narration, the coding number and square brackets should be typeset normally. For example, "Crohn's disease (CD) is associated with increased intestinal permeability[1,2]". If references are cited directly in the text, they should be put together within the text, for example, "From references[19,22-24], we know that..."

When the authors write the references, please ensure that the order in text is the same as in the references section, and also ensure the spelling accuracy of the first author's name. Do not list the same citation twice.

PMID and DOI

Pleased provide PubMed citation numbers to the reference list, *e.g.*, PMID and DOI, which can be found at http://www.ncbi.nlm.nih.gov/sites/entrez?db=pubmed and http://www.crossref.org/SimpleTextQuery/, respectively. The numbers will be used in E-version of this journal.

Style for journal references

Authors: the name of the first author should be typed in bold-faced letters. The family name of all authors should be typed with the initial letter capitalized, followed by their abbreviated first and middle initials. (For example, Lian-Sheng Ma is abbreviated as Ma LS, Bo-Rong Pan as Pan BR). The title of the cited article and italicized journal title (journal title should be in its abbreviated form as shown in PubMed), publication date, volume number (in black), start page, and end page [PMID: 11819634 DOI: 10.3748/wjg.13.5396].

Style for book references

Authors: the name of the first author should be typed in bold-faced letters. The surname of all authors should be typed with the initial letter capitalized, followed by their abbreviated middle and first initials. (For example, Lian-Sheng Ma is abbreviated as Ma LS, Bo-Rong Pan as Pan BR) Book title. Publication number. Publication place: Publication press, Year: start page and end page.

Format

Journals

English journal article (list all authors and include the PMID where applicable)

1 **Jung EM**, Clevert DA, Schreyer AG, Schmitt S, Rennert J, Kubale R, Feuerbach S, Jung F. Evaluation of quantitative contrast harmonic imaging to assess malignancy of liver tumors: A prospective controlled two-center study. *World J Gastroenterol* 2007; **13**: 6356-6364 [PMID: 18081224 DOI: 10.3748/wjg.13.6356]

Chinese journal article (list all authors and include the PMID where applicable)

2 **Lin GZ**, Wang XZ, Wang P, Lin J, Yang FD. Immunologic effect of Jianpi Yishen decoction in treatment of Pixu-diarrhoea. *Shijie Huaren Xiaohua Zazhi* 1999; **7**: 285-287

In press

3 **Tian D**, Araki H, Stahl E, Bergelson J, Kreitman M. Signature of balancing selection in Arabidopsis. *Proc Natl Acad Sci USA* 2006; In press

Organization as author

4 **Diabetes Prevention Program Research Group**. Hypertension, insulin, and proinsulin in participants with impaired glucose tolerance. *Hypertension* 2002; **40**: 679-686 [PMID: 12411462 PMCID:2516377 DOI:10.1161/01.HYP.0000035706.28494.09]

Both personal authors and an organization as author

5 **Vallancien G**, Emberton M, Harving N, van Moorselaar RJ; Alf-One Study Group. Sexual dysfunction in 1, 274 European men suffering from lower urinary tract symptoms. *J Urol* 2003; **169**: 2257-2261 [PMID: 12771764 DOI:10.1097/01.ju.0000067940.76090.73]

No author given

6 21st century heart solution may have a sting in the tail. *BMJ* 2002; **325**: 184 [PMID: 12142303 DOI:10.1136/bmj.325.7357.184]

Volume with supplement

7 **Geraud G**, Spierings EL, Keywood C. Tolerability and safety of frovatriptan with short- and long-term use for treatment of migraine and in comparison with sumatriptan. *Headache* 2002; **42** Suppl 2: S93-99 [PMID: 12028325 DOI:10.1046/j.1526-4610.42.s2.7.x]

Issue with no volume

8 **Banit DM**, Kaufer H, Hartford JM. Intraoperative frozen section analysis in revision total joint arthroplasty. *Clin Orthop Relat Res* 2002; (**401**): 230-238 [PMID: 12151900 DOI:10.1097/00003086-200208000-00026]

No volume or issue

9 Outreach: Bringing HIV-positive individuals into care. *HRSA Careaction* 2002; 1-6 [PMID: 12154804]

Books

Personal author(s)

10 **Sherlock S**, Dooley J. Diseases of the liver and billiary system. 9th ed. Oxford: Blackwell Sci Pub, 1993: 258-296

Chapter in a book (list all authors)

11 **Lam SK**. Academic investigator's perspectives of medical treatment for peptic ulcer. In: Swabb EA, Azabo S. Ulcer disease: investigation and basis for therapy. New York: Marcel Dekker, 1991: 431-450

Author(s) and editor(s)

12 **Breedlove GK**, Schorfheide AM. Adolescent pregnancy. 2nd ed. Wieczorek RR, editor. White Plains (NY): March of Dimes Education Services, 2001: 20-34

Conference proceedings

13 **Harnden P**, Joffe JK, Jones WG, editors. Germ cell tumours V. Proceedings of the 5th Germ cell tumours Conference; 2001 Sep 13-15; Leeds, UK. New York: Springer, 2002: 30-56

Conference paper

14 **Christensen S**, Oppacher F. An analysis of Koza's computational effort statistic for genetic programming. In: Foster JA, Lutton E, Miller J, Ryan C, Tettamanzi AG, editors. Genetic programming. EuroGP 2002: Proceedings of the 5th European Conference on Genetic Programming; 2002 Apr 3-5; Kinsdale, Ireland. Berlin: Springer, 2002: 182-191

Electronic journal (list all authors)

15 Morse SS. Factors in the emergence of infectious diseases. Emerg Infect Dis serial online, 1995-01-03, cited 1996-06-05; 1(1): 24 screens. Available from: URL: http://www.cdc.gov/ncidod/eid/index.htm

Patent (list all authors)

16 **Pagedas AC**, inventor; Ancel Surgical R&D Inc., assignee. Flexible endoscopic grasping and cutting device and positioning tool assembly. United States patent US 20020103498. 2002 Aug 1

Statistical data
Write as mean ± SD or mean ± SE.

Statistical expression
Express *t* test as *t* (in italics), *F* test as *F* (in italics), chi square test as χ^2 (in Greek), related coefficient as *r* (in italics), degree of freedom as υ (in Greek), sample number as *n* (in italics), and probability as *P* (in italics).

Units
Use SI units. For example: body mass, m (B) = 78 kg; blood pressure, p (B) = 16.2/12.3 kPa; incubation time, t (incubation) = 96 h, blood glucose concentration, c (glucose) 6.4 ± 2.1 mmol/L; blood CEA mass concentration, p (CEA) = 8.6 24.5 μg/L; CO_2 volume fraction, 50 mL/L CO_2, not 5% CO_2; likewise for 40 g/L formaldehyde, not 10% formalin; and mass fraction, 8 ng/g, *etc*. Arabic numerals such as 23, 243, 641 should be read 23243641.

The format for how to accurately write common units and quantums can be found at: http://www.wjgnet.com/1949-8462/g_info_20100312200347.htm.

Abbreviations
Standard abbreviations should be defined in the abstract and on first mention in the text. In general, terms should not be abbreviated unless they are used repeatedly and the abbreviation is helpful to the reader. Permissible abbreviations are listed in Units, Symbols and Abbreviations: A Guide for Biological and Medical Editors and Authors (Ed. Baron DN, 1988) published by The Royal Society of Medicine, London. Certain commonly used abbreviations, such as DNA, RNA, HIV, LD50, PCR, HBV, ECG, WBC, RBC, CT, ESR, CSF, IgG, ELISA, PBS, ATP, EDTA, mAb, can be used directly without further explanation.

Italics
Quantities: *t* time or temperature, *c* concentration, *A* area, *l* length, *m* mass, *V* volume.
Genotypes: *gyrA*, *arg* 1, *c myc*, *c fos*, *etc*.
Restriction enzymes: *Eco*RI, *Hin*dI, *Bam*HI, *Kbo* I, *Kpn* I, *etc*.
Biology: *H. pylori*, *E coli*, *etc*.

Examples for paper writing
All types of articles' writing style and requirement will be found in the link: http://www.wjgnet.com/esps/NavigationInfo.aspx?id=15

RESUBMISSION OF THE REVISED MANUSCRIPTS

Authors must revise their manuscript carefully according to the revision policies of Baishideng Publishing Group Co., Limited. The revised version, along with the signed copyright transfer agreement, responses to the reviewers, and English language Grade A certificate (for non-native speakers of English), should be submitted to the online system via the link contained in the e-mail sent by the editor. If you have any questions about the revision, please send e-mail to esps@wjgnet.com.

Language evaluation
The language of a manuscript will be graded before it is sent for revision. (1) Grade A: priority publishing; (2) Grade B: minor language polishing; (3) Grade C: a great deal of language polishing needed; and (4) Grade D: rejected. Revised articles should reach Grade A.

Copyright assignment form
Please download a Copyright assignment form from http://www.wjgnet.com/1949-8462/g_info_20100312200118.htm.

Responses to reviewers
Please revise your article according to the comments/suggestions provided by the reviewers. The format for responses to the reviewers' comments can be found at: http://www.wjgnet.com/1949-8462/g_info_20100312195923.htm.

Proof of financial support
For papers supported by a foundation, authors should provide a copy of the approval document and serial number of the foundation.

STATEMENT ABOUT ANONYMOUS PUBLICATION OF THE PEER REVIEWERS' COMMENTS

In order to increase the quality of peer review, push authors to carefully revise their manuscripts based on the peer reviewers' comments, and promote academic interactions among peer reviewers, authors and readers, we decide to anonymously publish the reviewers' comments and author's responses at the same time the manuscript is published online.

PUBLICATION FEE

WJC is an international, peer-reviewed, OA online journal. Articles published by this journal are distributed under the terms of the Creative Commons Attribution Non-commercial License, which permits use, distribution, and reproduction in any medium and format, provided the original work is properly cited. The use is non-commercial and is otherwise in compliance with the license. Authors of accepted articles must pay a publication fee. Publication fee: 600 USD per article. All invited articles are published free of charge.

百世登

Baishideng®

Published by **Baishideng Publishing Group Co., Limited**
Flat C, 23/F., Lucky Plaza,
315-321 Lockhart Road, Wan Chai, Hong Kong, China
Fax: +852-65557188
Telephone: +852-31779906
E-mail: bpgoffice@wjgnet.com
http://www.wjgnet.com